MASTER OF PHILOSOPHY

Temporal and Spatial Settlement of Subtidal Seed Mussels on the Southeast coast of Ireland

Chopin, Nicolas T.

Award date:
2024

Awarding institution:
Bangor University

Temporal and Spatial Settlement of Subtidal Seed Mussels on the Southeast coast of Ireland

Nicolas Chopin

A thesis submitted for the Degree of Master of Philosophy

In the School of Ocean Science

Marine Science Department

Bangor University, Wales

Supervisor: Prof. Shelagh K. Malham & Dr Peter E. Robins

School of Ocean Science

College of Ocean Science and Environment

Bangor University, Wales

Head of School: Prof. John Turner

Acknowledgements:

This research was an integral part of BIM (Bord Iascaigh Mhara) 2020 work program and was fully funded by the EMFF (European Maritime and Fisheries Fund), DAFM (Department of Agriculture, Food and the Marine of Ireland). I would also like to acknowledge the SFPA (Sea Fishery Protection of Ireland) for providing fishing figures, Bangor University staff, especially in SOS Menai Bridge, for overall support, as well as my colleagues in BIM. I want to especially thank Coílín Minto from ATU Galway, Elizabeth Tray from BIM and Isabelle Johansson for the gigantic support on R Studio, and Bangor University for the overall support. Last but not least, to my wife, Eimear O'Keeffe, who taught me everything about ArcGIS.

This thesis is the result of 16 years of fieldwork for BIM, collecting and measuring thousands of mussels, covering thousands of hectares of the seabed with the side scan sonar, and spending hundreds of days at sea.

Temporal and Spatial Settlement of Subtidal Seed Mussels on the Southeast coast of Ireland

Table of Contents

Temporal and Spatial Settlement of Subtidal Seed Mussels on the Southeast coast of Ireland

Tables of figures

Temporal and Spatial Settlement of Subtidal Seed Mussels on the Southeast Coast of Ireland

Author: Nicolas Chopin

Supervisors: Shelagh K. Malham, Peter E. Robins

Abstract:

Subtidal seed mussels are the sole resource of juveniles in the bottom-grown mussel industry in the Republic of Ireland. Understanding recruitment patterns allows for better management of the seasonal fishery and provides the industry with some production sustainability. From their planktonic larval phase to the fast-developing young seed or spat, mussels are subjected to various external factors such as shelf sea currents, wind-driven processes, sea temperature, food availability and substrate type, resulting in spatio-temporal variability in recruitment success through the years. This thesis proposes a methodology to assess the biomass of subtidal seed mussel beds and examines the effect of sea temperature on see mussel sizes at two locations in the Irish Sea.

Seed mussel surveys have been taking place on the coast of Ireland since 1970, providing settlement locations and indicative biomass figures to the bottom mussel farming industry and the regulatory bodies. Unlike intertidal settlements, subtidal seed mussel beds are permanently submerged, making their assessment more challenging. During 2020, using side scan sonar acoustic imagery and ArcGIS, it was possible to visualize and establish the extent of two subtidal seed mussel beds located along the southeast coast of Co. Wexford, one near Rosslare and a second in the Rusk Channel. Random sample locations for both sites were generated on mapping software, providing extensive ground-truthing, which was carried out using grab samples. Using the weight of seed mussel in each grab and the Inverted Distance Weight (IDW) interpolation method on ArcGIS, seed mussel biomass was estimated for each of the settlements. Post-fishery surveys were carried out using the same method, and the remaining biomass was estimated,

indicating that less than 10% of the original estimated biomass remained after the fishing effort. The original biomass estimations were then compared with the combined post-fishery biomass and the reported fishing figures from the industry. The variation between both figures indicated that the combined original biomass for both beds had been underestimated by less than 3% (or 182 metric tonnes), thus validating this estimation methodology.

Historically, the recruitment of subtidal seed mussel beds on the southeast coast of Ireland has been variable from year to year. According to the literature, the sea temperature is one of the main factors influencing the mussel life cycle. The seed mussel length records for the two main recruiting areas on the southeast coast of Ireland, namely Wexford-Rosslare and Cahore-Rusk Channel, collected from 2009 to 2022, give valuable insight into the seed length variation. Using a linear mixed model including the modelled sea temperatures for the expected larval phase until the first settlement (April, May, and June) and the recorded seed mussel length for each year, it was possible to assess the effect of sea temperature variations on the recruitment size. The model results for both areas indicated that smaller seed mussel size was related to lower sea temperature from April to June, in particular in 2013, when the lowest spring sea temperatures were observed. However, uncertainties generated by the prediction models indicate that low temperature may not be the only factor affecting the size of the seed mussel. Further scenarios, including other variables such as food availability, sediment mobility, and larval dispersion, should be considered.

Chapter 1: Understanding the Recruitment Variations of Mytilus sp. Juvenile Benthic Population on the Coast of Ireland

1.1. Introduction

Mussels are widely distributed globally and are one of the most studied species worldwide due to their biological, ecological, and commercial importance. They offer a range of ecosystem services, such as filter feeders, which act as a living "biofilter" that can help regulate nutrients within a bay (Chapter 9 in Smaal *et al.*, 2018). As bio-engineering organisms, the aggregation of mussels can form reefs that can provide sediment stabilisation along the coastline, thus helping reduce coastal erosion(Chapter 13 in Smaal *et al.*, 2018). They also provide a food source for larger animals such as birds (Hilgerloh, 1997) and can improve overall marine biodiversity (Sea *et al.*, 2022). In addition, they also represent a highly valuable source of seafood for human consumption, valued at €3.4 billion worldwide in 2016 (van der Schatte Olivier *et al.*, 2018; Avdelas *et al.*, 2021). Mussels have been harvested and farmed for centuries around the globe. Presently, farming is the most common way of producing various species of mussels. The main farmed species worldwide are the blue mussel *Mytilus edulis* Linnaeus, 1758; the Mediterranean mussel *Mytilus galloprovincialis* Lamarck, 1819; the Montevideo or Chilean mussel *Mytilus platensis* d'Orbigny, 1842; the bay mussel *Mytilus trossolus* Gould, 1850; the Asian green mussel *Perna viridis* Linnaeus, 1758 and the New Zealand mussel *Perna canaliculus* Gmelin, 1791. All these *Mytilus* species fall under what is commonly called the *Mytilus* complex, which is widely distributed from temperate to polar waters in both hemispheres (Koehn *et al.*, 2000). In Europe, the three main species in the wild and farmed are *Mytilus edulis*, *Mytilus Galloprovincialis* and *Mytilus trossolus* (Kijewski *et al.*, 2011). Those three species are morphologically similar; however, there appear to be growing adaptations due to local environmental variations (Elliott *et al.*, 2008; Telesca *et al.*, 2018; Capelle *et al.*, 2021a). Hybridisation between those species is common as they share similar distribution on European shores that are connected oceanographically in terms of larval dispersal and hence genetic connectivity (Bierne *et al.*, 2002; Beaumont *et al.*, 2004;

Coghlan and Gosling, 2007; Vera et al 2021) and similar reproduction patterns. The larvae pass through different planktonic stages before settling on a support such as rocks(King *et al.*, 1989), shells, gravel, hydroids, seaweed (Pulfrich, 1996)and already established mussel beds(Smaal *et al.*, 2017). However, oceanographic separation (e.g., peninsulas, ocean fronts) can limit gene flow between discrete populations (Vera et al., 2021). The duration of the planktonic phase depends on many factors, but growth is mainly driven by water temperature and food availability (Pechenik *et al.*, 1990). From fecundation to settlement, the *M. edulis* larvae can spend from four to ten weeks in the water column (Seed, 1969). On their last transformation, the larvae fix themselves on the seabed, from a depth range of the lower intertidal zone to 30 metres deep (pers. obs.), on the most suitable support available (Pineda *et al.*, 2010) using filaments (byssus threads) secreted by the byssal gland situated on the foot (Gosling, 2015). Following this stage, the aggregation of those young mussels on the seafloor can form "beds" that can spread over several hectares (Folmer *et al.*, 2014; Troost *et al.*, 2022). These beds supply the mussel farming sector with juveniles, which can be transplanted in designated growing areas.

Mussels are a readily available food source for coastal communities, and several farming techniques have been developed around the globe (i.e. rafts, longlines, bottom culture) to improve the harvesting and the culture of mussels (Smaal, 2002). The most popular technique is the submerged suspended culture (Smaal *et al.*, 2018). This method is used worldwide and with various species of mussel. The two main ways for suspended culture are the raft used in parts of Asia and suspended ropes used worldwide. Another technique in shallow lagoons consists of large metal trestles with suspended droppers. In France, "bouchots" appeared in the 13th century on the west coast following a shipwreck (Coste, 1861). They are essentially wooden poles planted in the intertidal zone and are used for both the collection of seed mussels and growth. This technique occurs along the west and north coasts of France. Finally, bottom culture mussels, evolving from commercial fishing, consists of transplanting juvenile mussels from naturally occurring beds and relaying them in sheltered areas to improve and manage their growth. This particular farming method is found mostly in parts of northern Europe (Ireland, Wales, the

Netherlands, Denmark) and the northeast coast of the United States of America (Newell *et al.*, 1991; Smaal, 2002).

In Ireland, the two prevailing farming techniques are suspended ropes used in sheltered bays around the coast and bottom culture used in shallow bays and intertidal zones. In both cases, farming depends on the collection of juvenile mussels, also known as seed mussels (Smaal, 2002). In suspended culture, the seed mussel can be collected on specially designed ropes that are submerged while mussel larvae are in the water column. While for the bottom culture, the larvae settle directly on the seabed where they aggregate and form beds that can be harvested and transplanted to licenced aquaculture sites. Although mussel farming has been carried out for generations, some challenges remain, in particular, the sourcing and availability of juveniles. For example, in the bottom-grown mussel Irish industry, the intake of wild seed mussels transplanted from 2007 to 2010 was steady at around 15,000 tonnes per year. From 2011 onwards, juvenile mussel recruitment dropped dramatically to around 3,000 tonnes in 2013. There has been a slow recovery since, but recruitment is still well below pre-2010 tonnage (BIM, 2019). A similar problem has been observed on the north coast of France, where the mussel fishery in east Cotentin has seen very little or no recruitment since 2016. The main difference between the French and the Irish situation is that in France, only adult mussels are fished for the market, whereas in Ireland, juvenile are fished and relayed in order to optimise their growth for the market. It is worth noting that the fishery in France has not been open since 2016; therefore, population recovery could have been expected, but it has not been the case (Le Gendre *et al.*, 2014a).

Seed mussel supply is the cornerstone of the mussel farming industry and is essential for wild population recruitment. Understanding relationships between species distribution, population connectivity, larval dispersal, and settlement patterns can provide insights into juvenile recruitment variations. Several endogenous and exogenous factors can affect the recruitment process from start to end: husbandry location and viability, larvae production, variability in ocean

dynamics and transport, species hybridisation, settlement spatial organisation and suitability of the sediment, climate variations and shifts, and how the fisheries are managed.

This thesis will focus on the subtidal blue mussel *Mytilus edulis* recruitment patterns on the southeast coast of Ireland, aiming at developing a better understanding of the seed mussel recruitment dynamics in this particular location. The objectives of this work are to develop a robust and repeatable method to assess the biomass of subtidal seed mussel beds and to identify the effect of seasonal water temperature variations on the size of those mussels.

1.2. Ecology

To assess the possible factors limiting seed mussel recruitment, it is important to understand the mechanisms of the production cycle of the blue mussel in subtidal systems, including benthic settlements (Fig.1).

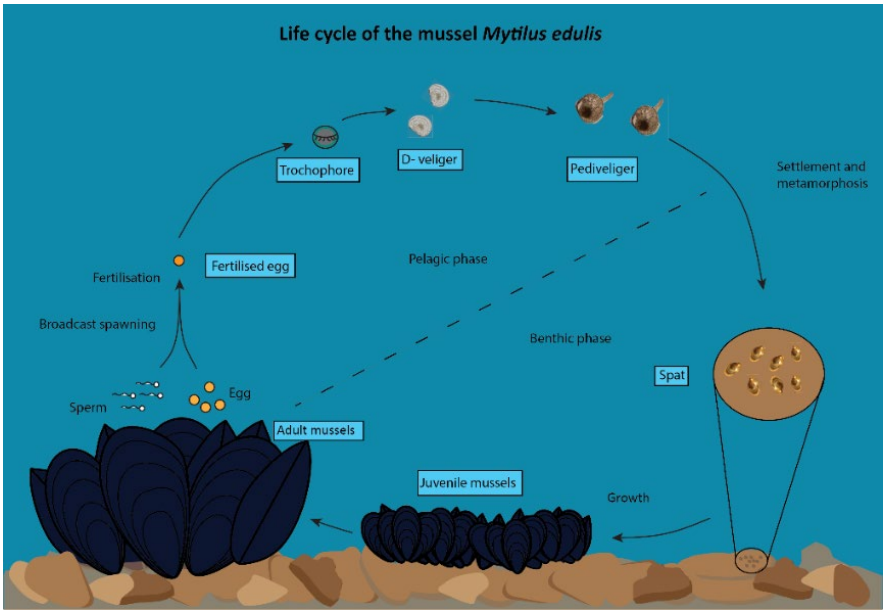

Fig. 1: The Life cycle of Mytilus edulis

1.2.1 Maturation

At the beginning of *Mytilus edulis* production cycle is the maturation of the broodstock. According to Chipperfield (1953), the maturation of *Mytilus edulis* starts when the water temperature reaches 7 degrees Celsius and is combined with suitable food availability. Maturation can occur

during the first year after the settlement of the larvae and is not related to the size of the individual (Seed, 1969).

In monitoring the maturation of the mussels, there are multiple methods for assessing gametogenesis for both males and females: a common and easy technique consists of measuring the ratio between the soft body tissue and the shell, known as the Condition Index (Davenport and Chen, 1987). The combination of the meat yield variation with water temperature monitoring can indicate the various stages of maturation and possible spawning (BIM, 2019). Nevertheless, the sole use of this technique is unreliable as the weight of the soft tissue varies throughout the year (Pleissner *et al.*, 2012; Pérez *et al.*, 2013). Therefore, this assessment method must be combined with a more in-depth analysis of the maturation level. A more reliable technique is to carry out regular checks on the status of the gonad using gonad squash techniques on the broodstock (Chipperfield, 1953; Seed, 1969; King *et al.*, 1989) and consists of assessing the level of gametogenesis under a microscope. However, using this method, it is difficult to distinguish the pre and post-spawning stages. Histological slides of the gonads are a much more consistent method than gonad squash (Seed, 1969) but are much more time-consuming and costly.

1.2.2 Spawning

The spawning cycle in northern Europe is typically twice per year, once during the Spring and the second event during Autumn (Chipperfield, 1953; King *et al.*, 1989; Pulfrich, 1996). Interannual environmental variations in weather and oceanographic conditions, such as sea temperature and dominating wind directions, have been shown to directly affect this reproduction cycle, mainly impacting broodstock maturation and food availability, meaning that spawning patterns can differ from year to year (Seed, 1969; Beukema, 1992; Beukema and Dekker, 2005). Bivalves can also undergo small spawning releases throughout the Summer rather than two specific events, which is termed "trickle spawning", which can occur in specific years (Gosling, 2022). Over the course of three years, Seed (1969) observed rapid gametogenesis following partial spawning, which could partly explain this trickle spawning pattern observed during some years. In most cases, water temperature variations appear to be the main exogenous trigger for bivalve

spawning (Chipperfield, 1953; BIM, 2020). Once gametes have been released into the water, they will act as a spawning stimulus for nearby ripe individuals (Gosling, 2015).

1.2.3 Planktonic life

Following spawning, the released fertilised eggs (Fig. 1) rapidly develop to reach the first transformation stage after 24 hours and become swimming ciliated trochophore larvae. Following the second transformation, the larvae become veliger with a D-shaped shell and are now around 100 µm. The veliger stage can last a few weeks, and the larvae will grow to 250 µm. The appearance of a dark eyespot and a foot signals that metamorphosis is near and the pediveliger larvae are ready to settle (Bayne, 1965; Gosling, 2015). The literature indicates that mussel larvae present different growth rates, from 8 μm^{-1} day to 25 μm^{-1} day (Bayne, 1964; Sprung, 1984c; Pechenik *et al.*, 1990). Those experiments used different temperatures exposures and different food concentrations. However, Gosling (2015) study shows a strong relationship between larvae growth and sea temperature.

The larvae's swimming behaviour varies during the development stages. The early young larvae tend to be close to the surface (Sprung, 1984b), while the older larvae are closer to the seabed (Pulfrich, 1996). Despite their swimming abilities, larvae have limited movement abilities and their distribution in the water column is largely affected by ocean currents (Knights *et al.*, 2006).

Throughout their planktonic phase, mussel larvae are usually considered as passive particles in the water column; therefore, their transport is influenced by tidal and surface wind-driven currents (Mc Quaid and Phillips, 2000; Knights *et al.*, 2006). The larval dispersal range can exceed 100 km; however, combining dispersal model and genetic analysis, it has been shown that effective larval transport is usually around 30 to 50 km from a broodstock to a successful larvae settlement (Gilg and Hilbish, 2003a, 2003b). In sheltered locations such as semi-closed bays and estuaries, the distance travelled by the larvae can be even further reduced, allowing some level of self-recruitment in the already established mussel settlements (Robins *et al.*, 2013; Smaal *et al.*, 2017). The last larval stage, known as pediveliger, is usually reached around 28 days

(Widdows, 1991), but this period can be extended up to six weeks (Bayne, 1965). The metamorphosis stage or primary settlement can happen when the pediveliger larvae reach the size of approximately 260 µm (Bayne, 1965). If food and/ or suitable substrate is not available, the larvae can delay metamorphosis and remain in the water column for a more extended period until they are ready to settle, but this can have a negative effect on feeding behaviour (Bayne, 1965; Pulfrich, 1996).

Once larvae metamorphosis takes place, the plantigrade, or "spat", usually settles on fibrous substrate first (Pulfrich, 1996 and pers. obs.), such as seaweed, hydroids or bryozoans. Following this first settlement, if conditions are not optimal for the development of the post-settled larvae or if the original support becomes unsuitable for the size of the small mussels (i.e., decaying seaweed), the spat can relocate to a more suitable substrate such as the seabed (Bayne, 1964; Seed, 1969; Pulfrich, 1996). This second settlement is usually influenced by a chemical cue from conspecifics such as old mussel shells or other mussels (Pulfrich, 1996; Morello and Yund, 2016; Wilcox and Jeffs, 2017).

1.2.4 Settlement extent

On the seabed, the seed and adult mussels organised themselves in patches that can form large colonies known as beds. Depending on the density of mussels on the seafloor, several patterns can be observed across mussel beds(Commito *et al.*, 2014). Other factors such as the type of substrate, the bio-accumulation of pseudo-faeces and faeces on high-density beds (Liu *et al.*, 2012), as well as local ocean currents (Folkard and Gascoigne, 2009; wa Kangeri et al., 2016), have been observed to influence the distribution of mussels across a mussel bed (Commito *et al.*, 2014; Bertolini *et al.*, 2017).

Mussel self-organisation has been observed on both wild mussel beds and cultivated plots (Commito and Dankers, 2001; Bertolini *et al.*, 2019). There are four patterns commonly found which are related to the abundance of mussels on the seabed (from low to high): i) isolated clumps, ii) open labyrinth, iii) tight mesh and finally, iv) near homogeneous (Liu *et al.*, 2013).

Knowledge of these typical structures can facilitate the accurate mapping of seed mussel bed extent, which can be integrated into a fisheries management plan, aid conservation measures, and provide stock assessment information on cultured plots. The extent of intertidal beds can be visually assessed at low water (Commito and Dankers, 2001; Capelle *et al.*, 2014). The assessment of subtidal beds extent is more complex and involves the use of specialised equipment such as sonar (Sotheran *et al.*, 1997; van Overmeeren *et al.*, 2009), underwater cameras (Hughes and Atkinson, 1997) or multibeam echo sounder (Wilson *et al.*, 2021).

1.3. Limiting recruitment factors

Despite the relative abundance of the various *Mytilus* species worldwide, several endogenous and exogenous factors have been highlighted in the literature that affect the recruitment of juveniles (Beukema and Dekker, 2005).

1.3.1 Mortalities

Mortalities are a main limiting factor of seed mussel bed recruitment. Predation, environmental and climate conditions can cause it, or a combination of possible pathogens and stress factors (Lupo *et al.*, 2021).

- Predation:

Research has demonstrated that seed mussels show a low survivability rate on natural beds until they can reach a size big enough to protect them from certain predators, namely birds and crabs such as *Carcinus maenas* (Elner, 1978; Smaal *et al.*, 2017). However, the common starfish, *Asteria rubens*, will feed on any available mussel, regardless of size. Starfish swarming patterns have been observed on both naturally occurring settlements and cultivated plots, resulting in the total loss of the mussel population in a particular area (Sloan and Aldridge, 1981; Dare, 1982; Calderwood *et al.*, 2016). Predation by the dog whelk *Lucella lapillus* has also been sporadically observed on mussel beds (Petraitis, 1998).

- Environmental and climate conditions:

Post-settlement larvae mortalities are also very high (Widdows, 1991) due to a lack of shelter from strong ocean currents (Pulfrich, 1996). Larvae tend to settle in a dynamic environment (Hunt and Scheibling, 1996), but strong currents can dislodge the settled spat and transport them to unsuitable grounds (Fuentes-Santos and Labarta, 2015). Established seed mussel beds can also be affected by tidal currents, with erosion usually starting at the centre of the settlement where the mussel is less firmly attached than at the edges of the bed (wa Kangeri *et al.*, 2016). The accumulation of faeces and pseudo-faeces on dense mussel beds forms a layer of soft sediment(Liu *et al.*, 2012), which can be a facilitating factor for erosion, with the tidal current creating an undercutting action in the soft sediment (wa Kangeri *et al.*, 2016). Although dislodged mussels can reorganise themselves on the seabed, large quantities of mussels have been observed high up on the shore following storms, resulting in mortalities (pers. obs.). Climate impacts are also highly variable and can have a significant effect on the survivability of mussels. Thermal stresses, such as sea temperature higher than 20^{o}C in the case of *Mytilus edulis*, have been shown to increase the risk of mortality for pre and post-spawning mussels (Clements *et al.*, 2018) as well as larvae survivability, especially when combined with low salinity (20) or high salinity (40)(Brenko and Calabrese, 1969).

- Pathogens and stress factors:

Mass mortality events, or MMEs, can sometimes be attributed to pathogens. Recurrent MME episodes have been investigated on both suspended rope cultures and “bouchots”; examples include the 2014 and 2015 mortality events in the Pertuis Charentais in France (Travers *et al.*, 2016). Although those mortalities appear to be multifactorial, the presence of a known bivalve pathogen, the bacteria *Vibrio splendidus* (Beaz-Hidalgo *et al.*, 2010), was confirmed in the samples collected at the time (Pépin *et al.*, 2017). High genomic abnormalities were also observed in those mussels, potentially originating from a leukaemia-like disease known as hemic neoplasia, which may be exacerbated by land pollution, local hydrodynamics and hybrid mussels with possible low immune systems (Benabdelmouna and Ledu, 2016). In 2015, 2016 and 2019, the MMEs in the Oosterschelde in the Netherlands, which resulted in 100% mortality on wild mussel beds, did not

indicate any traces of pathogens but appeared to be associated with a possible harmful algal bloom and the overall weak nature of mussels following intense spawning (Capelle *et al.*, 2021b).

1.3.2 Species distribution

Mussels can colonise various substrates, but species will perform differently depending on their preferred environment. Beaumont *et al.* (2004) showed that the larvae of *Mytilus galloprovincialis* will develop better in warmer water than *Mytilus edulis,* and their hybrids will develop slower regardless of the temperature variation. Salinity can also play a role in the geographical distribution of those species. Density differences between low and high-salinity waters can act as a physical barrier to possible introgression between *M*. *edilus* and *M. galloprovincialis* (Kijewski *et al.*, 2019).

There are multiple examples of introgression within the *Mytilus complex* worldwide, either between *M.edulis* and *M. galloprovincialis*, *M.edulis* and *M.trossolus* and between *M. galloprovincialis* and *M. trossolus* (Edward and Sibinski, 1987; Kijewski *et al.*, 2011; Gurney-Smith *et al.*, 2017; Larsson *et al.*, 2017; Kartavtsev *et al.*, 2018), all resulting with the production of hybrid individuals. Levels of hybridisation can be variable depending on the local competition with the other *Mytilus* species, and the development capability of the hybrid larvae can sometimes be limited (Bierne *et al.*, 2002; Beaumont *et al.*, 2004).

In Ireland, the two species *Mytilus edulis* and *Mytilus galloprovincialis,* as well as their hybrid, have been observed around the coast (Fig.2). *M.edulis* is the most dominant, especially in the Irish Sea, where no hybrid or *M. galloprovincialis* has been found (Gosling and Wilkins, 1981; Coghlan and Gosling, 2007; Gosling *et al.*, 2008; Lynch *et al.*, 2014, 2020). According to the research carried out by Gosling *et al.* (2008), *M.galloprovincialis* and hybrids appear to favour the rocky and exposed coast of the south and west coast of the island. Currently, the main limiting factor in the distribution of *Mytilus galloprovincialis* in northern Europe is its limited tolerance to low temperatures and its partial reproduction success in colder waters (Lynch *et al.*, 2020). However, results from Species Distribution Models (SDMs) indicate that its expected distribution

may exceed its current northern limits and that both *Mytilus edulis* and *galloprovincialis* geographical distribution limits are likely to change during the remainder of the 21st century (Fly *et al.*, 2015).

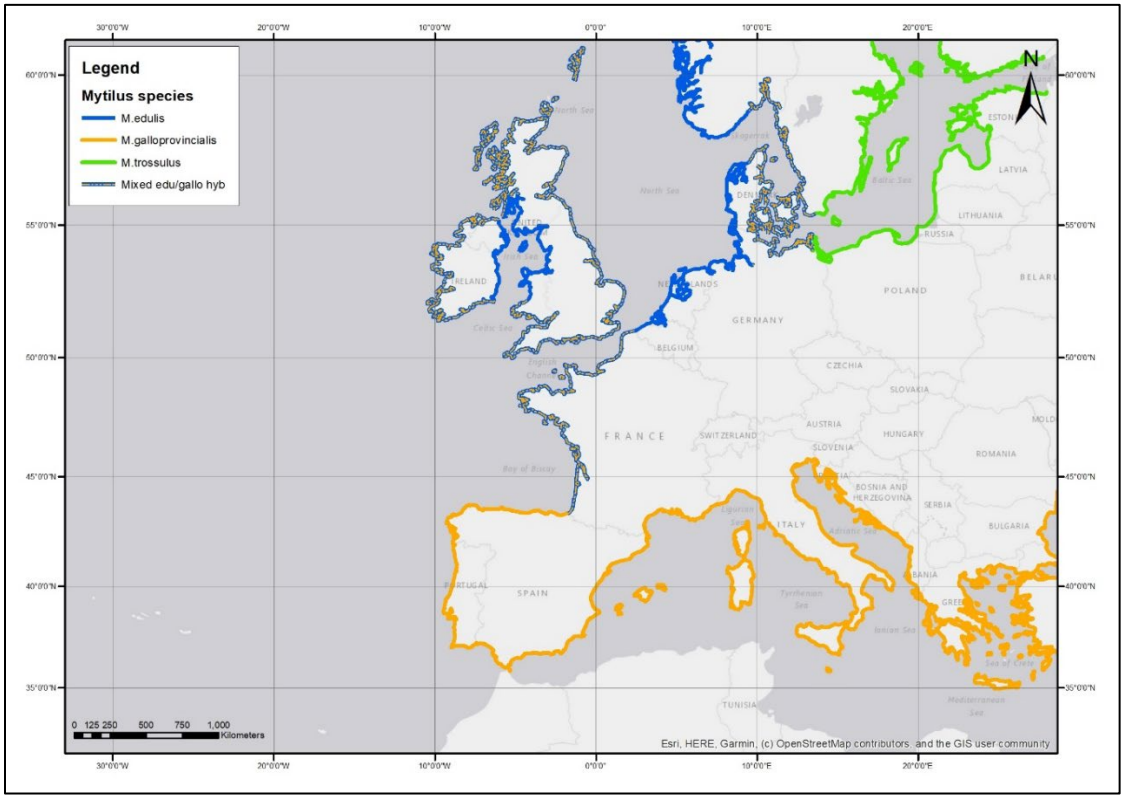

Fig. 2: Mytilus genus distribution in European waters (Hilbish et al., 2000)

1.3.3 Larval dispersal

As mentioned above, during their planktonic phase, mussel larvae distribution will mainly be driven by tidal and residual ocean currents (Gilg and Hilbish, 2003b, 2003a; Knights *et al.*, 2006). Determining those larval dispersal patterns can contribute to the understanding of mussel settlement formations.

The effects of wind-driven currents on surface waters (Verdier-Bonnet *et al.*, 1997; Mc Quaid and Phillips, 2000) can also affect the distribution of larvae, especially while located in the upper part of the water column during their first few weeks of planktonic life (Pulfrich, 1996). In general, bivalve larvae have limited swimming capabilities within the environment. However, they can move vertically in the water column once they pass the trochophore phase (between week one

to week two after fecundation), which could also contribute to the dispersion pattern (Garland *et al.*, 2002; Knights *et al.*, 2006; Morgan and Fisher, 2010). On the southeast coast of Ireland, tidal stages (flood, ebb and slack), as well as tide strength (spring and neap), appear to be the main factor of vertical distribution, with higher concentrations of larvae in the entire water column during flood tides as well as tidal flow-related larvae distribution stratification (Knights *et al.*, 2006).

Understanding larval dispersal patterns is essential to the overall mussel recruitment process. Hydrodynamic and particle tracking models (PTMs) can predict the possible outcomes of spawning events, such as the loss of larvae not settling on a suitable substrate (Robins *et al.*, 2013), the disruption of local currents gyres due to strong winds, the distribution of larvae following multiple spawning events within a short period and the effect of water temperature on the survival rate (Nicolle *et al.*, 2013). The effect of the wind and tidal currents can be combined or have independent effects mainly due to seabed topography, as shown by Nicolle *et al.* (2013) in their study of two bays on the north coast of France.

Adding larvae swimming behaviour (Blanton *et al.*, 1995; James *et al.*, 2019) to PTMs has shown that larvae will be dispersed at greater distances (Nicolle *et al.*, 2013). The addition of tidal or diel migration data to particles will give a more realistic outcome than passive dispersion (Robins *et al.*, 2013). Also, genetic studies carried out simultaneously can provide some model validation (Gilg and Hilbish, 2003b; Robins *et al.*, 2013; Azpeitia *et al.*, 2019).

1.3.4 Climate effects

Climate change directly affects marine ecosystems (Brierley and Kingsford, 2009; Hastings *et al.*, 2020), as observed in the variation of the distribution range of certain species (Pecl *et al.*, 2017). Since 1981, sea surface water temperatures across Europe have increased at a rate of 0.2^{0}C per decade (Minnett, 2014). A case study of Crassostrea gigas evidences an example of the consequence of those higher temperature*s*. King *et al.* (2021) observed that since 1995, the reproduction range of *C. gigas* has extended to the entire western shore of France. When

introduced in the 1970s, only sporadic events had been recorded north of La Rochelle; presently, areas like the Baie de Bourgneuf, just south of the Loire estuary, or the Rade de Brest in western Brittany, have turned into oyster spat collection zones (Dutertre *et al.*, 2010).

The effect of seasonal variations on mussel recruitment has been previously observed in the Wadden Sea, where it was shown that mussel recruitment rates were lower after milder winters, mainly due to higher predation (Beukema, 1992). It was further demonstrated that cold winters limit predators' propagation or delay their action on recently settled spat (Beukema and Dekker, 2014). Therefore, the increase in water temperature may have a positive effect on the predator population, thus limiting successful recruitment

In contrast, prolonged or unseasonal low temperatures can unbalance an entire ecosystem (deYoung *et al.*, 2008). An abrupt shift in the production cycle can be caused by external factors, such as fishing pressure, pollution and/or local tidal flow changes. Those changes, also known as regime shifts, can happen following a sudden perturbation or through a gradual accumulation of natural and anthropogenic factors; they are difficult to predict and can be difficult to reverse (Crépin *et al.*, 2012). Outcomes of these impacts can be variable and include limited stock recovery (Blöcker *et al.*, 2023), the increased resistance of the ecosystem to climatic stress following the change from a eutrophic system to an oligotrophic system (Derolez *et al.*, 2020), and a defined period of stable bivalve recruitment abundance followed by a period of low stable recruitment over (Powell *et al.*, 2008). For each scenario, management flexibility and adaptability are required through the period of the regime shift. These can be achieved by environmental monitoring to support decision-making and the establishment of mitigation measures for stakeholders, such as introducing diversification (Crépin *et al.*, 2012). An example of diversification would include developing farming of other species or the supply of juveniles from other locations.

1.3.5 Fishery management

Bottom mussel farming depends mainly on the supply and availability of juveniles from wild-seed mussel beds. The productivity return of relayed seed on the seabed is low in comparison with suspended cultures (Smaal, 2002). As a result, this resource must be closely managed to avoid overfishing and the resulting consequence of the possible decline of the entire industry (Baeta *et al.*, 2018). Management measures can include the introduction of fishing quotas/allocations based on the available biomass, fishing licences, fishery opening and closing dates and vessel monitoring during the fishing season (Maguire *et al.*, 2007; Le Gendre *et al.*, 2014a). In order to do this, the quantification and the mapping of the available biomass need to be established prior to the implementation of those measures.

The patterns formed by mussel aggregation can easily be observed on intertidal settlements using drones or satellite imagery (Crawford *et al.*, 2006). For subtidal beds, acoustic technologies facilitate mapping a large portion of the ocean floor (Brown *et al.*, 2011). Structures such as rock outcrops, sand ripples, sand bars, and biogenic reefs' acoustic signatures have been previously catalogued (Van Lancker *et al.*, 2007). Unlike burrowing invertebrates, the typical structures formed by mussel aggregations can easily be observed using acoustic devices such as side-scan sonar. Van Overmeeren *et al.* (2009) successfully used side-scan sonar technology on mudflats in the Netherlands to estimate mussel bed extent. Acoustic data on its own cannot quantify populations, so it must be complemented with ground truthing (Solan *et al.*, 2003; Diaz *et al.*, 2004). Automated classification of marine acoustic data still has some drawbacks with regard to accuracy (Cochrane and Lafferty, 2002; Diaz *et al.*, 2004; Brown *et al.*, 2005); therefore, a combination of an 'expert eye' for features identification and *in situ* samplings remain the best option to assess population in detail. On intertidal beds, it has been shown that mussels organised themselves in fractal patterns (Commito and Rusignuolo, 2000; Crawford *et al.*, 2006; Commito *et al.*, 2014), but the use of fractal analysis with acoustic data could be limited due to the level of detail from the generated acoustic images.

Fishery management must also incorporate a comprehensive understanding of the production cycle of local populations. By integrating various local oceanographic conditions, the available broodstock, the timing of spawning and settlement cycle, the larvae position in the water column and the type of preferred substrate, it is possible to accurately put in place dedicated settlement zones to optimise seed collection (Newell *et al.*, 1991). Unexploited seed mussel beds can produce larvae (Seed, 1969), which can then contribute to the self-recruitment of those beds or the creation of entirely new seed mussel settlements (Knights, 2012).

In Ireland, management measures have been implemented following a multi-agency project between 2000 and 2006. The outcome of the project was a set of recommendations for the industry and the management bodies, which included the setting of opening dates to avoid overlap with spawning and settling periods, the introduction of fishing prohibited areas, the increase of resource monitoring and the possible diversification of seed mussel source (Maguire *et al.*, 2007). Following this project, a full review of the bottom mussel farming industry was carried out across the entire island of Ireland, which resulted in the creation of a cross-border, inter-agency and industry consultation group: The Bottom Grown Mussel Consultative Forum. Its main task is to provide a management platform for the seed mussel fishery on an all-Ireland basis. It includes consultation with producers and other aquaculture and fisheries industry bodies. It also provides guidelines for the administration of the industry (i.e. tonnage allocations), environmental issues (i.e. invasive species) and business development (i.e. setting up MSC certification for the fishery) (BIM and Loughs Agency 2008).

1.4. Discussion

Several studies (Newell *et al.*, 1991; Le Gendre *et al.*, 2014a; Molinet *et al.*, 2017; Azpeitia *et al.*, 2019; Smaal *et al.*, 2021) have been carried out on mussel recruitment worldwide; this review focuses on seed mussel recruitment in a subtidal environment. A fundamental understanding of the life cycle of the mussels and the various issues that can affect each stage is essential to assess the limitations of the recruitment process.

The reproductive cycle of the local mussel population can be identified using knowledge of the availability, location and quality of the broodstock combined with the presence of suitable environmental conditions for maturation. The combination of weekly condition index (Davenport and Chen, 1987; Knights, 2012), water temperature measurement and gonad squash prove to be a valuable indicator of the broodstock readiness for spawning (Chipperfield, 1953; Seed, 1969; King *et al.*, 1989). Additional measurements of food availability could be important, although water temperature variation seems to be the main driver for spawning (Gosling, 2015). However, considering possible partial spawning followed by rapid reconditioning (Seed, 1969), it would be best practice to conduct maturation monitoring throughout the year to incorporate all possible spawning scenarios. Mussels can produce large quantities of larvae (Gosling, 2015), so quantifying the potential broodstock is probably less important than knowing its location. The location of the various matured mussels can be key to understanding larval dispersal within a given system (Gilg and Hilbish, 2003a).

Planktonic life is probably the most uncertain part of the early life cycle. The behaviour of the larvae within the water column will change depending on their age, particularly in the early stages when the trochophore larvae are situated close to the surface (Sprung, 1984b) and subjected to the wind-driven currents, tidal oscillations and residual circulation that will affect their dispersal. Once this early stage is over, the larvae appear to be able to migrate vertically - possibly synchronised by diel swimming patterns (Newell *et al.*, 1991; Knights *et al.*, 2006) - until they reach a suitable substrate around week 4-5 post-fecundation (Pulfrich, 1996). Accurately assessing the larvae's behaviour appears challenging, but realistic behaviour parameterised into PTMs can increase the accuracy of simulated larval dispersal and understanding of population connectivity (James *et al.*, 2019). Combining a comprehensive plankton monitoring program and local hydrodynamic study using GPS drifters and ADCPs can potentially give a greater insight into the behaviour of the larvae population at a given location (Morgan and Fisher, 2010; Haase *et al.*, 2012).

By their nature, intertidal mussel beds can be accessible at low water for sample collection or extent estimation. In the case of subtidal beds, like the ones in the Irish Sea, the depth of water, in most cases, 9 meters below the surface (BIM, n.d.), makes both those tasks rather challenging. However, a thorough seabed survey using acoustic technologies such as side-scan sonar (Sotheran *et al.*, 1997; van Overmeeren *et al.*, 2009), combined with extensive seabed sampling can help to find potentially suitable grounds such as bryozoans, hydroids and seaweed aggregation. More interestingly, growing seed mussel will start to self-organised on the seabed and form patterns (Liu *et al.*, 2013; Commito *et al.*, 2014), which can be clearly identifiable on the sonar imagery. Therefore, the generated acoustic image can potentially replace the visual assessment of the settlement. By running a comprehensive georeferenced sample collection on a defined mussel bed, it should be possible to assess the biomass accurately using interpolation tools from a Geographic Information System (GIS) software (Crawford *et al.*, 2006). This process could provide robust biomass figures for conservation objectives or fishery management.

Seed mussel recruitment limitation appears to be multifactorial, and understanding local recruitment cycles and dynamics related to spawning patterns, larvae dispersal, and settlement formation is paramount to managing this resource. However, water temperature appears to have a role in every step of the process, starting with the maturation of the broodstock (Chipperfield, 1953), then the development of the larvae (Brenko and Calabrese, 1969), and finally, the development of the seed mussel beds to some extent (Beukema *et al.*, 2015). It could be expected that seasonal sea temperature variations during the larvae phase would partially explain the recruitment abundance fluctuation from year to year.

To address the challenge of accurately assessing subtidal seed mussel beds, this thesis is proposing a new approach to estimate sub-tidal mussel settlement using side scan sonar technology combined with extensive sampling and GIS. Those results will also be verified by carrying out post-fishery surveys on those previously estimated commercial beds. It will also try to provide some answers on the reason behind the seed mussel bed recruitment variations observed from 2009 to 2022 along the southeast coast of Ireland by analysing the impact of sea

temperature variations during the larval phase on the seed mussel recruitment size on subtidal beds along the southeast coast of Ireland.

Chapter 2:
New approaches to mapping and quantifying the Biomass of Subtidal Seed Mussel Beds

2.1. Introduction

Around the globe, mussels are farmed for their high economic value as sustainably produced seafood and environmental importance (Smaal *et al.*, 2018; van der Schatte Olivier *et al.*, 2018). Ecologically, they are recognised for providing a range of ecosystem services such as bioengineers natural filters, and they also play a role in increasing biodiversity in their ecosystem by providing a source of food to protected species and structures for the development of epifauna (Smaal *et al.*, 2018). The earliest signs of consumption on the European continent date back 80,000 years (Zilhão *et al.*, 2020). In the European Union (EU), mussels for human consumption are mainly supplied by aquaculture, with 480,000 tonnes harvested in 2016, valued at around €450 million (Avdelas *et al.*, 2021). Mussels (*Mytilus sp.*) are produced on suspended ropes, bouchot poles and/or directly on the seabed (Smaal, 1991). In the Republic of Ireland, rope-grown mussels are primarily produced on the west coast, while bottom (seabed) mussels are produced in four locations around the coast: Lough Foyle, Carlingford Lough, Wexford Harbour and Castlemaine Harbour (Fig.3). The Irish bottom mussel industry produced 5,835 tonnes in 2021, with a sale value of €9.14 million (BIM, 2022). This industry solely relies on wild subtidal seed mussel beds (BIM and Loughs Agency, 2008), which require yearly reliable biomass assessment prior to the opening of the fishery (BIM and Loughs Agency, 2008; DAFM, 2018).

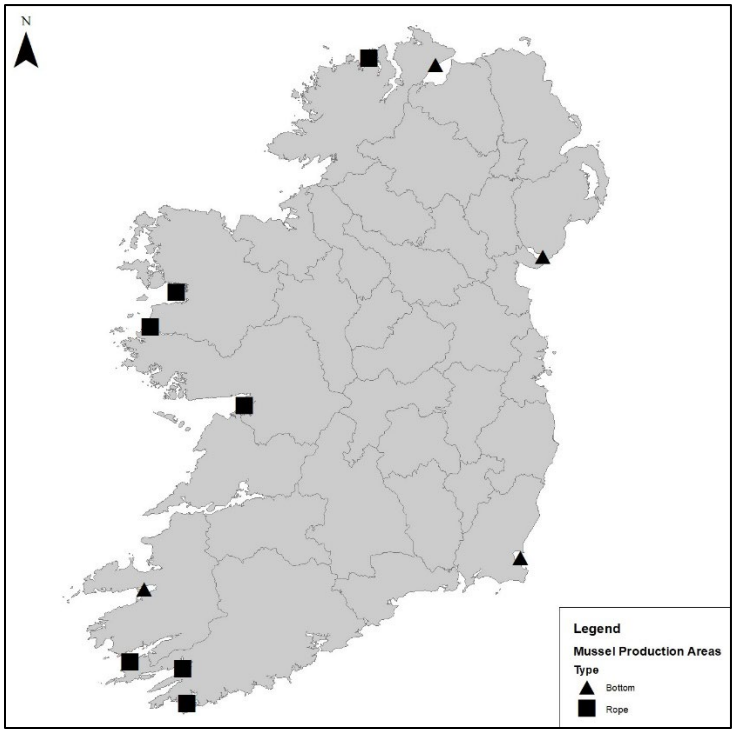

Fig. 3: Mussel production areas in the Republic of Ireland per farming type

Along the Irish coast, subtidal seed mussel beds are formed mainly in June, although there can also be a settlement in November, following the spawning of mature mussels from both farmed and wild stocks (Gosling *et al.*, 2008). The planktonic mussel larvae resulting from fecundation stay in the water column for four to five weeks, undergoing multiple transformations (Bayne, 1965; Seed, 1969) until settling on a suitable substrate such as hydroids, seaweed, gravel and conspecifics (Pulfrich, 1996; Morello and Yund, 2016; Wilcox and Jeffs, 2019). The planktonic larvae are subjected to tidal and residual ocean currents, which largely influence their spatial distribution and, hence, their settlement location (Gilg and Hilbish, 2003a). Once settled, the mussels spat then aggregate themselves, forming low-level structures that can spread over hundreds of hectares (Commito *et al.*, 2014; Liu *et al.*, 2014). Mussel spat that settles in June usually reaches 25 mm in length by the end of August (from the author's observations since 2008), allowing them to be transplanted in growing areas. The seed is fished using dredges and relayed on the same day on aquaculture licenses granted by the Department of Agriculture, Food and the Marine (DAFM). This subtidal seed mussel fishery in Ireland is not bound by minimal catching size, unlike harvesting fisheries like scallops (Marine Institute and BIM, 2020), cockles (Hervas *et al.*,

2008), or ready-for-market mussels (Cochard and Paul, 2016). The opening of the bottom mussel fishery in the Republic of Ireland is triggered by reaching the minimum threshold of 1,500 tonnes across any bed found.

There has been a range of publications that describe in-situ sampling and acoustic or visual data acquisition for mapping and estimating mussel population biomass (for example, Newell *et al.*, 1991; van Overmeeren *et al.*, 2009; Commito *et al.*, 2014; Cochard and Paul, 2016; Smaal *et al.*, 2017). From a commercial perspective, reliable surveys are essential to ensure sustainable fishing management measures are implemented. They also provide valuable biological data on the evolution of seed mussel beds, such as mussel growth, population size distribution within the settlement, and spatial organisation of the mussels on the seabed, as well as potential remaining biomass following fishing activities (BIM, n.d.; BIM and Loughs Agency, 2008).

Because of the depth of water in particular, assessing subtidal mussel beds can be challenging. Indeed, in the intertidal zone, aerial photography and land-based surveys can be carried out to map mussel beds (Commito and Rusignuolo, 2000). When settlements are subtidal and the water is relatively clear, video camera technology can be deployed to assess the spread of a population over time and can offer some indication of biomass density (Hughes and Atkinson, 1997). On mussel beds designated for commercial fishing, more intrusive methods using dredges and grabs can be used to collect physical samples (BIM, n.d.; Cochard and Paul, 2016). The main advantage of collecting physical samples is that it allows further analysis of the mussel's conditions, such as biometrics measurements, condition index and surface density. Due to the structural characteristics of high surface density mussel beds (Liu *et al.*, 2014), visual biomass estimations using video cameras may not represent population layers, and water turbidity can reduce the deployment of this type of equipment. In addition, because of the fractal distribution of mussel beds on the seafloor, surface densities can vary within one settlement (Crawford *et al.*, 2006; Bertolini *et al.*, 2017), thus requiring a substantial sample collection to provide an accurate picture of the distribution on the seabed. Mapping bivalve settlements living in the subtidal zone can be addressed by using acoustic equipment such as side scan sonar or backscatter data from

multibeam echo sounders (MBES) combined with quantitative samples collected with various sampling equipment such as quadrats, dredges, grabs and underwater videos (van Overmeeren et al. 2009; Sotheran et al. 1997). Those samples can then be interpolated using a multitude of statistical methods, such as Inverted Distance Weight (IDW), Kriging, and Random forest, to estimate the available biomass (Hervas *et al.*, 2008; Tully and Clarke, 2012; Marine Institute and BIM, 2020). Geographical Information System (GIS) software offers tools to carry out those various interpolations as well as providing a valuable platform to combine and visualise generated acoustic imagery and data from biological samples (Sotheran *et al.*, 1997; Diesing *et al.*, 2014; Dereli and Tercan, 2020). However, adverse sea conditions (above Force 4 on the Beaufort scale) and strong tidal currents (above 1.5 m/s) can greatly reduce data collection times in inshore waters (pers. obs.).

Historically, the seed mussel beds on the southeast coast of Ireland have been located in waters deeper than 10 m, in areas subjected to high turbidity levels due to the proximity of sandbanks and dynamic coastal waters (Bowers *et al.*, 2002). Through the years, those beds also presented highly variable seed mussel densities within each bed and between individual settlements (pers. obs.).

Due to the nature of the seabed (mainly gravel and shells) on the east coast of Ireland (Guinan *et al.*, 2020), it can be difficult to isolate seed mussel beds solely based on pixel values from backscatter data (Brown *et al.*, 2011). However, seed mussels' spatial organisation on substrate produces typical structures (Commito and Rusignuolo, 2000; Liu *et al.*, 2014). Such structures generated identifiable textures on the side scan sonar data, which can be marked for ground truthing. Further, side scan sonar can offer a large data collection swath compared to single beam echo sounders (Strong and Service, 2011).

A way of verifying the accuracy of the biomass estimation is to monitor fishing activities within previously designated beds by way of reports of fished tonnage by individual vessels, which is usually mandatory through all fisheries worldwide. In Ireland, as part of the fisheries regulation

in the Sea-fisheries and Maritime Jurisdiction Act of 2006 and amendments (Ireland, 2006), any vessel collecting wild subtidal seed mussels must report their daily estimated catch to the relevant authority. The compiled data indicates the tonnage of seed transplanted to growing grounds, which can be compared with the estimated figures for quality control. It is expected that, although dredgers take most of the biomass, some of it remains. Literature also indicates that the potential surviving biomass that remains through winter could provide an already established structure for newer stock to settle in the spring (Pineda *et al.*, 2010; Bertolini *et al.*, 2017).

Historical surveys have been carried out by Bord Iascaigh Mhara (BIM) since 1970 on the east coast of Ireland and have shown that seed mussels tend to settle in relatively similar locations from year to year (BIM and Loughs Agency, 2008; DAFM, 2018). The start of each survey season focuses primarily on those historical seed mussel beds. However, once those areas have been fully covered and show no sign of settlement, the survey is extended to grounds historically less reliable for seed mussel beds.

The aims of this study are: (1) to demonstrate that side scan sonar can provide an accurate tool to map subtidal seed mussel beds on circalittoral coarse sediment and fine sand grounds; (2) to show that Inverted Distance Weight (IDW) interpolation of targeted grab samples is a reliable method for seed mussel beds biomass estimation; and (3) to evaluate whether the combination of fishing data and post fishery biomass survey can validate the original estimation.

2.2. Methods

A survey protocol was designed in three stages and undertaken during the mussel survey season from June to October 2020: first, a preliminary stage aimed to mark potential settlement, then a biomass stage aimed to estimate the available seed mussel population prior to transplant, and finally a post fishery stage aimed to quantify the possible remaining biomass using the same methodology. The 2020 survey area had a footprint of 4,892 hectares, concentrated in the area between Wicklow Head (north) and Greenore Point, Co. Wexford (south), matching partially the historical distribution of seed mussel settlement on the east coast of Ireland (BIM and Loughs

Agency, 2008). However, no seed mussel beds were found north of Cahore Point, Co. Wexford. Therefore, the experiment focused along the east coast of County Wexford (Fig.4).

The amount of sea time available in 2020 was reduced due to the COVID-19 pandemic. Subsequently, updated acoustic data was not collected before the biomass estimation surveys. It was assumed that the period between the preliminary and the biomass estimation survey stages (1 month) would have little impact on the overall mussel spread on the seabed.

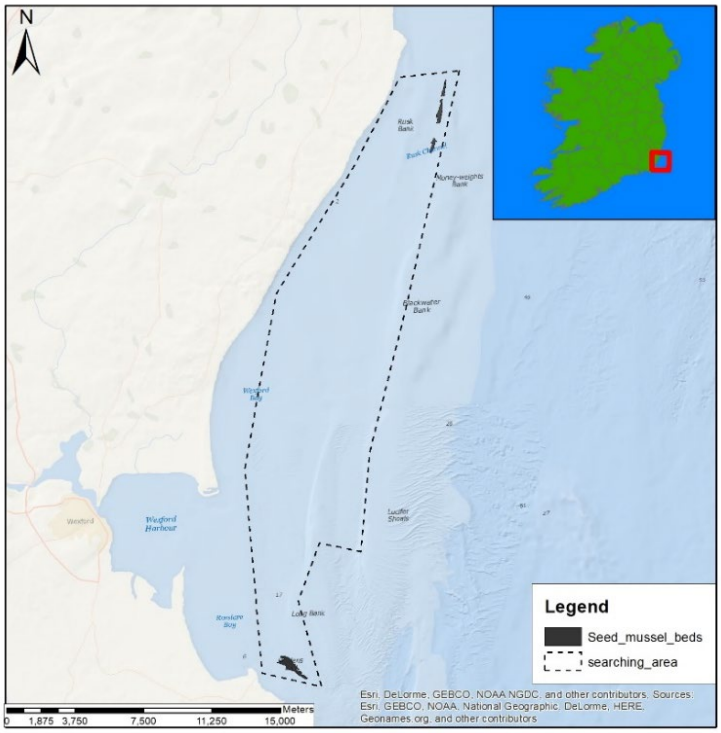

Fig. 4: 2020 subtidal seed mussel beds survey area along the east coast of County Wexford

Mussel samples were collected using a dredge and a grab during the three survey stages for biometric data analysis (see 2.2 Biological Data). The preliminary surveys took place between the 7th of July and the 7th of August 2020. The biomass surveys were carried out on the 18th of August for the Rusk Channel settlement and the 26th of August 2020 for the Rosslare bed. The 2020 seed mussel fishery campaign was opened on the 9th of September 2020 on the east coast of Ireland. Post-fishery surveys took place in October 2020: the 7th and 8th for the Rusk Channel and the 15th for Rosslare.

2.2.1 Acoustic Data

Geophysical and oceanographic background

The survey area is located on the southeast coast of Ireland. The bathymetry in the area where the beds were located is comprised between - 10 and -20 m (Fig.5). The topography presents multiple sand banks established in a north-south direction, which creates channels as narrow as 1,500 m wide for the Rusk Channel. The seabed presents large areas of sand ripples, mainly on the shoulders of the sand banks (Fig.5). The seed mussel beds are mainly located on circalittoral coarse sediment (EUNIS class A5.14) and fine sand or muddy sand (EUNIS class A5.25 or A5.26) (Guinan *et al.*, 2020).

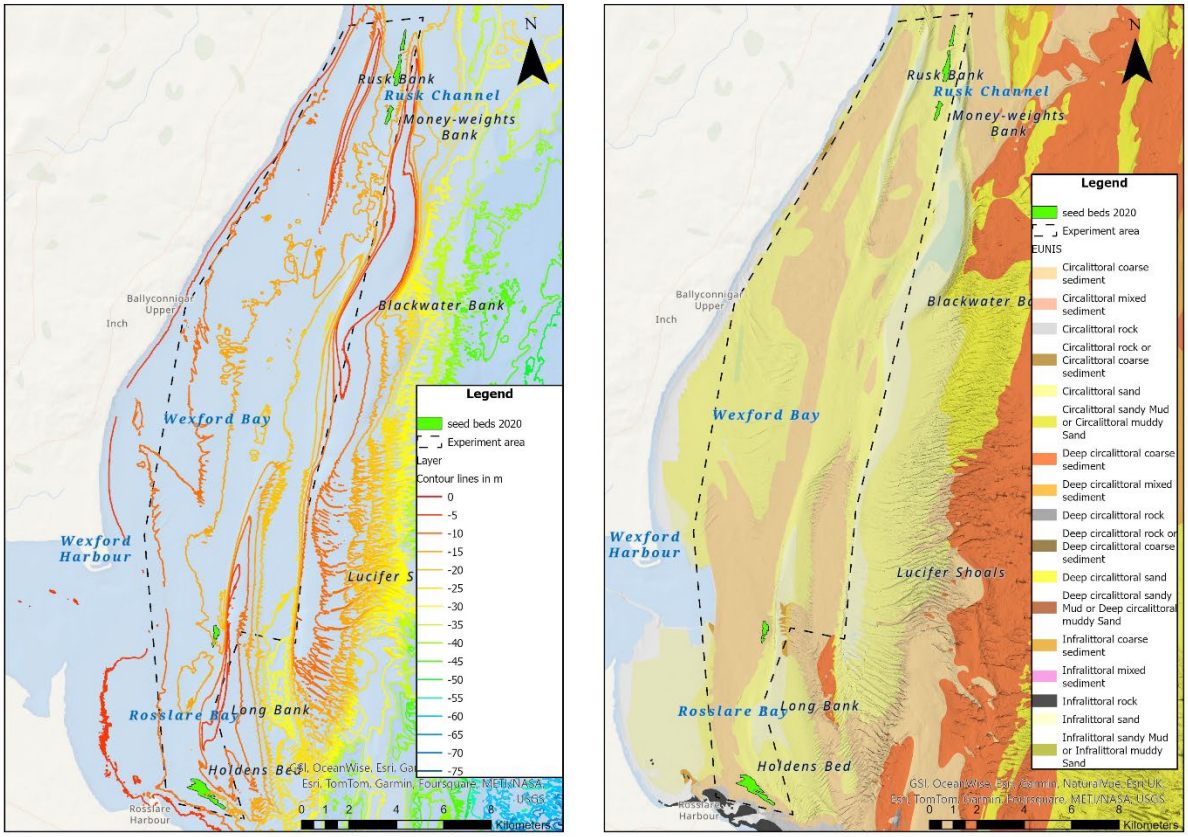

Fig. 5: Bathymetry, geomorphology and seabed classification maps of the experiment area

The western shore of the Irish Sea presents much less tidal range than the eastern shore and also less current velocity; however, tidal currents around Rosslare can reach up to 1.5 m s^{-1} (Robins *et al.*, 2013). Previous works in the area indicated that the dominating current is in a north-to-south direction (BIM, 2019).

Acquisition

The data at each location was collected using the 4125 Edgetech® Digital Dual Frequency side scan sonar system working simultaneously in 400kHz and 900kHz. The system comprises a tow fish, a 100 m towing cable, a topside processing unit that connects the cable, and a laptop that displays and records the data. The laptop is also connected to a GPS on board the survey vessel so the data can be exported for geoprocessing. The tow fish is deployed using 9 mm Dyneema® rope from a drum winch on deck for safety and ease of operation.

Although high frequency (900kHz) offers greater feature details, its reliable swath range for the surveys was too limited (50 m on each side of the tow fish). Therefore, all the data was collected in 400 kHz with an effective swath of 2 ×100 m. A weight was added to the tow rope 5 m ahead of the tow fish to maximise this swath and reduce the nadir. From experience, the tow fish altitude is key for data quality; exceeding 8 m from the seabed decreases swath efficiency (nadir increase) and exposes the tow fish to turbulence from tidal currents and survey vessel propellors wash. To maintain this optimal altitude, towing speed and cable length must be set before data recording. For these surveys, the towing speed was set between 3 and 6 knots, and the cable length was around three times the depth of the concerned area. Due to the length of the cable deployed, a layback was applied to the data so that the position of the tow fish could be deducted from the vessel position. The layback was calculated using the distance and the offset of the GPS antenna to the towing point (the towing block on the gantry), the height of the towing point to the surface of the water, the depth of the tow fish (from tow fish pressure sensor) and the length of cable deployed from the towing point (Fig.6).

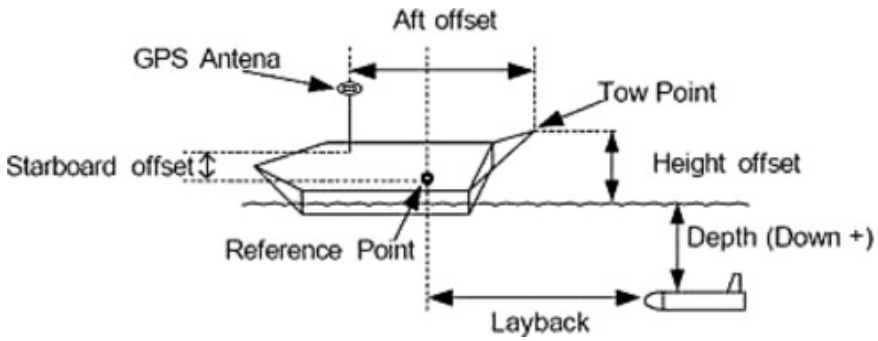

Fig. 6: Detail of layback calculation

To collect optimum acoustic data, the weather conditions, such as the speed and direction of the wind and the tidal currents, as well as the wave height and frequency, are crucial. The wind speed cannot exceed Force 4 on the Beaufort scale (between 5.5 and 8 ms^{-1}) (from the author's experience and observations). The effect for wind, even below Force 4, against opposite-direction tidal currents (i.e. a southerly wind against an ebbing tide going south) increases the waves' steepness while reducing their wavelength, resulting in rougher sea conditions (Unna, 1942; Lapworth, 2011). Such conditions increase the pitch and roll of the tow fish underwater, adding to a tugging motion of the vessel on the towing cable that will interfere with the acoustic data.

Controls were set up once the tow fish was deployed using the native Edgetech® software Discover. Suitable layback was applied for video gain (28 to 34 dB) and Time Variable Gain or TVG (32 to 36 dB). The bottom track was set on the clearest sonar channel to process the data. Over the past ten years, a catalogue of acoustic features has been produced internally in BIM on a similar base to the MESH project (Van Lancker *et al.*, 2007) to help with data acquisition. Acoustic feature identification was facilitated by an *ad-hoc* catalogue established by the author, consisting of ground truthing features collected over ten years of survey (BIM, 2016) and supported by techniques by Van Lancker *et al.* (2007). Relevant features were marked using Edgetech Target logger software. To ensure full coverage of the surveyed areas, the Coverage Map software was used alongside Discover (Plets and Dix, 2013). This software displays the track of the tow fish as well as the swath range of each transducer. The distance between each survey line allowed for a maximum of 10% overlap between swaths. For ease of processing, the recording was switched off at the end of each line and restarted once the turning manoeuvre was finished and the tow

fish was realigned with the survey vessel. The data was recorded using the Edgetech native format (*.JSF*).

Data processing

The data collected from the Rusk Channel and Rosslare search areas were processed immediately on board the survey vessel using Chesapeake Technology SonarWiz 6 software. The software has built-in importing preferences for each file format to return the best resolution. For the JSF files, the following was applied: Auto JSF scalar, extra TVG set at 40 dB/100m and ADC gain. For each file, the bottom track was redefined to remove most of the nadir so that both starboard and port side data join as seamlessly as possible, although due to seabed topography, some survey lines were not as clear as others. Empirical Gain Normalisation (EGN) was applied to the first survey line using all the data for each area. This process removes acoustic interferences, increases texture details, and smooths the residual nadir. Once the data on the first survey line appeared satisfactory, the EGN was applied to all the other lines within each surveyed area. The mosaic created was then exported in GeoTIFF format (georeferenced image) using 0.2 m per pixel resolution. The drawback of such a high resolution is that the image created is relatively large. However, the level of detail and textures are preserved. The created images were imported in ArcGIS 10.6.1 following the process designed by the author (detailed online: https://youtu.be/G3vETJpjA2Y).

Side scan sonar has been successfully used with ground truthing equipment to assess the mussel population (van Overmeeren *et al.*, 2009). As mentioned, seed mussel beds can have a similar backscatter pixel value as the seabed when composed of gravel and shells, making automated feature extraction through image analysis unreliable (Cochrane and Lafferty, 2002; Crawford *et al.*, 2006). The structures built from the accumulation of mussels generate distinctive textures (Fig.7) similar to other characteristic seabed features, such as rock outcrops and sand waves, that are easily identifiable on MBES data (Van Lancker *et al.*, 2007). Using ArcGIS, possible borders were manually traced, following the seed mussel accumulation texture (Brown *et al.* 2011;

Diesing *et al.* 2020). The targets marked during the side scan sonar survey were imported on the same map and transferred to the vessel plotter for the ground truthing survey.

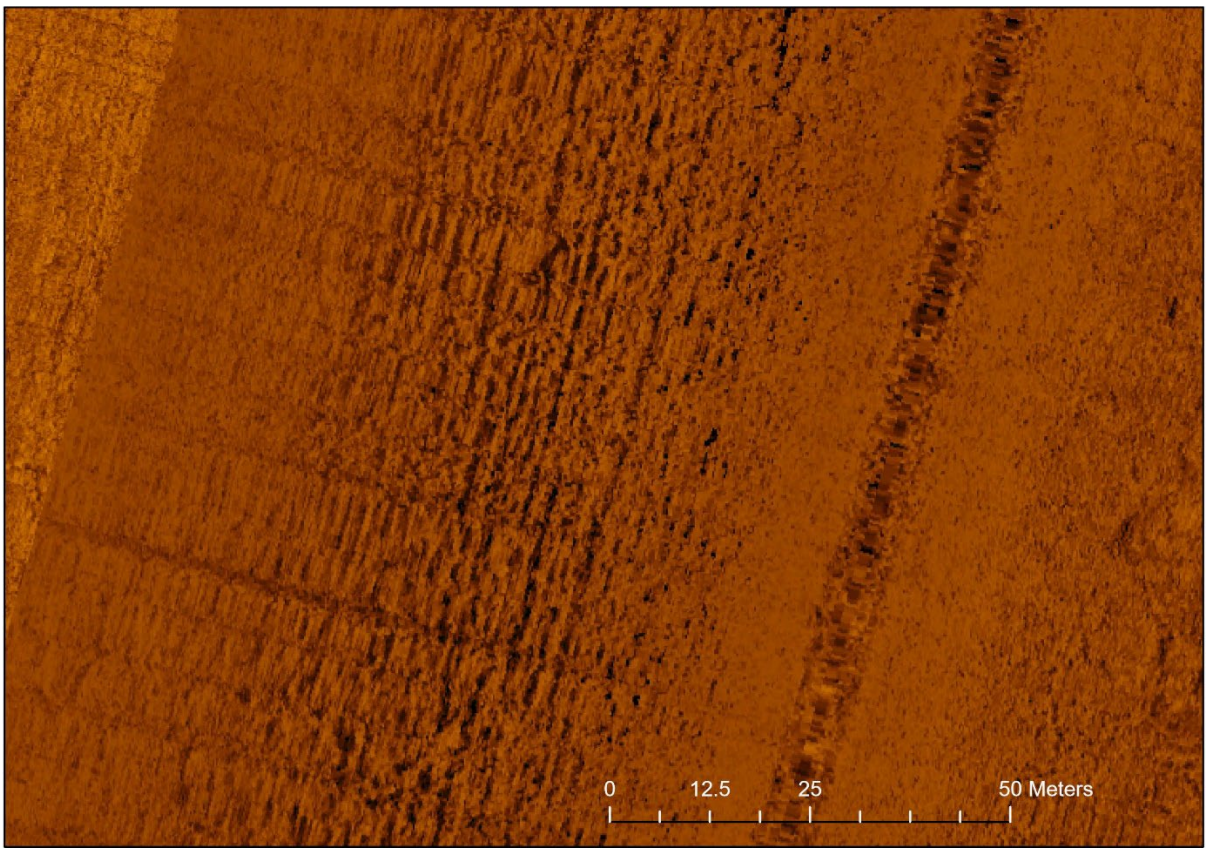

Fig. 7: Mussel pattern texture detail on side scan sonar data

2.2.2 Biological data

Two sampling techniques were used on the Rosslare and the Rusk Channel study sites to assess the extent of the mussel biomass and the mussel size range in the targeted mussel settlement areas. The techniques also indicated other species present.

Dredging

Multiple dredge tows were carried out at each location based on previously established acoustic targets to confirm the presence/absence of seed mussel. The main advantage of dredging is that it can be carried out in most weather and tide conditions, unlike the grab that requires calm seas and light tidal currents. The dredge comprises a 36 mm stainless steel chain belly and a top diamond mesh of 70 mm inner mesh measurement, and its dimensions are 1 × 1 m. To ensure

reliable contact with the seabed, a 5 m 19 mm link chain is set up between the dredge and the towing rope. Depending on the depth, weather, and tidal conditions, 3 to 3.5 times the water depth was used as the deployed length of towing rope (9mm Dyneema®). Upon contact with the seabed, GPS position and water depth were recorded. The average towing speed was between 1.5 to 3 knots for a towing distance of 50 to 120 m. A comprehensive suite of details was also recorded for each tow, such as position in WGS 84 of the start and end of the tow, the average depth, the tide speed and direction, the towing speed, the date and start time, the weather conditions, and a succinct description of the content of the dredge.

Following the qualitative visual assessment of the dredge content, by tipping the content of the dredge in a box on the deck of the survey vessel, each tow was classified as following: seed (mussel for at least a 1/3 of volume of the dredge), signs of seed (less than a 1/3 of the volume of the dredge or quantity of individuals <10 mm), shells and stones and finally other species (including, bryozoans, hydroids, echinoderms). All the data was transferred on ArcGIS, keeping all the details in the file attribute table. Sub-samples were collected at random throughout the dredge for biometric analysis.

Grab sampling

A Day grab with a 0.1 m^2 footprint was used at both locations. From personal experience, tidal currents over 0.8 m/s can cause the contact of the grab with the seabed to be unreliable, and the excessive motion of the vessel in such strong currents can render its deployment unsafe for the crew. Coastal sea level variability can differ markedly from tide table predictions, especially as the tide propagates away from the location/timing of the tidal prediction, but also due to residual atmospheric processes (e.g. storm surges and waves) and interactions of coastal waters with the seabed and undulating coastal topography and bathymetry (e.g. islands, sand banks, rocky reefs) (Hibbert *et al.*, 2015). These variations make predicting the available sampling window challenging, ranging from a few minutes to several hours. Although grabs represent only a small footprint on the overall extent of the settlements, they give valuable data on the layer organisation of the mussel bed and an indication of the nature of the substrate.

Random sampling points were generated within the border of each settlement area on ArcGIS using the XTools 18.1 extension. For Rosslare and Rusk Channel beds, the generating point factor was set at a minimum of 40 points with a minimum distance of 20 m between each point. All samples were collected within a 20 m radius of the generated sampling points. On deployment of the grab, its position was recorded, as well as the depth, weather condition, date and time, tide speed and direction. Each sample was cleaned on a 1000 µm sieve to remove fine sediment, and a brief description of the content was also recorded. Samples of each grab were processed on location using an electronic scale (10 grams precision), recording the total weight of the sieved sample, the net weight of the mussel and the weight of other materials, including other species, all considered waste. A percentage of waste was then calculated. Following those results, the grabs were then classified into four categories, for mapping purposes, similar to the dredge content classification detailed above: seed (with net sample weight superior to 250 g of mussel), signs of mussels (with net sample weight inferior to 250 g of mussel or the presence of mussel spat on stones), stone shells (from grabs containing sand, gravel, stones or shells and no mussels) and other species (from grabs content dominated by non-mussel species such as starfish, clams or seaweed). Unsuccessful grabs (i.e., jaws remaining open or jammed by stones) were retaken until successful or representative of the expected nature of the seabed. Samples from a single grab or sample pool were then set aside for biometrics analysis (see 2.2.3-Biometrics processing). Th recorded mussel weights for each grab sample were used to generate the biomass estimation for both mussel beds.

For the biomass estimation survey, 44 sampling points were randomly generated within the established boundaries of the mussel bed in Rosslare. Because of their proximity to the bed's border and the weather conditions during the sampling, two grabs were collected outside the settlement. The other 42 were taken within the seedbed, and their corrected position was recorded.

Due to its smaller size compared to the Rosslare settlement, 32 random grab sampling stations were generated for the Rusk channel. Four extra stations were added to the auto-generated ones,

giving 36 over the three sub-beds. Again, five samples were taken outside the estimated bed because some stations were too close to the settlement border; however, none of those presented seed mussels. Four other samples, taken within the estimated bed, also showed no mussel.

For the post-fishery survey, 31 sampling points were generated for the Rosslare bed, with all samples collected over two slack tides on the same day. For the Rusk Channel bed, 35 samples were collected over two days due to limiting tide conditions (slack water time in the day).

Biometrics processing

Three subsamples of 100 individuals were set aside for measurements for each location. Shell length (anterior to posterior) was recorded with an electronic calliper. Summary statistics in Excel were generated for each subsample, and a size range distribution per bed was calculated by pooling the three subsamples' measurements for each location using Excel histogram analysis.

Biomass estimation

Using the grab data, the biomass of seed mussel per location was estimated using the Inverted Distance Weight (IDW) algorithm on ArcGIS 10.6.1 (ESRI, n.d.). A similar method was previously used successfully for cockle population estimation (Hervas *et al.*, 2008). IDW interpolation uses selected neighbouring points to estimate the potential biomass distribution. This research used the six closest points to each sampling point during the pre-fishery survey and the three closest points during the post-fishery survey. The main reason for the variation between pre- and post-fishing was the density distribution of the grabs during both surveys. A preliminary IDW raster was created and reclassified for each survey according to the sample mussel weight range. Every reclassified raster was then transformed into multipart polygons related to each class range, and areas were calculated using in-built ArcGIS tools. The mean mussel weight per grab (or 0.1 m^2) for each class was extracted using the summary tool in the shapefile attribute table and used to estimate the biomass for each classified polygon. The total biomass per area was calculated by adding each class, and all results were converted into industry-relatable units: area in hectares

and biomass in metric tonnes. To assess biomass variation pre- and post-fishing, IDW reclassified raster for each survey was compared also using the ArcGIS raster calculator tool. Pre-fishing, post-fishing and biomass variation maps were created for both surveyed locations.

2.3 Results

2.3.1 Preliminary surveys

Preliminary surveys consisting of acoustic data and biometric sample collection were carried out during the last two weeks of July 2020 on historical seed mussel bed locations on the southeast coast of Ireland.

Acoustic Data

Typical seed mussel patterns were observed at three locations within the surveyed areas. The first potential settlement covered 52.85 hectares and was located in the channel east of Rosslare (Fig.8a). A second area, in the Rusk Channel, was divided into three distinctive sub-settlements or sub-beds representing a total of 41.52 hectares (Fig.8b).

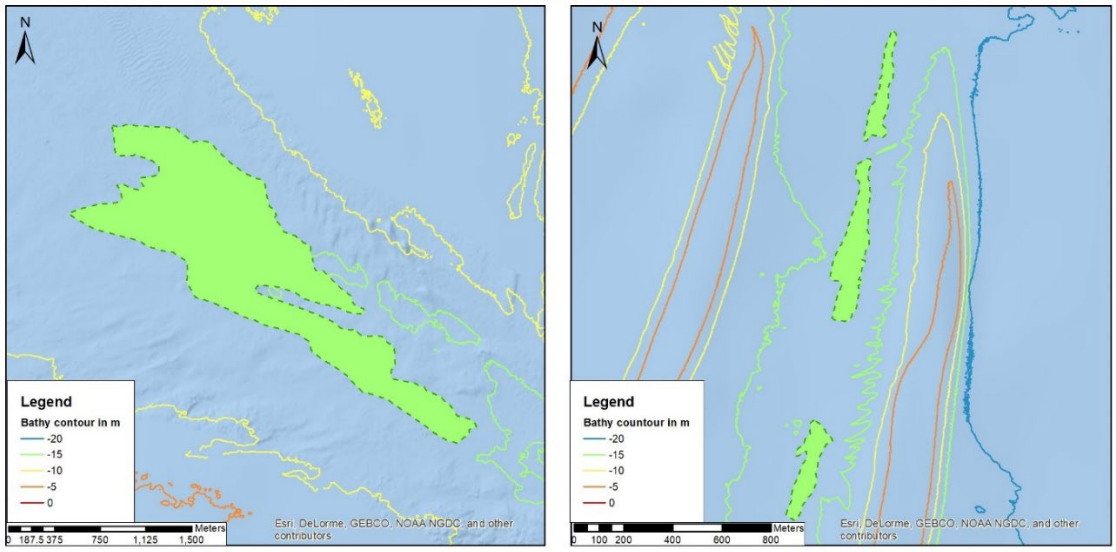

Fig. 8: Estimated seed mussel beds generated from acoustic data: a) Rosslare and b) Rusk Channel

The smaller bed outside Wexford Harbour was found to have been fully depleted by starfish predation shortly after the original survey; therefore, it has not been integrated further. Based on the established acoustic feature catalogue, 21 marks (9 for the Rosslare bed and 12 for the

Rusk Channel) displaying relevant seed mussel pattern texture were recorded between the two potential seed mussel beds.

Biological data

Both sampling surveys confirmed the extent of the two possible mussel beds generated from the side scan sonar data, with both settlements displaying distinctive geometry. The Rosslare settlement stretched over 1,911 m at its longest and 547 m at its widest, while the Rusk Channel beds stretched over 4,069 m long and 275 m wide. These two different geometries can be partially explained by the effect of local tidal currents (wa Kangeri *et al.*, 2016) at each location, likely due to their distinctive underwater topography: a broad channel contained between low-level sandbanks for Rosslare and a narrow and steep channel for the Rusk bed (shown as depth contours in Fig.8). However, the southern end of the Rosslare bed appears also to be affected by the narrowing of the channel.

Rosslare: All geopositioned marks were checked by towing the dredge through each mark as per their location on the vessel plotter, and a visual assessment of their content was recorded (as detailed in *2.2.1-Dredging)*. The average towing length from contact with the seabed to lift off was 62±14 m, and the depth ranged from 13 m to 14 m. Eight of the nine investigated acoustic targets contained an average of 60 kg of mussel, confirming that the features observed on the side scan sonar data were indeed mussel beds. The two dredge samples collected from the last investigated targets did not show any mussels. The tows conducted in Rosslare were mainly composed of small stones, common starfish *Asteria rubens* and spider crabs *Maja brachydactyla*, this bycatch representing less than 10% of the total weight content of the dredge. The average size of the mussels was 31.62 mm (minimum: 6.61 mm, maximum: 51.69 mm); however, the size frequency (Fig.9) shows a distinctive bimodal distribution of the population classes (Dankers *et al.*, 2001; Johansson *et al.*, 2024) that could correspond to two different settlement times (King *et al.*, 1989) or growth rate differences (Huston and Deangelis, 1987). The larger class size comprised 34 and 46 mm, representing over 61% of the sampled mussels. The smaller class was comprised between 12 and 20 mm, representing 22% of the sampled mussels.

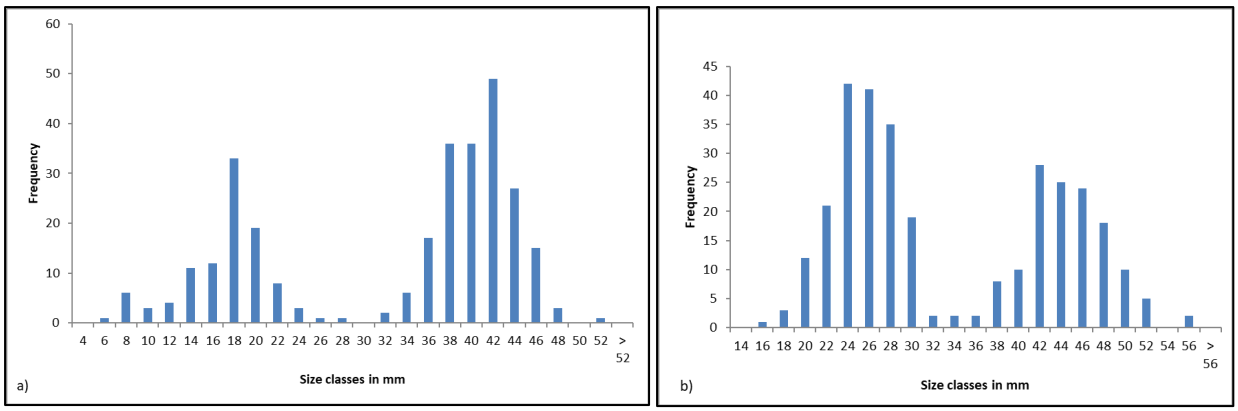

Fig. 9: Seed mussel size distribution in Rosslare during a) July and b) August 2020 surveys

Rusk Channel: From the 12 tows recorded in the Rusk Channel area, seven contained between 30 kg and 80 kg of seed mussel. The bycatch from those tows was mainly composed of mixed sediment and small stones, representing 25% of the weight of the samples collected. In addition to those 12 dredge tows, five more tows were carried without using acoustic markings. The average water depth in the surveyed area was 16.29 m (maximum 18 m, minimum 15 m). The average tow length was also longer than during the Rosslare survey, with 103 m (shortest: 71 m, longest 173 m). The average size of the seed in the Rusk Channel was 19.1 mm (maximum: 32.4 mm, minimum: 5.4 mm). The population size range was 27.02 mm) and size distribution (Fig.10) potentially indicated multiple larvae settlement within a short period.

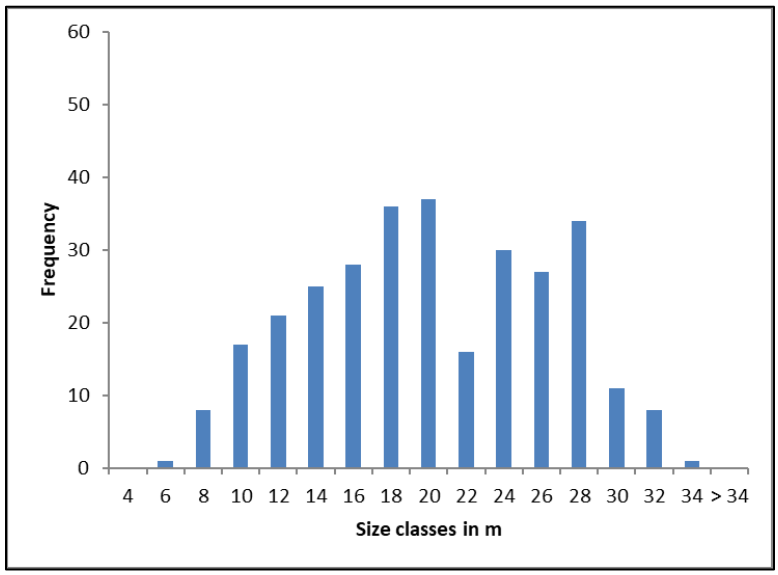

Fig. 10: Population size distribution in the Rusk Channel in July 2020

2.3.2 Biomass estimations

Considering that the fishery was due to open at the start of September, it was deemed more relevant to carry out biomass estimations in August rather than in July. The surveys focused on collecting grab data and biometric samples.

Rosslare: Mussel seed was observed in 35 grabs and seven grabs contained only sediment and stones/gravel. Marginally higher densities were observed in the centre of the seed mussel settlement than in the north, and south extremities (Fig.12a). A high level of bycatch was also collected for each sample, representing 51% of the average grab weight (highest level: 91%, lowest level:12%). The weight of seed mussel per grab (0.1 m^{-2} footprint) averaged 0.6 kg while the maximum weight recorded was 2.28 kg and the minimum was 0.04 kg. This wide density range confirmed that the seed mussels did not form a uniform seabed covering pattern.

The IDW raster generated from this data highlighted the higher density in the central part of the settlement (Fig. 12a). Matching the grab weight range mentioned above, 11 density classes were defined to calculate the potential biomass of the bed. Following the IDW interpolation process in this paper, the estimated mussel biomass available within the previously established 52.82 hectares was 2,738 tonnes (Table in Appendix).

Biometric data for 310 individual mussels collected during this survey showed an increase in the mean size to 32.61 mm (+0.91 mm from July 2020), the minimum size to 15.41 mm (+8.8 mm from July 2020) and the maximum size to 54.96 mm (+3.27 mm from July 2020), which coincided with decreasing size range by 5.53 mm from July (Fig. 9). Between the two sampling periods, (from July to August), the minimum size increased from 6.61 mm to 15.41 mm. The two distinct seed populations observed in the July samples, the smaller 12 to 20 mm class and the larger 34 to 46 mm class, were still evident through the August survey samples. Those two mussel size classes were then represented by the 22 to 28 mm class and the 42 to 48 mm class, with the smaller size class dominating the population distribution throughout the samples (22 and 28 mm), which also correlated with the decrease in the size range (Fig. 9).

Rusk Channel: The mussel quantity in the 27 successful samples was highly variable, with an average weight of 0.95 kg per grab (minimum weight: 0.1 kg, maximum weight: 2.28 kg). The higher weight grabs were mainly collected in the south sub-bed and the southern half of the middle sub-bed. As anticipated from the preliminary survey dredge data, the north sub-bed presented a more scattered mussel distribution. The overall settlement in the Rusk Channel showed higher surface density than the Rosslare bed. Indeed, 13 grabs contained over 1 kg of mussels, corresponding to an average of 1.49 kg grams or nearly 15 kg/m^2. However, the Rusk Channel samples were also characterised by high levels of bycatch, mainly composed of mixed coarse sediment, shells and small stones representing an average of 42% of the total grab sample weight (highest: 94% in the north sub-bed, lowest: 2% in the south sub-bed).

The IDW raster showed potential high mussel density for both south and middle sub-beds (Fig. 12a). From the density range detailed above, ten density classes were defined to run the biomass estimation process. For the potential 41.57 hectares defined previously from the acoustic survey, it was estimated that the Rusk Channel seed bed contained 3,588.5 tonnes (Table in Appendix).

No updated biometric data was recorded because of the short time between the preliminary survey (end of July) and the biomass estimation survey (mid-August) at this location.

2.3.3 Post-Fishery Surveys

The Rosslare and Rusk Channel beds were finally re-surveyed at the end of the fishing season using the same protocols to quantify the potential remaining biomass.

Post-fishery acoustic survey

The side scan sonar was deployed so that the footprint originally surveyed was resurveyed. Most of the mussel pattern features on both beds had disappeared, and dredge marks were still clearly visible a week after the end of the fishing (Fig. 11). However, few areas showing the distinctive pattern at both locations remained. For Rosslare, two small areas were observed in the centre

and along the south border. Some seed mussel patterns remained for all three sub-beds in the Rusk Channel. Following acoustic image analysis, the footprint of the remaining biomass in Rosslare was estimated at 3.29 hectares and 9.58 hectares in the Rusk Channel.

a)

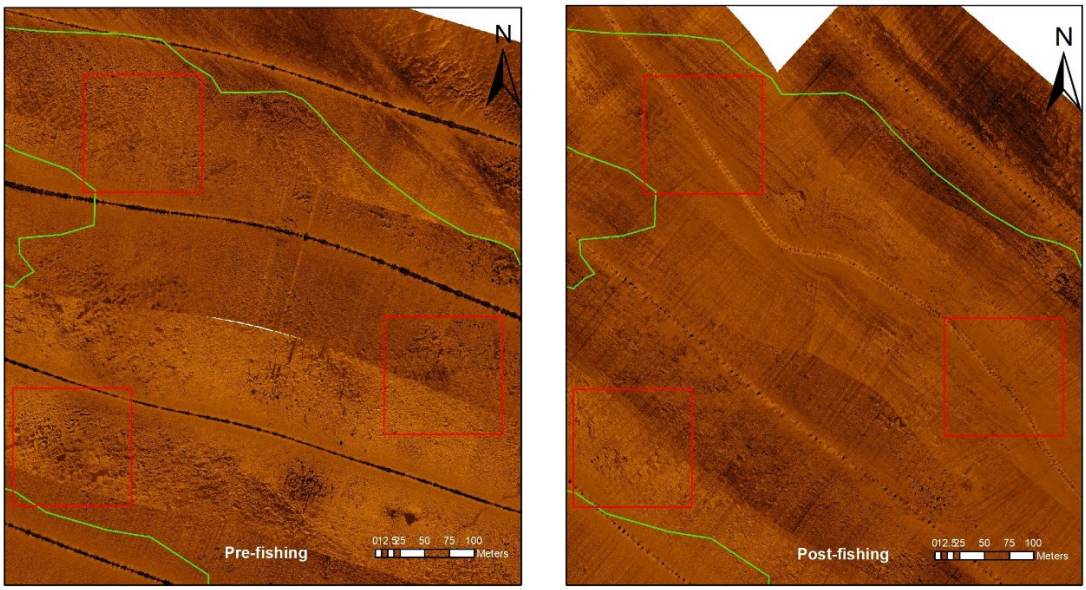

b)

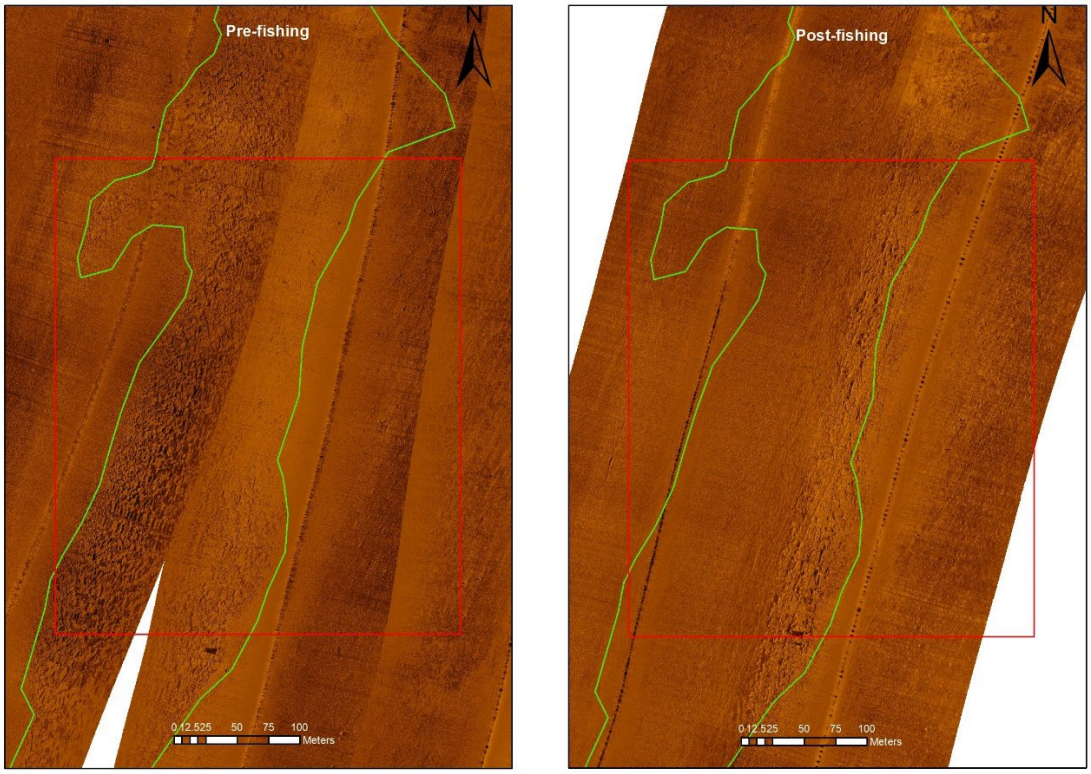

Fig. 11: Acoustic image of Rosslare (a) and the Rusk Channel (b) pre and post-fishing

Notes: The green line indicates the border of the original bed. In the pre-fishing pictures, mussel features are sharp within the bed: in the three red squares in the top picture and along the west border of the bed in the bottom. On the post-fishing, most of those have disappeared, the ground is smooth and featureless, and dredge marks can be observed, mainly on the bottom left picture.

Post -fishery biomass estimation

Random sampling points were generated within the original footprint of the settlements, which assessed biomass.

Rosslare: Post-fishing sampling was limited due to the number of stones found at the location, which affected the efficiency of the grab. The equipment was deployed 41 times in total but was jammed by stones ten times over various sampling stations. Seed mussel was found in 24 samples, characterised by low quantities of mussels, as 22 grabs presented less than 0.15 kg of seed. The average weight of the samples collected in Rosslare was 0.14 kg (maximum: maximum: 2.02 kg, minimum: 0.005 kg). The location of the heaviest sample recorded (2.02 kg) matched with the identified acoustic mussel pattern. However, further sampling in its proximity did not indicate the potential remaining mussels and the extent of the possible remaining biomass. As expected, relatively high levels of other materials were found within the marked seed bed, mainly composed of gravel, coarse sediment, and broken shells, also known as shell ashes. The other material averaged 85% of the grab weight (highest: 99%, lowest: 6%), 35% higher than pre-fishing.

To avoid skewed results, the calculated biomass estimates were adjusted by removing the sample containing 2.02 kg from the process as it was considered an outlier, as no other mussels were found at the sample location. When used with the IDW algorithm, the estimated volume of remaining biomass appeared unrealistic with what was observed *in situ*.

From the remaining samples, eight classes were used to generate the IDW raster (Fig. 12b). The remaining biomass was estimated to be 195.71 tonnes (Table in Appendix), scattered throughout the original bed. ArcGIS raster calculator tool was used to compare estimated density variations between pre- and post-fishing (Fig. 12c). The highest variations were observed in the central part of the mussel bed, where the biomass was estimated as the most abundant during the pre-fishing survey.

Rusk Channel: 20 samples were recorded with less than 0.15 kg of seed per grab. The average seed weight per sample was 0.12 kg (maximum: 0.54 kg, minimum: 0.01 kg). The grab contents were also characterised by the high level of other material similar to that observed in Rosslare, accounting for 81% of each grab weight on average (highest: 98%, lowest: 39%), which is nearly double the amount of what was found during the pre-fishing survey. However, the seabed presented less stone and equipment jamming was less of an issue.

To create the IDW density raster(Fig. 12b) and the biomass estimation figures, 11 weight classes were designed(see tables in Appendix). The remaining biomass, concentrating on the northern side of the middle sub-bed, was estimated at 417.56 tonnes (Table in Appendix). A weight density variations raster was also generated to compare biomass distribution before and after the fishery Fig. 12c). High-density areas established in the pre-fishing survey indicated the greatest variations, mainly for the south and southern sides of the middle sub-bed.

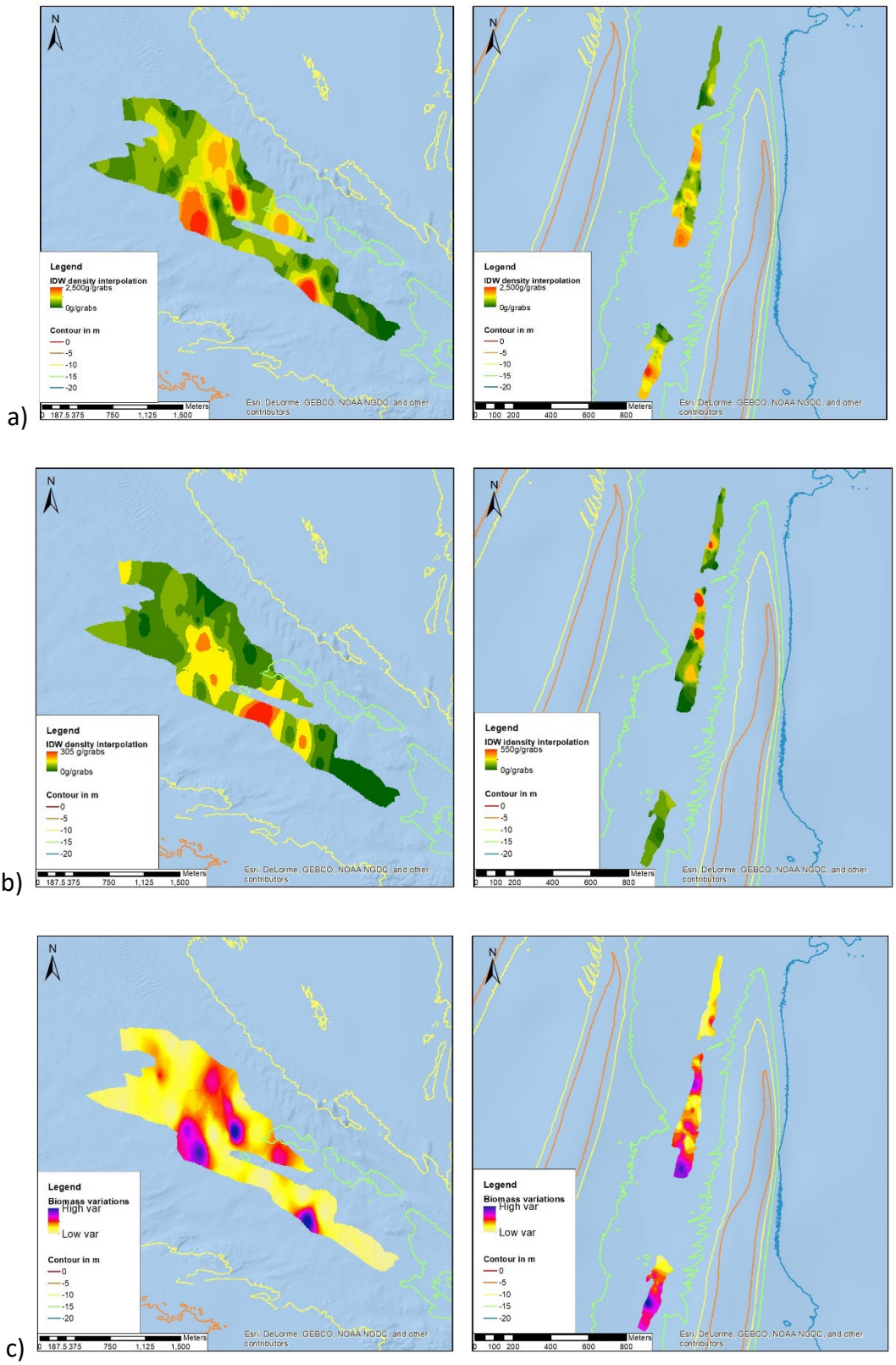

Fig. 12: Biomass estimations maps with IDW interpolation before fishing (a), after fishing (b) and the density variations between both stages(c) for Rosslare l bed (left) and the Rusk Channe (right).

Biometrics

There was significant growth in the mussels remaining at both locations compared to the data collected before the opening of the fishery. In Rosslare, although the maximum size had slightly decreased (1.1 mm regression), all other size classes increased between 3 and 10 mm. This growth is even more obvious for the Rusk Channel bed, with an increase of 12 mm for the minimum size, 13 mm for the median size and 11 mm for the maximum size (Fig. 13). The mussel size range (based on length) decreased on both beds, which is likely due to the removal of most of the biomass at both locations, but also exponential growth of younger individuals.

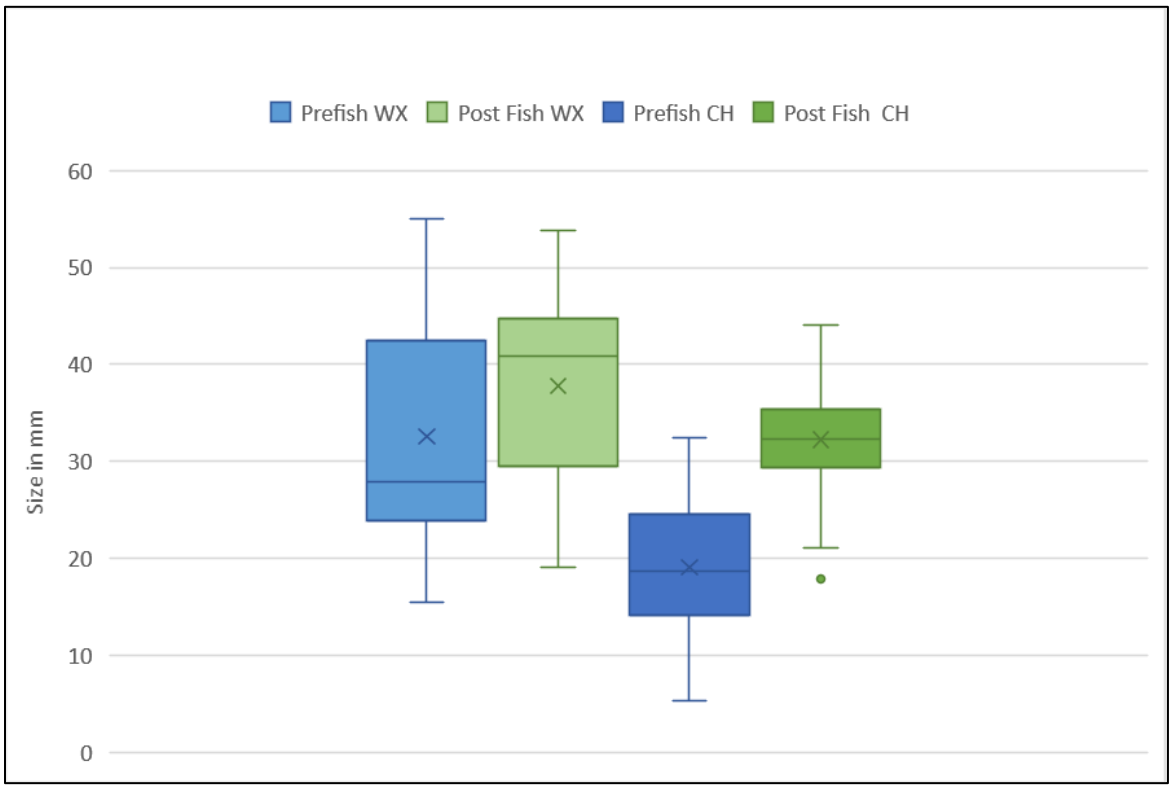

Fig. 13: Box plot of Pre and post-fishing seed mussel sizes for Rosslare (WX) and the Rusk Channel (CH)

The size distribution patterns remained similar in Rosslare with the two distinctive populations observed in July, with the larger cohorts (36 to 50mm) displaying an increase in numbers, indicating rapid growth, typical of younger mussels (Aldrich and Crowley, 1986). The size distribution in the Rusk Channel during the pre-fishing survey did not display an overall dominating class; this was not the case in post-fishing, as nearly a quarter of the mussels measured (21% of 300 individuals) were between 32 and 34 mm.

2.4. Discussion

The results indicated that side scan sonar provides a reliable tool to map subtidal seed mussel beds on mixed sediment ground, as distinctive seed mussel bed features can be observed within the data. IDW interpolation of targeted samples provides a robust method to estimate seed mussel biomass accurately. The combination of fishing data and post-fishery biomass survey validated the original biomass estimation as the estimated tonnage from both the Rosslare bed and Rusk Channel bed were similar to the sum of the transplanted tonnage and the remaining biomass post-fishing for each of those beds.

Reliability of the side scan sonar

As shown in previous publications (Diaz et al. 2004; van Overmeeren et al. 2009; Solan et al. 2003), side scan sonar is a reliable tool to map benthic populations, generating recognisable textures within acoustic data. However, due to the particular nature of the seabed in the area surveyed in this experiment (coarse sand and gravel), automated feature extraction based on pixel values was not possible (Brown *et al.*, 2002). Combining high-resolution acoustic data mosaic with extensive ground truthing based on typical mussel bed features made it possible to establish satisfactory bed boundaries using GIS (Brown *et al.*, 2011). Although this method required some experience in recognising mussel bed features on acoustic data, it was made more accessible by producing an imagery catalogue that guided meaningful features observed and confirmed in previous surveys.

There are numerous advantages to using side scan sonar for this type of survey. The swath coverage from the towfish is greater than MBES or other acoustic devices such as RoxAnn/RoxSwath for similar depth, mainly due to the equipment being towed at an average depth of 7 m below the surface and the orientation of the transducers. In the area surveyed during this experiment, the effective swath was always comprised between 180m to 200 m, independent of the depth of water. Swath on hull-mounted transducers can reduce in shallow waters (< -100m) and, therefore, would require more survey lines at tighter intervals. The sonar swath allowed the seed mussel bed areas to be covered in a couple of hours, making the time

available on the survey vessel more efficient. The towing depth also prevents interference from thermocline, halocline and planktonic bloom (pers. obs.). Another advantage is that the data is usually processed within an hour following its acquisition. In comparison with MBES data, which requires extensive cleaning and processing time, the sonar files only require nadir removal and mild gain correction through SonarWiz 6 prior to the mosaic GeoTIFF being generated. Finally, shadows produced by features on the seabed are more pronounced using side scan sonar, making their identification easier by eye.

A possible disadvantage of using side scan sonar is that it can require extensive sample collection to ground-truth the data. During this experiment 136 grabs were collected between the biomass surveys (pre and post-fishing) across the two sites in Rosslare and in the Rusk Channel. It is conceivable that if two more seed mussel beds were found during 2020 in other locations, the amount of grabs would have doubled, involving twice the amount of time to collect and analyse. Collecting and processing all those samples consume time and resources (Godet *et al.*, 2009), and because of the searching area and, on occasion, challenging weather conditions, the number of samples can sometimes be insufficient to produce a reliable biomass estimate. As an improvement of the methodology developed in this experiment, the combination of limited sampling and data bootstrapping has been used on challenging fish stock assessment (Stewart and Hamel, 2014) and could improve future surveys. Data bootstrapping could also provide openings to other estimation methods based on geostatistical routine and predictive models carried out on other shellfish stocks (Smith and Addison, 2003; Marine Institute and BIM, 2020). Using high-resolution MBES data could likewise provide solutions to reduce the impact of sample collection. Derived bathymetry variables such as rugosity, slope, and hardness related to seabed features could automatically extract those features from bathymetric data (Wilson *et al.*, 2021). Combining good quality back scatter data from MBES and side scan sonar images could also provide an interesting process (Fakiris *et al.*, 2019). By relating mussel features from the sonar image to pixel values from the back scatter, it would be possible to create a seabed classification map indicating the extent of the mussel bed. The addition of high-resolution bathymetry could

also provide a grid on which the sonar image could be draped, providing a 3D visualisation of the mussel beds.

Inverted Distance Weight (IDW) interpolation with targeted samples

IDW interpolation has already been used to produce large-scale density maps for other bivalve populations using biological samples (Hervas *et al.*, 2008; Tully and Clarke, 2012). This study only collected samples within the boundaries generated from the side scan sonar data. It resulted in over 83% of grabs containing mussel seed during the biomass estimation survey across both locations. All the samples collected outside the bed's boundaries did not show mussels, thus validating the areas generated from the acoustic data. Interestingly, maps produced with the IDW interpolation pre and post-fishing showed substantial surface density variations, mainly in areas that yield higher weight densities pre-fishing. It could indicate selective fishing patterns from the fleet, possibly concentrating the fishing effort in high-weight density zones. However, this could only be confirmed by overlaying VMS (Vessel Monitoring System) data from the vessels, which was not available at the time of this experiment.

Further investigation would also be required to assess a possible correlation between the acoustic features from the side scan sonar imagery and the density distribution maps. As mentioned above, sample collection and processing consume a lot of time and labour; streamlining this process using a digitised data collection system with ad-hoc recording format such as Field Maps (ESRI, n.d.) combined accurate GNSS positioning can remove data manual entry and transfer time. Also, automated classification and estimation using historical data and sonar imagery would drastically reduce the sampling requirements (Frederick *et al.*, 2020; Janowski *et al.*, 2022). Finally, a comparative study between the various interpolation methods (IDW, Kriging, Spline) would be interesting to assess potential differences in biomass estimations.

Validation using fishing data and post-fishery survey

The introduction of the post-fishery biomass assessment in the overall methodology indicates that the mussel dredgers fleet does not remove the entire settlement. Indeed, both seed mussel

settlements displayed some remaining biomass, accounting for less than 10% of the original estimated available stock of 6,326.48 tonnes. According to 2020 reported figures from the SFPA (Sea Fishery Protection Authority of Ireland), approximately 5,895 tonnes of seed mussels were transplanted from the two seed beds identified in this experiment. It is worth noting that those reported tonnages are not established using weighing instruments due mainly to the fishing and transplanting method (dredges emptied directly in vessel holds that are then pumped out on growing grounds); therefore, those figures are at the appreciation of the vessel operator.

Combining this reported transplanted tonnage with the post-fishing estimated figures produced in this research showed that the potential overall biomass for both beds increased to 6,508 tonnes. This figure partially validates the methods used in this paper as the original biomass was underestimated by 182 tonnes, representing less than 3% of the total of reported transplanted figures and estimated biomass left on those two beds. The post-fishery acoustic survey also showed remaining seed mussel features. However, further investigation by targeting those features was not carried out, and it is believed that this could have improved the quantification of remaining biomass.

It is unknown if the remaining mussels would provide a viable source of larvae for recolonisation, considering larval dispersal patterns (Gilg and Hilbish, 2003a; Coscia *et al.*, 2013; BIM, 2019). Established mussel beds are known to facilitate larvae secondary settlement (Pulfrich, 1996; Morello and Yund, 2016; Wilcox and Jeffs, 2017), although the survivability of the remaining mussels over the winter period could be questionable (Steenbergen *et al.*, 2005). From the various seed mussel surveys carried out by BIM since 2008, it appears that overwintered seed survivability on wild beds is variable along this coast (BIM source, unpublished). As cited in this paper, the 2020 seed survey reports described a bed of overwintered mussels being fully depleted by predation from *Asteria rubens* in late spring but also part of the Rosslare bed likely providing a bridgehead for the 2020 spring larvae settlement. Because of the high probability of the destruction of the remaining mussel biomass by predation or dislodgement (Troost *et al.*, 2022), it can be hypothesised that the post-fishery stock will not benefit any wild mussel bed

regeneration. In contrast, the transplanted stock will have better survivability and productivity on cultivated grounds (Smaal *et al.*, 2017), subsequently providing a more reliable source of larvae production during the farming cycle. Also, it is likely that the most represented cohort in August (16 to 18 mm) was related to the most represented cohort in October; this would correspond to an average growth rate of 7 mm month^{-1}, similar to those reported for farmed mussels in the literature around Europe (Rodhouse *et al.*, 1984; Pérez-Camacho *et al.*, 1995).

Previous methodologies designed to assess the biomass of mussel beds have used different acoustic data collection such as a combination of single beam ground discrimination system and Optimum Allocation Analysis (AAO) through ground truthing with dredges (Strong and Service, 2011), side scan sonar imagery using FK filtering and quadrat sampling (van Overmeeren *et al.*, 2009), or just dredge samples (Troost *et al.*, 2022). The estimated biomass in those methodologies either does not mention biomass verification through fisheries transplanted figures or assumes that all the biomass has been removed from the beds. This current research highlights that around 10% of the original biomass remains on the seabed, so this should be added to the reported transplanted figures from the industry. Also, the literature indicates that density is not homogenous on mussel beds (Commito and Rusignuolo, 2000; Liu *et al.*, 2014); therefore, extrapolating density from dredge tow may be misleading, especially while not including ground contact consistency, possibility of overflowing and losses due to mesh size. Because of the fluidity of mussel aggregations on soft sediment compared to other bivalves, precise grab sampling is possible, thus providing a detailed density distribution through multiple sampling, as shown in this research. The methodology carried out in this experiment has improved the reliability of biomass estimation of BIM subtidal seed mussel surveys. Since 2010, side scan sonar data collection, Day grab sampling, real-time on-board GIS data display, introduction of IDW estimation and post-fishing surveys have been major improvements in comparison with earlier survey methods using only dredge tows and limited coverage seabed discrimination systems. The methodology designed in this chapter has been implemented in 2021 and 2022; however, the level of accuracy reached previously was not replicated as the biomass was underestimated by 11% in 2021 and 16% in 2022 (unpublished figures). The main reason for this discrepancy is that

a post-fishery survey was not carried out on all beds in 2021 and 2022 and that all settlements could not be estimated in 2022 due to extensive recruitment on the seabed (reported transplanted tonnage: 11,379 tonnes in 2022 against 5,895 tonnes in 2020, sources SFPA). Although the side scan sonar provided a reliable mussel bed extent, it appears that the biomass estimation accuracy was due to the combination of extensive grab sampling within those boundaries.

This experiment also had many interesting, related observations, mainly with the Rosslare seed mussel population biometric measurements. Firstly, the July population size distribution histogram presents a clear break in the population size range between 28 and 32 mm and what appears to be two distinct cohorts. This bimodal distribution indicates possible settlement later in 2019 or early 2020 for the first-class range and a more traditional settlement in late spring for the second class. Several examples of variable spawning patterns have been recorded in the literature supporting this hypothesis (Chipperfield, 1953; R. Seed, 1969; Beukema, 1992; Gosling, 2015). In opposition, the seed mussel size range in the Rusk Channel settlement appeared to indicate different growth rates within the bed (Liu et al., 2012). This settlement also corresponds to a traditional spring spawning pattern.

Secondly, the 310 individual mussels collected on the Rosslare settlement during this experiment showed an increase in the mean size to 32.61 mm (+0.91 mm from July 2020), the minimum size to 15.41 mm (+8.8 mm from July 2020) and the maximum size to 54.96 mm (+3.27 mm from July 2020), which coincided with decreasing size range by 5.53 mm from July (Fig. 7). The minimum seed mussel size recorded increased from 6.61 mm to 15.41 mm from July to August. This steep increase can indicate a rapid growth rate of smaller/younger individuals (Aldrich and Crowley, 1986), as no signs of predation were observed on this particular bed.

Finally, there are high discrepancies in the recruitment of juvenile mussels on the seabed. According to the all-Ireland reported figures from the SFPA, transplanted seed mussel tonnage decreased from over 18,000 tonnes in 2008 to less than 3,000 tonnes in 2013. The numbers have

been slowly recovering since but not to the level reported pre-2010. This phenomenon is not limited to Ireland; this trend has also been observed in Normandy (Cochard and Paul, 2016). However, this fishery harvests commercial-size mussels instead of transplanting seeds on growing grounds. Seed mussel recruitment limitation is multi-factorial and not limited to settlement issues of larvae on the seabed (Dardignac-Corbeil and Prou, 1995; Pulfrich, 1996; South, 2016). Even if a robust seed mussel survey methodology is designed, the efforts will be futile if no settlement is found. Therefore, it is essential to understand the dynamics of local mussel populations by designating and protecting potential husbandries, monitoring their maturation cycle, understanding local larval distribution, and assessing larvae settling behaviour. In addition, it is worth investigating improving returns from the available resources and looking into other sources of juveniles to ensure the industry's survival.

Chapter 3:
The relation between sea water temperature and recruitment variations of subtidal seed mussel on the southeast coast of Ireland

3.1. Introduction

Subtidal seed mussel beds are the sole supply of juveniles for the Irish bottom mussel farming industry. In the Republic of Ireland, most beds are located in nearshore waters on the southeast coast and have been seasonally assessed for biomass since 1969 by An Bord Iascaigh Mhara (BIM) prior to the opening of the fishery (BIM, n.d.). In 2007 and 2008, several recommendations were set for future research to ensure better management of Ireland's subtidal seed mussel resource (Maguire *et al.*, 2007; BIM and Loughs Agency, 2008). Noticeably, (Maguire et al., 2007) recommended (i) establishing the factors driving the survivability of the resource and the possible stability of overwintering seed, (ii) understanding the long-term recruitment patterns in the Irish Sea and Celtic Sea, (iii) improving the accuracy of larval dispersion modelling, and (iv) investigating the possible correlation between seabed type and recruitment success. State agencies and academics have conducted multiple studies linked to those recommendations, including assessing the reproduction capacity of subtidal seed mussels (Knights, 2012), understanding larvae distribution patterns (Robins *et al.*, 2013; BIM, 2019; Demmer *et al.*, 2022), improving biomass estimation survey techniques (BIM, n.d.) and establishing the genetic distribution (Gosling *et al.*, 2008; Lynch *et al.*, 2020).

Since 2008, the reported seed mussel transplanted tonnage dramatically dropped from 18,134 tonnes to 2,626 tonnes in 2013 (Fig. 14), losing 9,639 tonnes between 2008 and 2011 despite no increase in the fishing fleet (sources from the Sea Fisheries Protection Agency - SFPA). Most studies took place either well before (Gosling *et al.*, 2008; Knights, 2012; Robins *et al.*, 2013)or after(BIM, 2020; Lynch *et al.*, 2020; Demmer *et al.*, 2022) this period, and most were too limited

in time; therefore, this variation in the pattern of subtidal seed mussel recruitment was not fully captured.

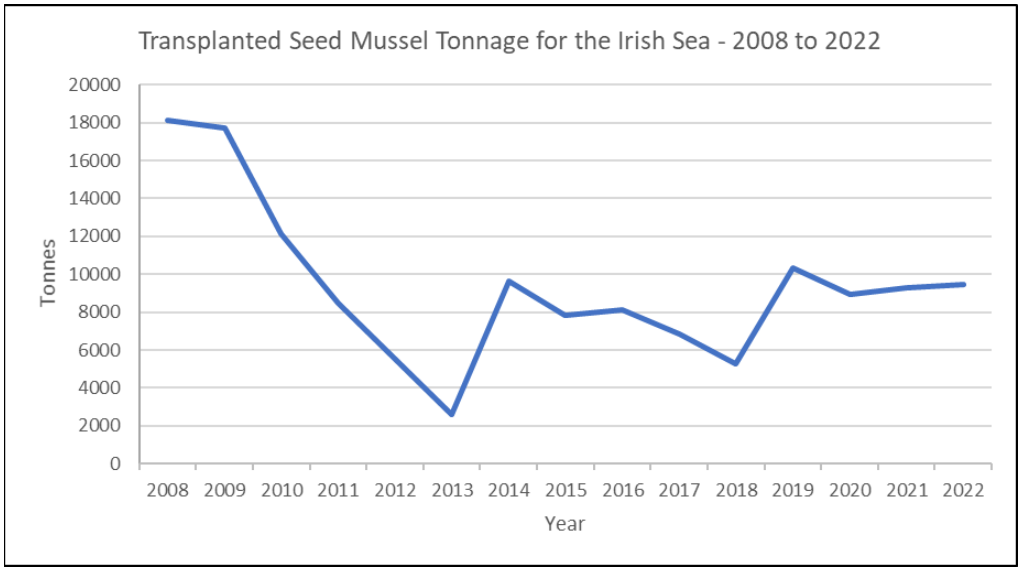

Fig. 14: Reported transplanted seed mussel tonnage variations from 2008 to 2022 (SFPA)

Mussels have a seasonal reproduction cycle, which can be divided into the following phases: broodstock maturation, spawning, planktonic larvae, settlement on substrate, and post-settlement growth (Gosling, 2015). The cycle of the subtidal seed mussel on the southeast Irish coast usually occurs between January (maturation) and July (formed settlement of new mussels following the planktonic phase of the larvae). Several exogenous and endogenous factors can directly affect this reproduction cycle; this includes larvae dispersal, predation, species diversity, fisheries management and sea temperature variations, all of which make seed mussel recruitment success highly variable (Beukema and Dekker, 2005).

Following spawning, the larvae's transport and spatial distribution are mainly driven by tidal and residual currents (Gilg and Hilbish, 2003a; Knights *et al.*, 2006), including wind-driven currents (Garland *et al.*, 2002; Demmer *et al.*, 2022). The combined effect of these currents may result in driving the larvae to unsuitable settlement and fishing environments (Robins *et al.*, 2013), such as deeper waters (below 30 meters), unsuitable substrate (rocky reefs) or intertidal grounds, which cannot be fished in Ireland, as seen in Dingle bay in 2018, where a significant amount of young seed mussels were discovered on intertidal rocks (BIM, 2019). Depending on

environmental conditions, mussel larvae spend between 1 month and 1 ½ months in the water column(Bayne, 1965; Widdows, 1991) before settling on suitable support on the seabed, including shells and stones, fibrous hydroids, hornwrack (*Flustra foliacea*) or brown seaweed (Seed, 1969; Pulfrich, 1996). It is during that post-settlement phase that the young mussel spat can be subjected to high mortalities, mainly due to relocation to an unsuitable environment following dislodgement from tidal currents (Fuentes-Santos and Labarta, 2015). The kinetic energy generated by winter storms (Feser *et al.*, 2015) in coastal waters can also be a facilitating factor for the dislodgement of mussels settled on the seabed (wa Kangeri *et al.*, 2016) as observed south of Rosslare, Co. Wexford, following storm Barra in December 2021 (Fig. 15).

Fig. 15: Seed mussel dislodged following storm Barra in December 2021 (Credits – Mark Doyle)

Predation on young mussels also greatly affects recruitment success. Subtidal beds can be subjected to high levels of predation, mainly from the common starfish *Asteria rubens* (Calderwood *et al.*, 2016). Since 2010, BIM surveys mention two mussel beds being fully depleted by common starfish, noticeably in 2013 when at least 3,000 tonnes of seed were lost between July and August. The second bed, composed of overwintered mussels from 2019, displayed over

90% coverage of starfish in early July 2020 (BIM, n.d.) and was fully consumed by mid-August 2020.

From a species distribution aspect, mussel species perform differently depending on their preferred environment (Beaumont *et al.*, 2004). *Mytilus edulis* and *Mytilus galloprovincialis,* as well as their hybrid, are present around the coast of Ireland (Gosling and Wilkins, 1981; Coghlan and Gosling, 2007; Gosling *et al.*, 2008; Lynch *et al.*, 2020). *M. edulis* is the more commonly observed mussel species, followed by hybrids and then *M. galloprovincialis* (Lynch *et al.*, 2020). Neither *M. galloprovincialis* nor hybrids have been observed in the Irish Sea, as indicated in various publications from 1981, 2007 and 2020 (Gosling and Wilkins, 1981; Coghlan and Gosling, 2007; Lynch *et al.*, 2020), possibly due to a seasonal thermal front developing between the Celtic Sea and the south Irish Sea (Brown *et al.*, 2003).

Sea water temperature variation is a critical factor throughout the biological cycle of the mussels. It is considered one of the main drivers for broodstock maturation and spawning (Chipperfield, 1953; King *et al.*, 1989) and larvae development (Brenko and Calabrese, 1969; Gosling, 2015). Considering that mussel gametogenesis can start when the water temperature reaches 7^{o}C (Chipperfield, 1953), low water temperature during early spring could delay both the maturation and spawning period and also the larvae settlement and growth. In opposition, high water temperature during the autumn could allow for reconditioning of the broodstock and partial spawning (Seed, 1969), providing a late settlement. The development of larvae also depends on water temperature, as low temperatures can generate a delayed metamorphosis, affecting feeding and the overall condition of the settled larvae (Bayne, 1965). Once settled, the optimum temperature for *Mytilus edulis* scope for growth (SFG) during the Spring is situated around 15 ^{o}C, while slight decreases occur at 10 ^{o}C and 5 ^{o}C (Fly and Hilbish, 2013). Further, the effects of climate change have been observed and documented on a range of marine ecosystems worldwide (Beaugrand and Reid, 2003). Noticeably, the recorded sea surface temperatures (SST) have steadily increased by 0.2^{o}C per decade in Europe since 1981 (Minnett, 2014; Feser *et al.*, 2015). The annual SST projected trend shows a possible increase of 0.05 ^{o}C to 0.5 ^{o}C decade^{-1} from 1976

to 2099 (Alexander *et al.*, 2018). These sea temperature changes can be an important stress factor for mussels and it can affect their overall physiology (Zippay and Helmuth, 2012) and so, mussel recruitment patterns.

The occurrence of subtidal seed mussel beds on the east coast of Ireland is well documented and has been recorded since 1904 (BIM, n.d.; Browne, 1904). The seed mussel surveys are conducted annually from April to September, after which the seed mussel fishery can open. During the survey, samples are collected from each identified bed for biometric analysis, including the average length of the seed and the size distribution. Between the period 2009 to 2022, the average seed mussel length recorded varied from year to year. Such variations could be explained by the sea temperature fluctuation during the larval phase (April to June), which is known to impact larvae development (Bayne, 1965; Pechenik *et al.*, 1990; Zippay and Helmuth, 2012).

This study assessed whether there is any correlation between subtidal seed mussel recruitment and sea temperature variation during the larval phase. Using a sea temperature dataset from Copernicus and seed mussel length data from 2009 – 2022, the research will focus on two areas off the southeast coast of Ireland where recurring seed mussel beds have been surveyed. The seed size differences will be assessed from transplanting time between 2009 to 2022. Any correlation between recruitment patterns through those years and sea water temperature will also be assessed, using recorded seed mussel sizes from historical surveys and reanalysis of sea temperature data.

3.2. Methodology

3.2.1 Seed mussel data

Seed mussel beds have been delineated from acoustic imagery since 2009. They frequently occur at the same discreet locations along the east coast. As a result, it was possible to divide the east coast into six distinct regions for this study. These regions were distributed from north to south and were labelled Howth-Lambay, Wicklow, Glassgorman, Cahore-Rusk Channel, Blackwater and

finally, Wexford-Rosslare (Fig. 16). Analysis of the cumulative figures for seed mussel area for each region shows that Wexford-Rosslare represents 30%, Wicklow represents 26%, Cahore-Rusk Channel represents 17%, Howth-Lambay and Glassgorman each represent 11%, and finally, Blackwater represents 5%. Wexford-Rosslare and Cahore-Rusk Channel were the only regions where beds recurred most frequently throughout the analysis (2009 to 2022). Therefore, this research will focus on those two regions: Wexford- Rosslare and Cahore-Rusk Channel.

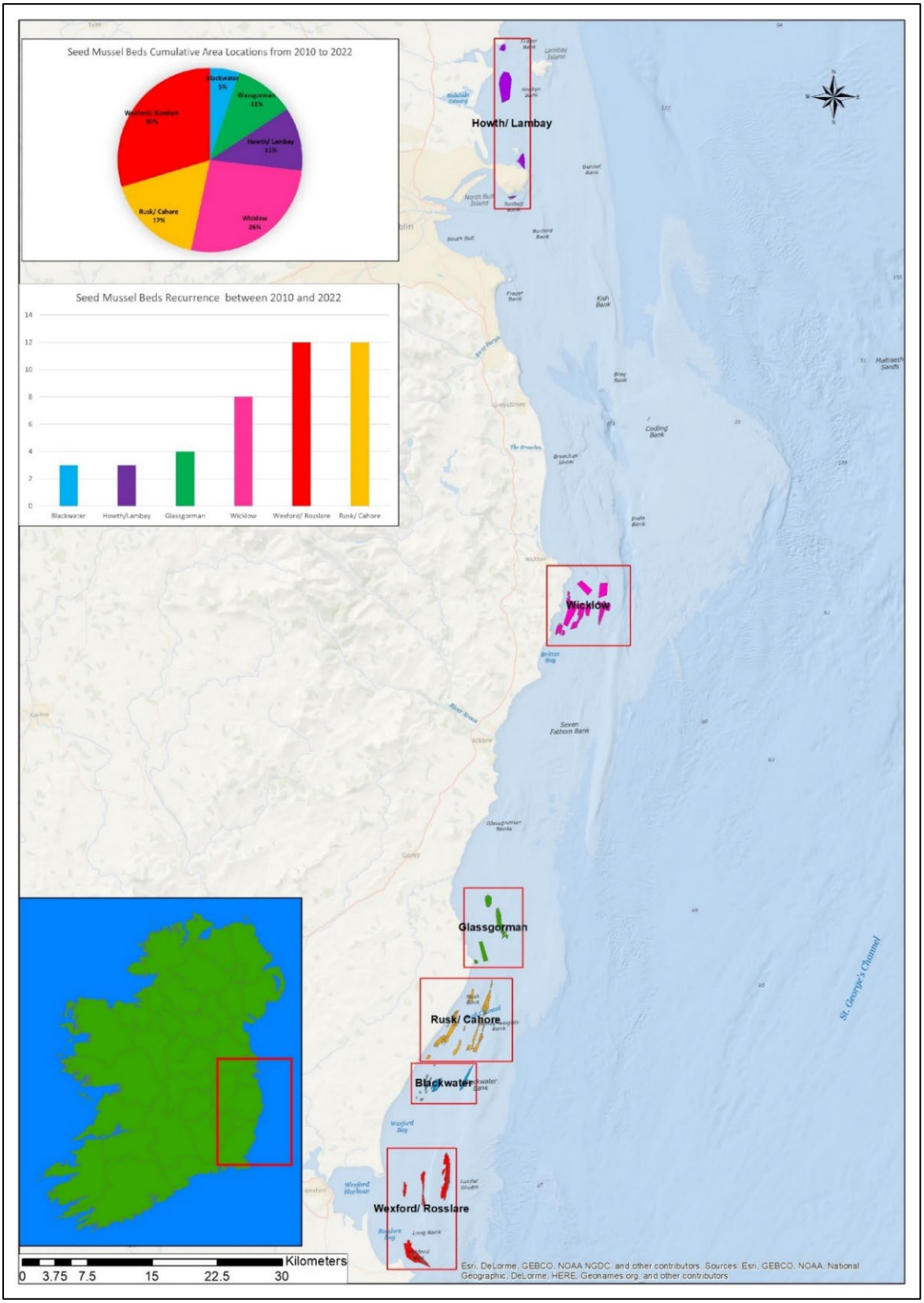

Fig. 16: Subtidal seed mussel beds distribution on the east coast of Ireland from 2009 to 2022

Samples were collected at the two chosen regions to measure the size of the mussels. The samples were collected annually from 2009 to 2022 during the survey season (from April to August) using a Day grab or a dredge. Each sample contained a minimum of 99 individuals. They were measured using a digital calliper (0.01 mm accuracy) to ascertain the average mussel length in each region. Overwintered mussels were present in some samples. However, they were not included in the analysis because this study focuses only on newly recruited seed mussels. The exclusion of overwintered mussels was based on visual characteristics, mainly the presence of epifauna such as bryozoans and barnacles on the shells (Svane and Setyobudiandi, 1996; European Environment Agency, 2019). A bimodal distribution of the size frequency for one location is also an indicator of two temporal separate settlements.

3.2.2 Sea temperature data

The temperature data was extracted from the Copernicus Marine Environment Monitoring Services (CMEMS), which used the nested regional ocean model NEMO 3.6 (Copernicus Marine Service, 2022) using ArcGIS PRO version 3.02 (ESRI). The temperature model outputs 7 x 7 km tiles displaying average daily Sea Bottom Temperatures (SBT) (Fig. 17). Mussel larvae only spend limited time on the surface layer during their planktonic cycle (Sprung, 1984b); therefore, only the SBT was used for the analysis. The daily mean temperatures for the SBT from April 1st to June 30th were used to calculate a daily cumulative temperature (DCT) and an average sea bottom temperature. This 91-day period corresponds to the time the larvae appear in the water column until they settle on the seabed and start growing (King *et al.*, 1989; Knights *et al.*, 2006). This was calculated annually for the years 2009 to 2022 for both Wexford-Rosslare and Cahore-Rusk Channel regions. Only tiles overlapping with the seed mussel beds were selected for this study, and the data for those overlapping tiles were again averaged to provide a single temperature value for each region for each year.

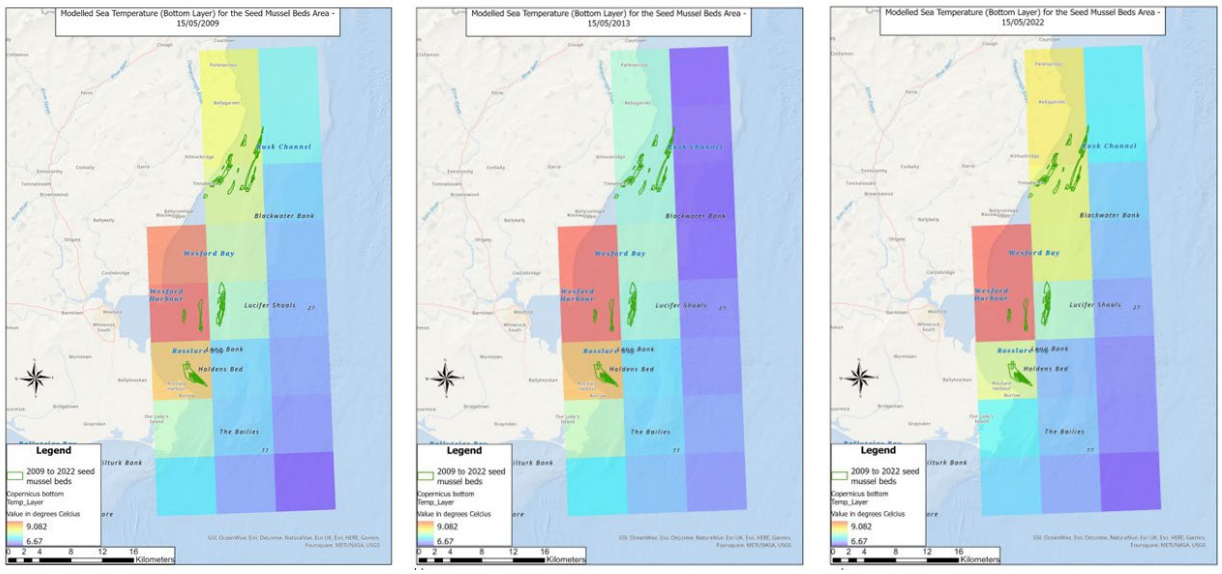

a) b) c)

Fig. 17: Example of modelled sea bottom temperature (SBT)in the southwest Irish Sea for: a) 15/05/2009, b)15/05/2013 and c)15/05/2022

3.2.3 Statistical analysis

A dataset with the temperature and the seed mussel biometrics was created for each location. This dataset comprised the average SBT per year, the DCT for each year, the individual measurements of each mussel per sample (in mm), the sampling year and the sampling week. Both regions were analysed separately.

The data were imported into R Studio (R Core Team, 2022). Two additional variables, 'Season' and 'Temperature Variation,' were generated (details in Appendix). The sampling weeks were classed as 'early' (between weeks 15 - 22), 'halfway' (weeks 23 - 30), and 'late' (weeks 31 - 38) to produce the 'Season' variable. The DCT was classed as 'low' (DCT ≤970), 'medium' (DCT values between 971 and 1040), and 'high' (DCT values between 1041 to 1107) to generate the 'Temperature Variation' variable. These data were then used to generate two plots using ggplot2 (Wickham, 2016), one indicating the sample size distribution for each year relative to the `Season' (Fig. 18 and 21) and another showing the sample size distribution in relation to the `Temperature variation' (Fig. 19 and 22). These plots were created for each region in the study. Box plots showing the size distribution for each year were colour-coded according to `Season' and `Temperature variation' (Fig. 20 and 23).

The possible effect of temperature variations on the seed mussel sizes was investigated using a linear mixed model (LMM) (Dingemanse and Dochtermann, 2013; Clements *et al.*, 2021) in R Studio using the lme4 package (Bates *et al.*, 2015). An LMM was chosen primarily because of the sample design (samples were collected within the defined boundaries and not randomly along the coast) and the multiple input parameters used (SBT, sampling week, year and mussel length). LMM also allow the inclusion of a random effect and interaction term. In this experiment the sampling year (random effect) captures the variability of each year while the effect of temperature on seed mussel size over time (interaction term) is included as a combine variable. However, those models also require assumptions evaluation for potential autocorrelation of the residuals, resulting in further model adaptation.

The following section documents the formulae trialled in the LMM. The first model run used the following formula:

$$Y_{log1} = \beta_0 + \beta_1 \cdot X_1 + \beta_2 \cdot X_2 + \alpha + \epsilon$$

Where the dependent variable (Y_{log1}) was the recorded length in mm of the mussel samples expressed in the natural logarithm number, β_0 is the intercept, the first independent variable (X_1) was the year and sampling week expressed as a decimal value (for example 2009.33 for Week 11 of 2009), the second independent variable (X_2) was DCT, the random effect associated with the grouping factor (α) expressed the sampling year, (ϵ) and represents the residual error term.

Model fitting was initially improved by normalising the recorded mussel length with the Box-Cox lambda transformation ($Y_{\lambda 1}$) using the MASS package (Venables and Ripley, 2002) in RStudio. The model was run again using the following formula:

$$Y_{\lambda 1} = \beta_0 + \beta_1 \cdot X_1 + \beta_2 \cdot X_2 + \alpha + \epsilon$$

To further improve this linear mixed model, the DCT values were replaced by the average SBT values (T). In addition, an interaction term ($X_1 \cdot T$) consisting of the sampling time and the temperature (SBT) was introduced to the original formula. The addition of the interaction term enables the combined effect of sampling time and SBT on the logarithm seed mussel sizes ($Y_{\log 2}$)

to be examined rather than the effects of those variables at an individual level. The model was rerun using the following formula:

$$Y_{\log 2} = \beta_0 + \beta_1 \cdot X_1 + \beta_2 \cdot T + \beta_3 \cdot X_1 \cdot T + \alpha + \epsilon$$

The Box-Cox lambda transformation on seed mussel length was used again to improve model fitting, and the final model was developed:

$$Y_{\lambda 2} = \beta_0 + \beta_1 \cdot X_1 + \beta_2 \cdot T + \beta_3 \cdot X_1 \cdot T + \alpha + \epsilon$$

Where the dependent variable ($Y_{\lambda 2}$) was the transformed recorded length in mm of the mussel samples, the first independent variable (X_1) was the year and sampling week expressed as a decimal value, the second independent variable (T) was the average temperatures, the interaction term ($X_1 \cdot T$) was the week number expressed as a decimal value for each year by the average sea temperature values, the sampling year as a vector provided the random effect (α).

Residuals were plotted for the different model outputs to assess how well each model fit using normal histograms and quantile residual plots (see Appendix). The results of each final model were exported to a table in HTML using the Stargazer package (Hlavac and Marek, 2022). Finally, the model's predictions were plotted using the ggeffect package (Lüdecke, 2018). In addition, to ensure that assumptions were met, evaluations based on diagnostics, including linearity, normality of the residual (Shapiro-Wilk test), homoscedasticity and independence of errors (Durbin-Watson test), were done using the lme4 package also.

All the scripts and the detailed process in RStudio are available in the Appendix.

3.3. Results

The main objective of this study was to assess the effects of sea temperature and the seasonal time of sampling on seed mussel size in the Wexford-Rosslare region and the Cahore-Rusk Channel region from 2009 to 2022. The results indicate that low sea temperatures have a negative effect on the size of seed mussels regardless of the time of year in which the sampling was undertaken.

3.3.1 Seed mussel size variations

A table summarising the statistics for annual sea temperatures and mussel length was produced for each region (Tables 1 and 2). The tables also including the time of year (Sampling Week) the samples were collected.

Wexford/Rosslare:

Wexford/Rosslare	*2009*	*2010*	*2011*	*2012*	*2013*	*2014*	*2016*	*2017*	*2019*	*2020*	*2021*	*2022*
Average Temperature	11.25	11.28	11.76	10.95	10.24	11.63	11.21	12.01	11.53	11.41	11.06	12.13
Minimum Temperature	8.18	7.45	9.04	8.67	6.06	8.15	8.19	9.49	8.86	7.77	8.37	9.18
Maximum Temperature	14.74	14.55	14.15	13.67	13.81	15.15	14.37	15.11	15.13	14.29	14.59	14.99
Daily cumulative (n=91)	1023.65	1026.32	1070.00	996.23	932.22	1057.95	1019.89	1093.15	1048.91	1038.04	1006.45	1103.65
Sampling Week	17	15	32	25	26	27	35	27	32	29	33	31
Average length (mm)	24.97	20.89	18.58	12.45	11.05	15.48	22.62	37.73	26.51	31.61	34.39	35.67
Minimum length (mm)	17.29	11.85	4.51	4.02	2.73	5.96	7.80	5.34	8.18	5.88	9.73	5.30
Maximum length (mm)	50.53	33.17	29.55	21.76	19.12	21.21	35.56	57.87	34.90	51.69	53.78	61.84
Count	101	151	151	142	300	100	600	506	300	294	390	603

Table 1: Data summary table for the Wexford/ Rosslare Sector – 2009 to 2022

The above table relates to the Wexford-Rosslare region. In general, the average sea temperatures are relatively stable, with the exception of 2013. In 2013, the lowest sea temperature and lowest seed mussel length were recorded. Most sampling took place in the middle of the year (Weeks 25 and 35), with the exception of 2009 and 2010, when sampling was undertaken much earlier in the year (Weeks 15 and 17). The average length recorded was larger than expected for this time of year given the reproduction cycle of mussels (King *et al.*, 1989), and therefore indicates that those mussels settled the previous Autumn and overwintered. No sample was collected in 2015 and 2018 due to this sector's absence of seed mussel beds.

Mussel length distribution graphs were generated and colour-coded by the qualitative categories DCT (Fig. 18) and sampling time (Fig. 19).

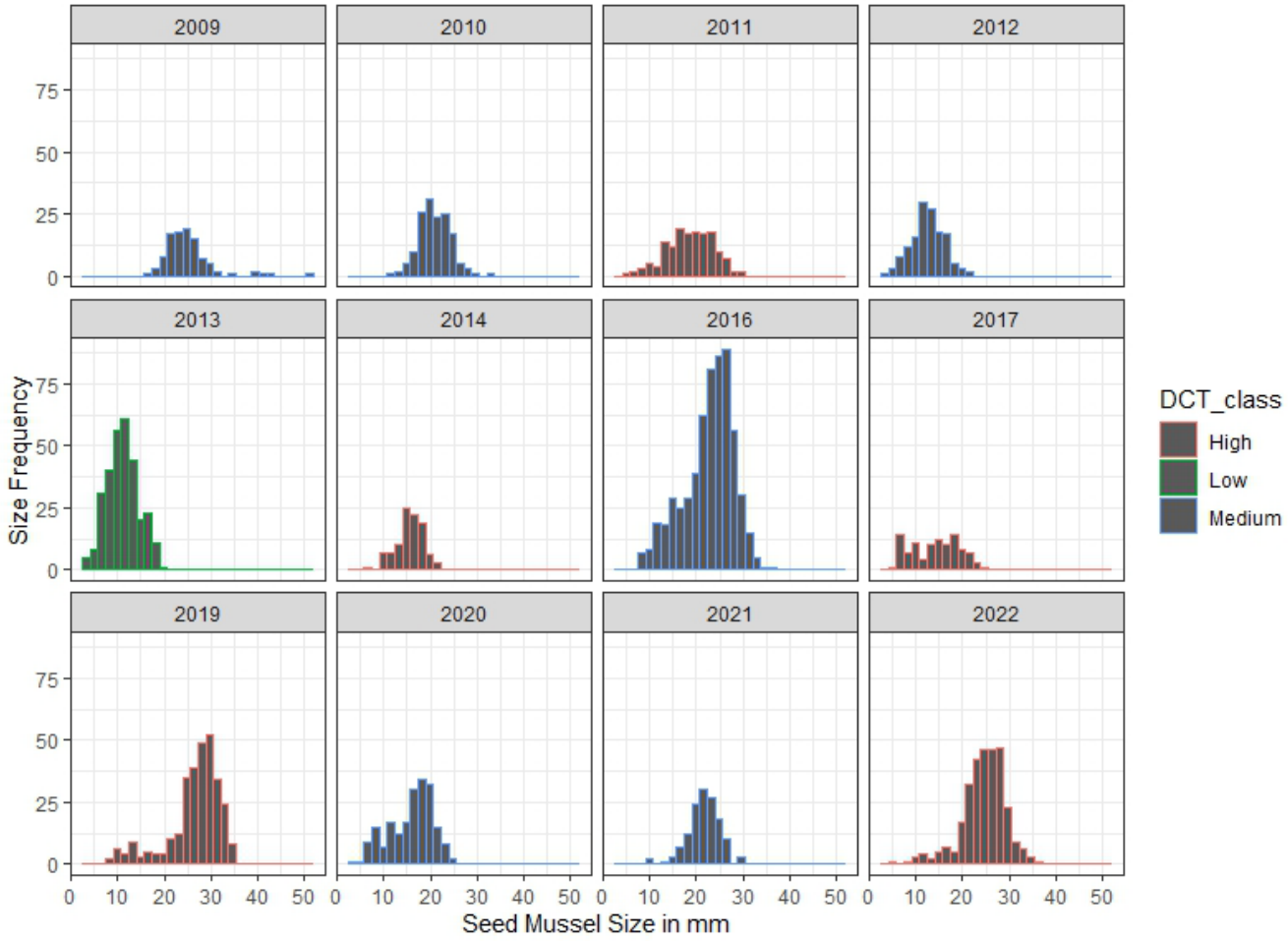

Fig. 18: Seed mussel length distribution and DCT variations from 2009 to 2022 for Wexford/ Rosslare

For sample length distribution and DCT variation (Fig. 18), we had one year (2013) with low cumulative temperatures, six years with medium cumulative temperatures (2009, 2010, 2012,2016,2020 and 2021), and five years with high cumulative temperatures (2011, 2014, 2017, 2019 and 2022). A decrease in the DCT can be observed between 2011 and 2013. The lowest DCT also corresponded to a small mussel length distribution in 2013. 2012 and 2017 also present a small length distribution. However, the DCT for each year was respectively medium and high for the years 2019 and 2022, presenting a larger length distribution and also high DCT. The year 2016 can also be considered representative of mostly larger mussels with a medium DCT value.

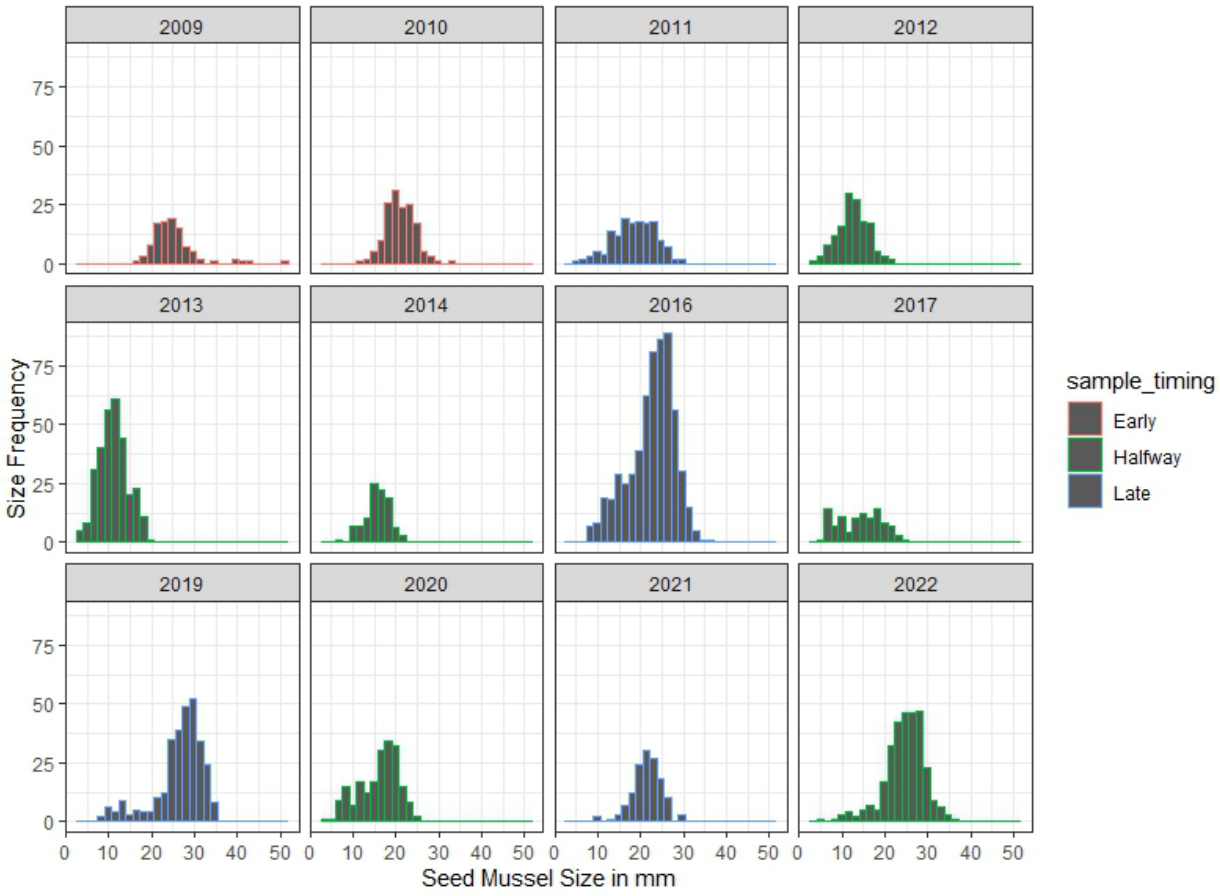

Fig. 19: Seed mussel length distribution and sampling time from 2009 to 2022 for Wexford/ Rosslare

For the sample length distribution and the sampling time (Fig. 19), there were two early samplings (2009 and 2010), six samplings halfway (2012, 2013, 2014, 2017, 2020, 2022), and four late samplings (2011, 2016, 2019 and 2021). 2012, 2013 and 2017 present smaller mussels while sampling took place midway. The samples from 2016 and 2019 present a larger cohort but also at a later stage. Medium-length distribution was observed early in 2009 and 2010.

Figure 18 shows the cumulating mussel size distribution, DCT class and sampling time where the size decrease from 2009 to 2013 is clear, with the year 2013 showing the smallest size distribution and the lowest DCT. The early sampling and relatively large size distribution are also clear for 2009 and 2010.

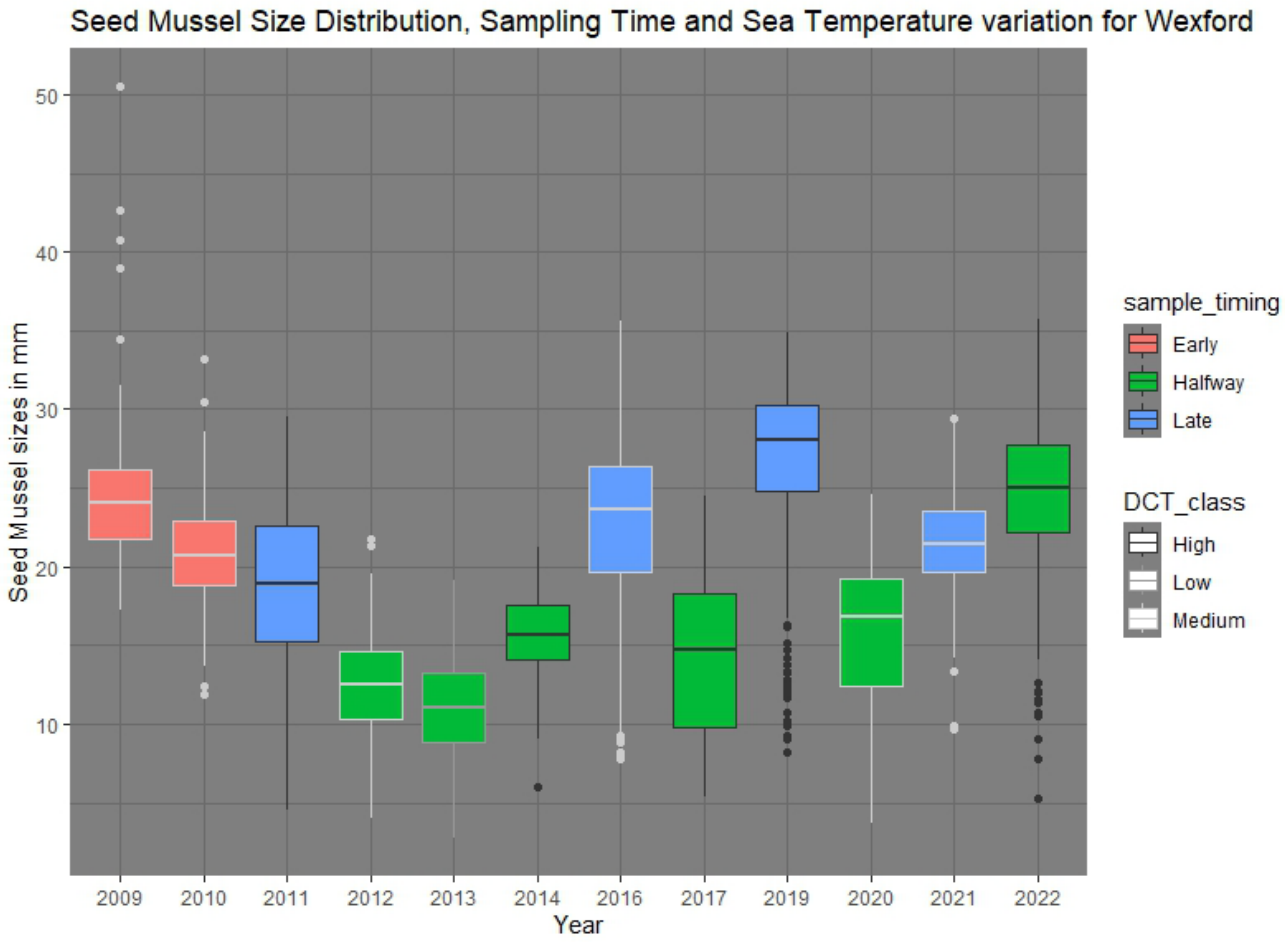

Fig. 20: Seed mussel size distribution, with Daily Cumulative Temperature classes and sampling time period for the Wexford/Rosslare sector from 2009 to 2022

Cahore/ Rusk Channel

Cahore/Rusk	*2009*	*2010*	*2011*	*2012*	*2013*	*2014*	*2015*	*2016*	*2018*	*2019*	*2020*	*2021*	*2022*
Mean Temperature	10.85	10.87	11.55	10.74	9.90	11.46	10.49	10.86	10.68	11.23	11.13	10.99	11.82
Minimum Temperature	7.74	7.08	8.77	8.55	6.08	8.14	7.54	7.97	6.81	8.68	7.52	8.44	9.09
Maximum Temperature	14.27	14.62	14.10	13.79	13.40	14.89	14.34	14.23	14.98	14.69	14.45	14.24	14.68
Dayly cumulative (n=91)	987.76	989.29	1050.70	977.10	900.71	1042.76	954.32	988.34	971.69	1022.03	1013.01	1000.30	1075.51
Sampling Week	25	38	17	28	29	27	36	33	27	28	32	34	27
Average length (mm)	32.22	18.26	28.31	12.61	11.12	12.97	26.52	21.49	11.97	19.68	19.08	28.03	31.70
Minimum length (mm)	23.21	6.85	17.12	3.91	4.45	3.62	12.75	5.10	3.01	5.73	5.38	10.36	2.94
Maximum length (mm)	42.16	32.21	40.03	25.61	20.12	21.80	37.34	30.52	25.88	32.70	32.40	38.74	57.62
Count	99	198	150	202	100	200	102	400	200	500	300	300	1000

Table 2: Data summary table for Cahore/ Rusk Channel Sector – 2009 to 2022

The above table relates to the Cahore-Rusk Channel region. Similar to Wexford-Rosslare, the average sea temperatures are relatively stable for all years with the exception of 2013. Again, it can be observed that the lowest sea temperature and lowest seed mussel length were recorded, proving that results from Wexford-Rosslare are not outliers. Most sampling also took place in the

middle of the year (Weeks 25 and 36), with the exception of this time in 2011, when sampling was undertaken much earlier in the year (Week 17). It was observed again that the mussel length was larger than expected at this time of year, indicating that these mussels overwintered, as was the case in Wexford-Rosslare in 2009 and 2010. No sample was collected in 2017; no seed mussel settlement was found in this location.

The data recorded was plotted in the same way as for the Wexford/ Rosslare area, showing the size distribution histograms per year against the DCT (Fig. 21) for the area and showing the same histograms but with the sampling time (Fig. 22).

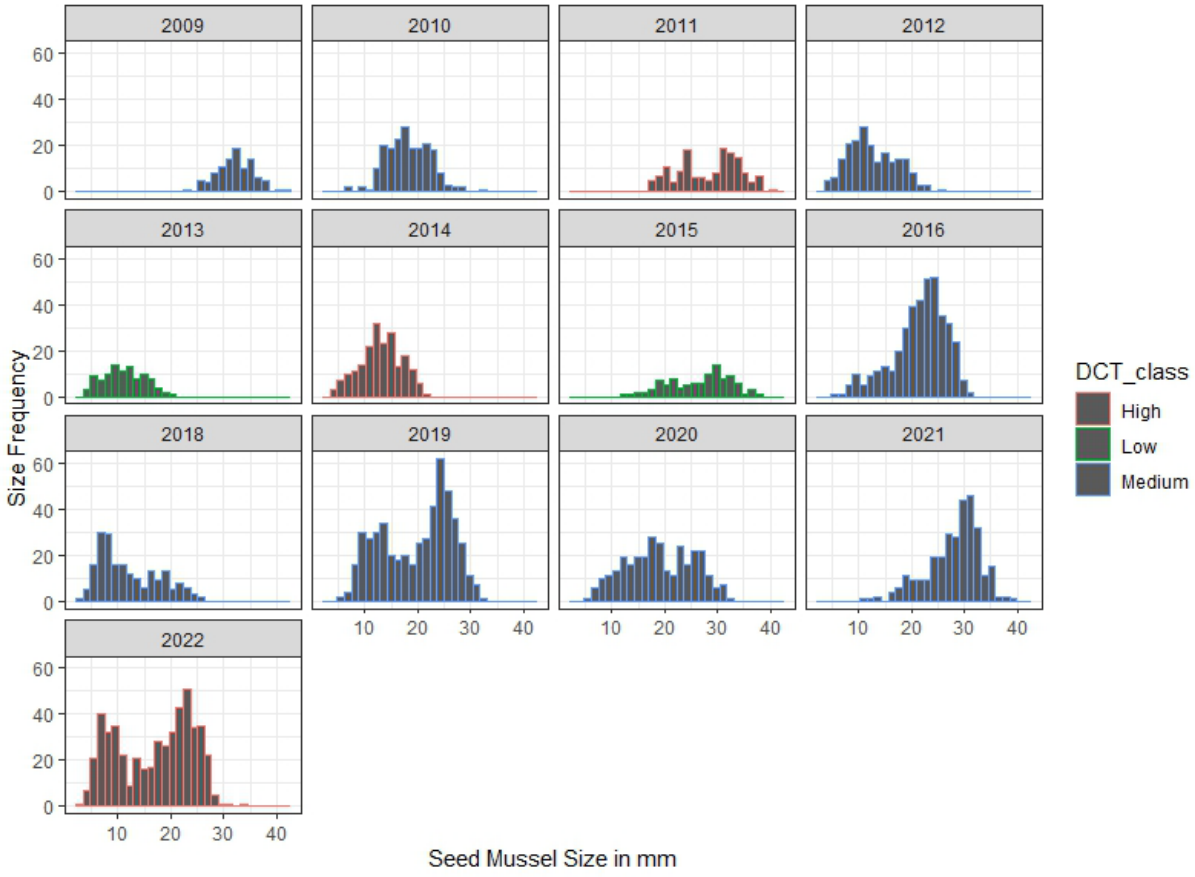

Fig. 21: Seed mussel length distribution and DCT variations from 2009 to 2022 for Cahore/ Rusk Channel

For the size distribution with DCT classes (Fig. 21), there were two years with low daily cumulated temperatures (2013 and 2015), eight years presenting medium DCT (2009, 2010, 2012, 2016, 2018, 2019, 2020, 2021), and three years with high DCT (2011, 2014, 2022). There was a decreasing pattern of the DCT between 2011 and 2013, followed by an increase in 2014 and a

drop to lower values in 2015. The low size range distribution in 2013 corresponds to a low DCT value, but it does not appear to be the case for 2015, which also presents a low DCT value but larger size range. The low size range distribution in 2012 does not correspond to a low DCT value. The larger range in 2021 presents a medium DCT value, while 2014 and 2022 present a medium size distribution, while the DCT value for both years is high.

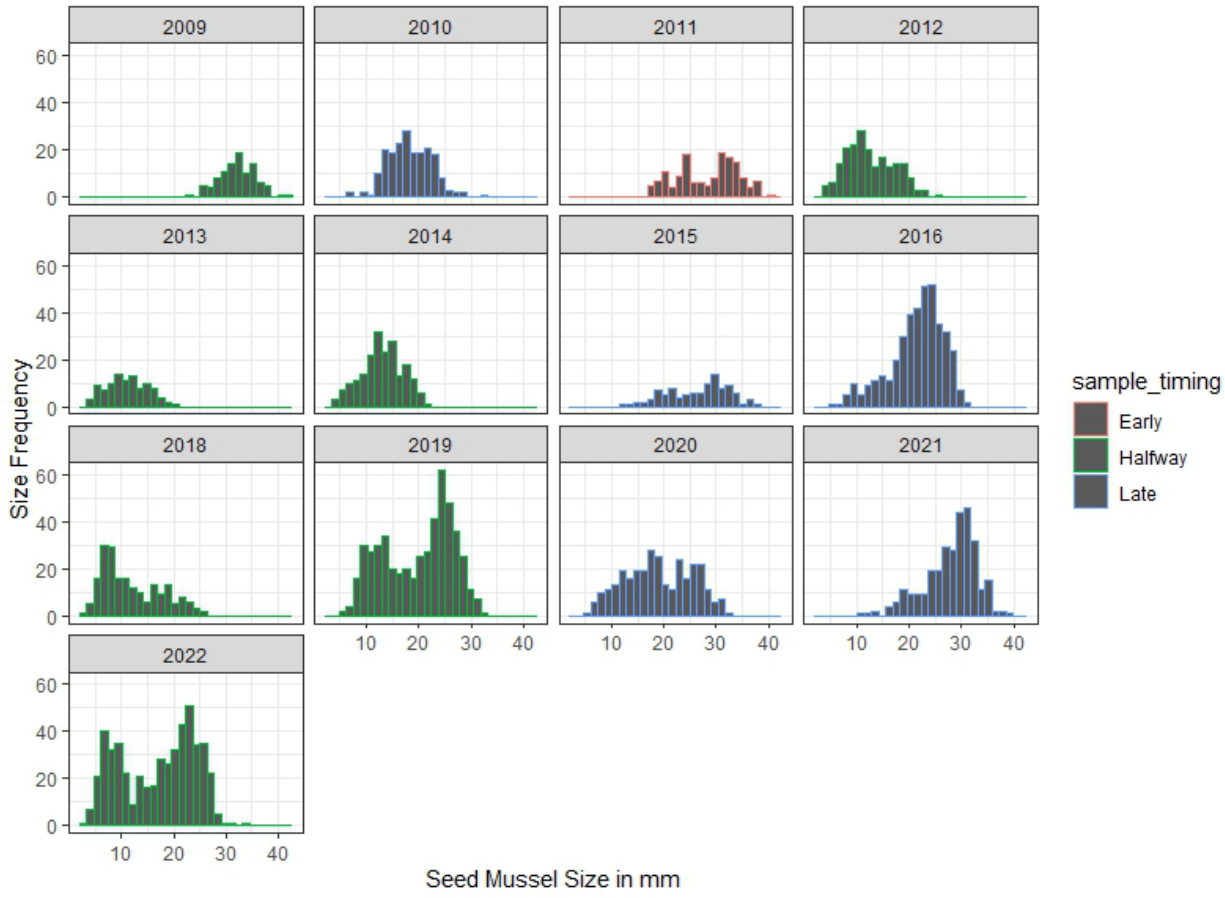

Fig. 22: Seed mussel length distribution and sampling time from 2009 to 2022 for Cahore/ Rusk Channel

In terms of size distribution and sampling time (Fig.22), there was one early sampling (2011), seven halfway samplings (2009, 2012, 2013, 2014, 2018, 2019, 2022), and five late samplings (2010, 2015, 2016, 2020, 2021) periods. 2009 presented a large size range while the sampling time was halfway. 2011 sampling was earlier than the other years but presented a large range: 2013 and 2014 present small cohorts. The large range size in 2015, 2016 and 2021 corresponds with late sampling.

The cumulative boxplot graph (Fig. 23) does not present any clear pattern of size decrease between 2011 and 2013. However, 2011 presented a large size range with an early sampling stage and a high DCT value. Despite sampling midway through the period, 2013 presents one of the lowest size ranges and a low DCT value. 2015 also presented a low DCT value. However, sampling took place later in the year, which did not affect the recorded length of seed mussel.

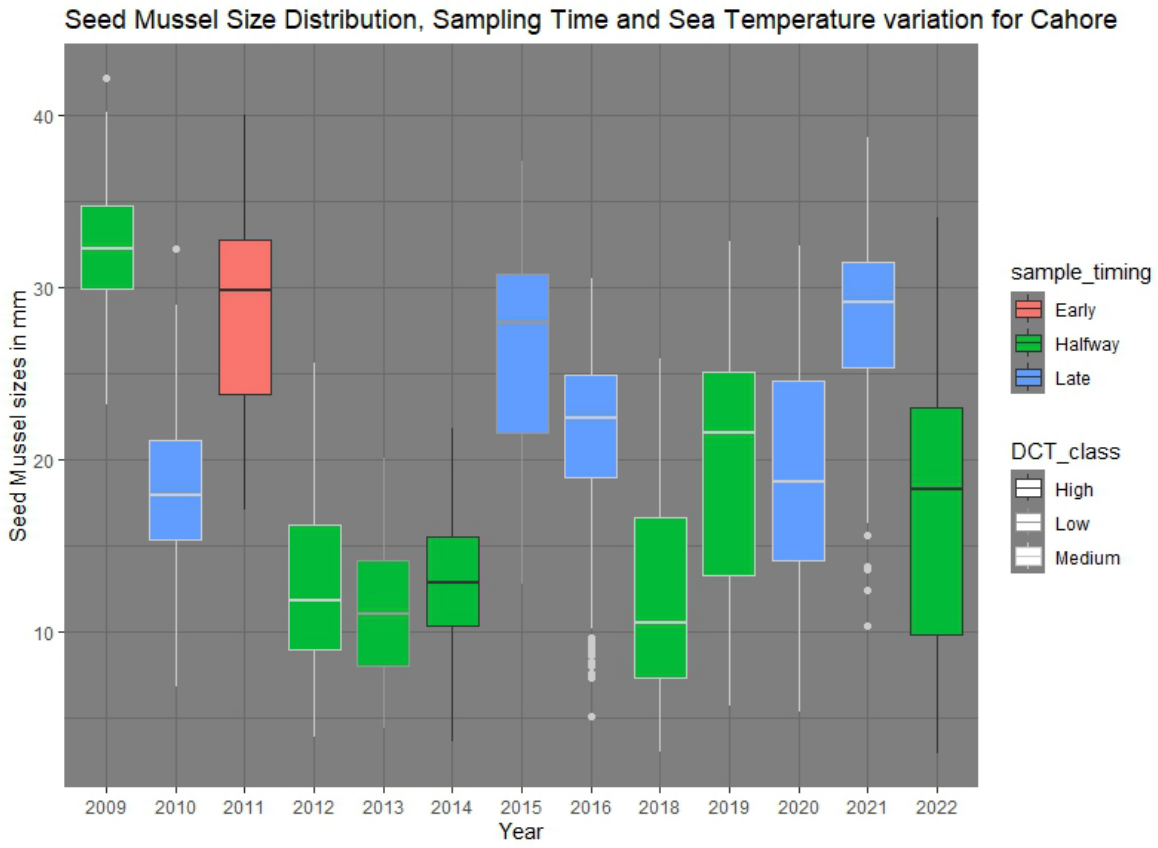

Fig. 23: Seed mussel size distribution, indicating Daily Cumulative Temperature classes and sampling time period for the Cahore/ Rusk Channel sector from 2009 to 2022

3.3.2 Significance of the effect of temperature on the size of the seed

The results produced from the first model presented issues with the residual fitting (heavy tailing for both locations). The Box-Cox Lambda transformation of the recorded seed mussel sizes improved the normalised histogram and reduced the tailing on the plotted residuals. However, the transformation of the mussel size increased the Restricted Maximum Likelihood (REML) in the model results, posing model fitting issues. After further trials, it was found that the model with the best fit was a model using the transformed seed mussel sizes (Box-Cox Lambda), the average Sea Bottom Temperatures (SBT), the decimal expression of the sampling week for each year, and an interaction term between the decimal expression of the sampling week and the average SBT. The results for the final model for both locations indicate that low SBT during the larvae phase has a significant effect ($p<0.01$) on the seed mussel sizes, as both coefficients for SBT were negative (Tables 3 and 4).

	Dependent variable:
	lba_size
deci_year	-2,328.080***
	(597.586)
sb_temp	-106.217***
	(28.361)
deci_year:sb_temp	209.966***
	(53.071)
Constant	1,191.693***
	(319.066)
Observations	2,584
Log Likelihood	-7,135.947
Akaike Inf. Crit.	14,283.890
Bayesian Inf. Crit.	14,319.040
Note:	*p<0.1; **p<0.05; ***p<0.01

Table 3: Model results for Wexford/ Rosslare

	Dependent variable:
	lba_size
deci_year	-1,482.542***
	(217.035)
sb_temp	-72.312***
	(11.929)
deci_year:sb_temp	129.656***
	(18.445)
Constant	840.031***
	(138.882)
Observations	3,251
Log Likelihood	-7,482.293
Akaike Inf. Crit.	14,976.590
Bayesian Inf. Crit.	15,013.110
Note:	*p<0.1; **p<0.05; ***p<0.01

Table 4: Models results for Cahore/ Rusk Channel

Lastly, the final model results were used to generate prediction plots to visualise the relationship between the SBT during the larvae phase and the size of the seed mussel. Those plots also include regression lines with predicted intervals for both regions.

The relationship between the SBT and the seed mussel size appears to be positive in the Wexford-Rosslare region (Fig.24), where lower sea temperatures during the larval phase corresponded to lower mussel length (2012 and 2013). Above 11 degrees, this relationship is not as clear; some of the largest recorded seed mussel lengths (2009, 2016, and 2019) do not correspond to the highest sea temperature (as of 2017 and 2022). However, the error bands from the prediction model indicate a greater level of uncertainty in the relationship between lower temperatures and smaller mussels than in the one between high temperatures and larger mussels.

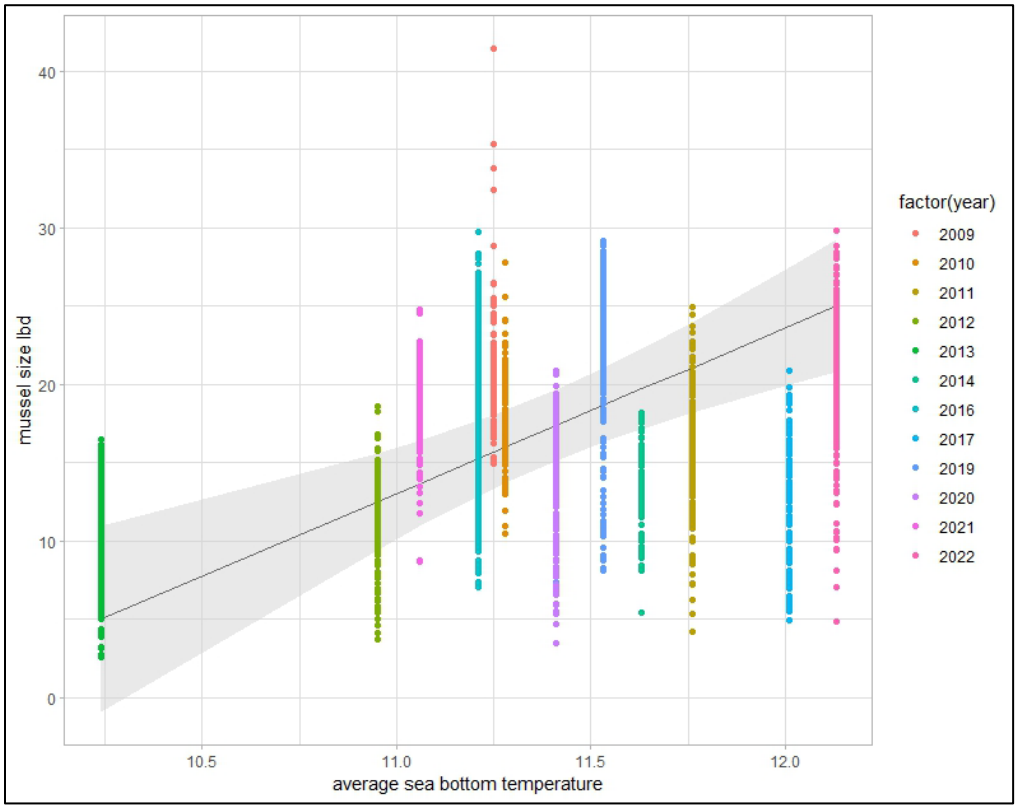

Fig. 24: Wexford/ Rosslare model prediction results, including regression line and predicted interval

For the other region (Cahore-Rusk Channel) (Fig. 25), the regression line indicates that the relationship between sea temperature and mussel length, although still positive, is not as pronounced as in the Wexford-Rosslare region. The lowest recorded length in 2013 still corresponds to the lowest SBT value, but the largest recorded length in 2009, 2011, 2016 and 2021 do not correlate with the highest temperatures observed (2011, 2014 and 2022). From a prediction aspect, the width of the error bands indicates a greater level of uncertainty.

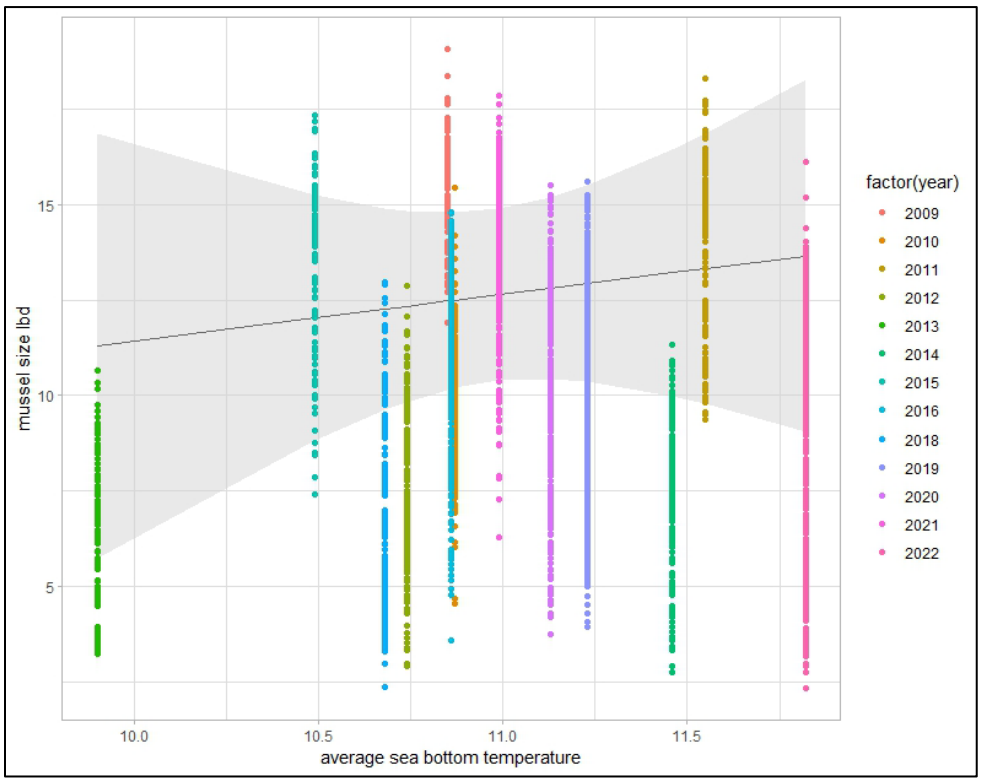

Fig. 25: Cahore/ Rusk Channel model prediction results, including regression line and predicted interval

Detailed scripts of the procedure and results for each scenario are available in the Appendix.

3.3.3 Evaluation of the assumptions based on diagnostic results

Evaluations of the last iteration of the model for both locations indicate that assumptions were not fully met (see graphs in Appendix). Plots generated for residuals versus fitted to assess linearity suggested non- linear relationships. Looking at the normality of the residuals, assumptions were partially met. Q-Q plots still showed some level of deviation in the tails, indicating that although residuals were approximately normal, they were not perfectly normal. Checking for homoscedasticity, the residuals for both Wexford and Cahore last models have some level of heteroscedasticity, indicating that the assumption of constant variance is violated. Finally, the Durbin-Watson test for both locations indicates a significant positive autocorrelation, meaning the residuals errors are not independent.

3.4. Discussion

This study found that low water temperature during the larval phase has an impact on the size of the related seed mussels. It also demonstrated that the length of seed mussels at the recruitment locations varies from year to year and can include overwintering seed mussels. Finally, it identified that sea temperature may not be the only factor explaining the year-to-year seed mussel length variations in the wild.

The coefficient estimates from the LMMs in both regions show that lower sea bottom temperatures negatively affect the length of the seed mussels. Furthermore, the negative coefficient for sea bottom temperature in both cases implies that as temperature decreases, the predicted size of the seed also decreases. The coefficient for the interaction term suggests that the effect of temperature on seed mussel sizes changes with time, but it remains negative, implying that lower temperatures are consistently associated with smaller sizes. Consequently, it is possible to conclude that lower sea bottom temperatures during the planktonic phase are likely affecting the size of the seed mussels settled on the seabed. The lowest average and daily cumulative sea temperatures over the expected spring larvae cycle were recorded in 2013 for both studied regions. This also corresponded to the observation of smaller mussel lengths on the beds (Fig.22 and 23). Lower temperatures during the larvae cycle have been shown to delay metamorphosis (Bayne, 1965) and to slow down larvae growth when reaching below 10^{o}C (Brenko and Calabrese, 1969). The average SBT during the 2013 spring was 10.24 ^{o}C (lowest: 6.06 ^{o}C) for the Wexford/ Rosslare sector and 9.90 ^{o}C (lowest: 6.08 ^{o}C) for the Cahore/ Rusk Channel sector. It is, therefore, possible that the 2013 mussel larvae may have developed slower than in other years.

Year-on-year variations of the seed mussel length, sampling time and sea bottom temperatures were observed throughout the data. In the Wexford-Rosslare region, the results indicate that 2009 and 2010 likely correspond to seed mussel settlement occurring the previous autumn, as both years presented relatively large mussel cohorts at an early stage in the year (Week 15 and 17). Autumn settlement, occurring in 2010, also appeared to be the reason for larger seed mussel

length observed in the early part of 2011 (Week 17) in the Cahore-Rusk Channel region. Considering the environmental conditions in winter would not be suitable for spawning (Chipperfield, 1953; Aldrich and Crowley, 1986; King *et al.*, 1989), it is unlikely that there would be a subsequent settlement in January which would have produced these mussels. The average growth of newly settled seed mussels is around 7 mm per month (Pérez-Camacho *et al.*, 1995; pers. obs.); when the animals are submerged, it is highly unlikely that this growth would observed during the winter months as they present unsuitable conditions for larvae growth (Pechenik *et al.*, 1990; Silke and Cusack, 2012). In this case, it is likely that the 2011 mussels resulted from a late autumn spawning, as observed by King *et al.* (1989) and that the seed mussel continued to grow at a lower rate during the winter months.

Finally, a decreasing trend for sea water temperature was observed from 2011 to 2013 year (Tables 1 and 2). This trend correlates with a reduction in the mussel length for those years (Fig. 20 and 23). However, temperature decreasing trend was also observed between 2019 and 2021, but it did not result in smaller mussels for those years (also in Fig.20 and 23). Both prediction models (Fig. 24 and 25) indicate a degree of uncertainty with regard to the effect of sea temperature on mussel size, being more pronounced in the results for the Cahore-Rusk Channel region. This uncertainty implies that although sea temperature during the planktonic phase appears critical, more so in the Wexford-Rosslare region, other factors such as food availability, predation, and tidal currents might need to be considered. Indeed, based on the diagnostics results, the assumptions of linearity, homoscedasticity, normality, and independence of residuals are not fully met in the model used in this study. This suggests that this linear mixed model may not be entirely appropriate in its current form and would require to be refined, mainly to address the presence of autocorrelation.

The literature review undertaken at the start of the project provided sufficient evidence to suggest that sea temperature is the main environmental variable which affects seed mussel growth (Bayne, 1965; Pechenik *et al.*, 1990; Zippay and Helmuth, 2012). The literature review also highlighted that sea temperatures affect the level of predation (Beukema and Dekker, 2014); as

a result, predation was not used as a variable in this study. In addition, there is also a lack of data on predation of seed mussel beds in Irish waters. The other environmental variables that could be considered are tidal currents and food availability. Tidal currents and food availability might explain some of the uncertainties in the current models. Hydrodynamic models have frequently been used to track the dispersal of larvae (Robins *et al.*, 2013; Demmer *et al.*, 2022), but their application in studies on established beds is less frequent. Fuentes et al. (2015) noted that hydrodynamics forces appear to be the main cause of mortality of larvae post-settlement due to dislodgement and transport to unsuitable growing grounds. Food availability is obviously a factor which influences growth (Sprung, 1984a); however, studies have shown both positive and negative relationships between mussel growth and food concentration (Sarà *et al.*, 1998; Bergström and Lindegarth, 2016). Furthermore, it has been observed that sea temperature below 12^{o}C has a negative effect on the ingestion of food by mussel larvae (Sprung, 1984c, 1984a). Therefore, food availability was not considered in this study.

In conclusion, there are a multitude of factors affecting seed mussel settlements, which makes it challenging to assess the reasons for recruitment variations. This study proved that sea temperature is one of the main factors affecting mussel recruitment, but other environmental factors could be considered for predicting recruitment patterns. Development of local models of larvae dispersion (Le Gendre *et al.*, 2014b; Demmer *et al.*, 2022) can improve understanding of larval transport pathways from source to sink. Furthermore, high-resolution modelled data for chlorophyll, currents, seabed type, seabed shear stress, and sediment mobility could help understand and predict variations in seed mussel recruitment.

Chapter 4: Conclusion

The objective of this thesis was to gain a better understanding of the dynamics of subtidal seed mussel recruitment on the southeast coast of Ireland. The management of seed mussel beds, either for conservation or exploitation purposes, can greatly benefit from the collection of dependable data such as their spatial distribution, abundance, size and also their response to different environmental conditions.

A large number of studies have been carried out on mussel species, covering subjects including genetic distribution, larvae dispersion, effects of predation, spatial organisation on the seabed and survivability. However, because of their coastal distribution, it is clear that mussel population dynamics are affected by coastal environmental factors. Mussel beds are located in sheltered shallow waters and mudflats but also in rocky and coarse sediment (more dynamic) open waters. This variability of habitats can make the identification of mussel beds challenging. Intertidal settlement can be visually assessed on foot at low water; however, subtidal beds require the deployment of remote sensing equipment, such as acoustic devices, and extensive ground truthing to provide reliable data.

This study has shown that side scan sonar provides an effective and reliable tool to map the extent of seed mussel beds located in subtidal areas. Using GIS software to combine the generated acoustic imagery with extensive sampling, it was possible to calculate an accurate estimation of the seed mussel biomass. This method was verified by using a similar process to estimate the remaining biomass post-fishery added to the reported fishing figures. The final results indicated that the original biomass was underestimated by 3% in comparison with the combined fishing figures and remaining biomass. Although this method has proven to be successful, it still requires manual digitisation of the beds' boundaries and the collection of substantial numbers of samples. However, those processes can be streamlined by, for example, the introduction of new machine learning technologies to extract the seed mussel settlement extent from the generated side scan sonar image to remove any possible human error or using statistical bootstrapping of the samples

to make their collection more efficient. High-resolution MBES data could also be integrated into the designation and visualisation of the seed mussel bed extent and topography. Backscatter data merged with a small-scale bathymetric grid can be draped with the side scan sonar mosaic, allowing for 3-D visualisation of the seed mussel bed. This would provide a great insight into the relationship between sonar features, bed elevation and seabed type, as previously observed on the intertidal seed mussel beds. It is planned in the years following the experiment carried out in this thesis to investigate subtidal seed mussel topography using mini Autonomous Underwater Vehicles (AUVs), which combines high-frequency side scan sonar and photogrammetry. One of the challenges faced in the estimation of subtidal seed mussel beds is the biomass coverage variation throughout the bed. Although the side scan sonar data provides mussel features visualisation, it has very limited capacity in translating the biomass density variations. Real colour photogrammetry of the seed mussel settlement combined with high-frequency side scan sonar could allow for a more realistic definition of the mussel bed extent and biomass coverage variations, thus directly related to more precise biomass estimations. However, those biomass estimations are entirely dependent on successful seed mussel recruitment, which, as indicated in this thesis, is difficult to predict.

Sea temperature variations are one of the main limiting factors affecting the maturation of the adult mussels, the larval development, and the overall growth of the mussels. The study also demonstrated that during years with relatively low sea bottom temperatures during spring, the growth of seed mussels where reduced. By selecting two of the most productive locations for seed mussel beds on the southeast coast of Ireland and by using seed mussel lengths recorded between 2009 and 2022, it was possible to visualise recruitment size variations between those years. The results from statistical models combining those measurements with weekly-averaged sea bottom temperature and sampling period (week) indicated that sea bottom temperature affected seed mussel growth on both sites. However, only considering sea bottom temperature may not explain all recruitment variations. Additional independent variables, such as food availability and seabed shear stress, which were not included in the model used in the thesis, should be considered for further investigations. As indicated in chapter 1, food availability is

directly linked to growth and seabed shear stress is the first cause of seed mussel bed erosion. Those two parameters, added to sea temperature variations, appear to be the most common limiting factor of seed mussel bed recruitment. Translating those variations through a time period instead of a single point in time would also be more relevant and could indicate the combined effect of those variables on recruitment patterns. Analysis of various scenarios based on historical data generated from oceanographic models could provide valuable insight into the reasons behind poor and good recruitment years. Prediction models used in a similar way could also provide possible early indicators of recruitment success.

Because of the complexity of the planktonic and settlement phases, further investigation should take place by using larval dispersal models that include larvae behaviour based on their age, statistical models considering other environmental variables generated by local-scale oceanographic models that relate to the recruitment of mussels, full broodstock quantification, qualitative assessment of mussel larvae and reliable biomass surveys for seed mussel beds.

References

Aldrich, J. C., and Crowley, M. 1986. Condition and variability in Mytilus edulis (L.) from different habitats in Ireland. Science, 52: 273–286.

Alexander, M. A., Scott, J. D., Friedland, K. D., Mills, K. E., Nye, J. A., Pershing, A. J., and Thomas, A. C. 2018. Projected sea surface temperatures over the 21st century: Changes in the mean, variability and extremes for large marine ecosystem regions of Northern Oceans. Elementa, 6.

Avdelas, L., Avdic-Mravlje, E., Borges Marques, A. C., Cano, S., Capelle, J. J., Carvalho, N., Cozzolino, M., *et al.* 2021. The decline of mussel aquaculture in the European Union: causes, economic impacts and opportunities. Reviews in Aquaculture, 13: 91–118.

Azpeitia, K., Rodríguez-Ezpeleta, N., and Mendiola, D. 2019. Settlement and recruitment pattern variability of the mussel Mytilus galloprovincialis Lmk. from SE Bay of Biscay (Basque Country). Regional Studies in Marine Science, 27: 100523. Elsevier B.V. https://doi.org/10.1016/j.rsma.2019.100523.

Baeta, M., Breton, F., Ubach, R., and Ariza, E. 2018. A socio-ecological approach to the declining Catalan clam fisheries. Ocean and Coastal Management, 154: 143–154. Elsevier. https://doi.org/10.1016/j.ocecoaman.2018.01.012.

Bates, D., Maechler, M., Bolker, B., and Steve Walker. 2015. Fitting Linear Mixed-Effects Models Using lme4. Journal of Statistical Software.

Bayne, B. L. 1964. Primary and Secondary Settlement in Mytilus edulis L. (Mollusca). The Journal of Animal Ecology, 33: 513. https://www.jstor.org/stable/2569 Accessed:

Bayne, B. L. 1965. Growth and the delay of metamorphosis of the larvae of Mytilus edulis (L.). Ophelia, 2: 1–47. Taylor & Francis Group. http://www.tandfonline.com/doi/abs/10.1080/00785326.1965.10409596 (Accessed 18 July 2019).

Beaugrand, G., and Reid, P. C. 2003. Long-term changes in phytoplankton, zooplankton and salmon related to climate. Global Change Biology, 9: 801–817.

Beaumont, A. R., Turner, G., Wood, A. R., and Skibinski, D. O. F. 2004. Hybridisations between Mytilus edulis and Mytilus galloprovincialis and performance of pure species and hybrid veliger larvae at different temperatures. Journal of Experimental Marine Biology and Ecology, 302: 177–188.

Beaz-Hidalgo, R., Balboa, S., Romalde, J. L., and Figueras, M. J. 2010. Diversity and pathogenecity of Vibrio species in cultured bivalve molluscs. Environmental Microbiology Reports, 2: 34–43.

Benabdelmouna, A., and Ledu, C. 2016. The mass mortality of blue mussels (Mytilus spp.) from the Atlantic coast of France is associated with heavy genomic abnormalities as evidenced by flow cytometry. Journal of Invertebrate Pathology, 138: 30–38. Elsevier Inc. http://dx.doi.org/10.1016/j.jip.2016.06.001.

Bergström, P., and Lindegarth, M. 2016. Environmental influence on mussel (Mytilus edulis) growth - A quantile regression approach. Estuarine, Coastal and Shelf Science, 171: 123–132.

Bertolini, C., Geraldi, N. R., Montgomery, W. I., and O'Connor, N. E. 2017. Substratum type and

conspecific density as drivers of mussel patch formation. Journal of Sea Research, 121: 24–32. Elsevier B.V. http://dx.doi.org/10.1016/j.seares.2017.01.004.

Bertolini, C., Cornellissen, B., Capelle, J., Koppel, J., and Bouma, T. J. 2019. Putting self-organization to the test: labyrinthine patterns as optimal solution for persistence. Oikos: oik.06373. John Wiley & Sons, Ltd (10.1111). https://onlinelibrary.wiley.com/doi/abs/10.1111/oik.06373 (Accessed 9 August 2019).

Beukema, J. J. 1992. Expected changes in the wadden sea benthos in a warmer world: Lessons from periods with mild winters. Netherlands Journal of Sea Research, 30: 73–79.

Beukema, J. J., and Dekker, R. 2005. Decline of recruitment success in cockles and other bivalves in the Wadden Sea: Possible role of climate change, predation on postlarvae and fisheries. Marine Ecology Progress Series, 287: 149–167.

Beukema, J. J., and Dekker, R. 2014. Variability in predator abundance links winter temperatures and bivalve recruitment: Correlative evidence from long-term data in a tidal flat. Marine Ecology Progress Series, 513: 1–15.

Beukema, J. J., Dekker, R., van Stralen, M. R., and de Vlas, J. 2015. Large-scale synchronization of annual recruitment success and stock size in Wadden Sea populations of the mussel Mytilus edulis L. Helgoland Marine Research, 69: 327–333. Springer Berlin Heidelberg.

Bierne, N., David, P., Boudry, P., and Bonhomme, F. 2002. Assortative fertilization and selection at larval stage in the mussels Mytilus edulis and M. galloprovincialis. Evolution, 56: 292–298.

BIM. (n.d.). Seed Mussel Survey Reports. http://www.bim.ie/our-publications/aquaculture/ (Accessed 18 December 2019).

BIM, and Loughs Agency. 2008. The Rising Tide - A Review of teh Bottom Grown Mussel Sector on the Island of Ireland. 173–173 pp. https://www.agriculture.gov.ie/media/migration/publications/2008/Mussel_Report08.pdf.

BIM. 2016. Side Scan Sonar Features Catalogue. https://www.researchgate.net/publication/358640202_Side_Scan_Sonar_Features_Catalogue_related_to_Aquaculture_and_Inshore_Fishing_Activities#fullTextFileContent.

BIM. 2019. 2018 Spring Mussel Larvae Monitoring, Aquaculture Technical Report. http://ispp.ie/wp-content/uploads/2019/03/2018-Spring-Mussel-Larvae-Monitoring-min.pdf.

BIM. 2020. Spring Mussel Larvae Monitoring 2019. https://bim.ie/publications/aquaculture/.

BIM. 2022. Annual Aquaculture Statistical Report. 2–3 pp.

Blanton, J. O., Wenner, E. L., Werner, F. E., and Knott, D. 1995. Effects of wind-generated coastal currents on the transport of blue crab megalopae on a shallow continental shelf. Bulletin of Marine Science, 57: 739–752.

Blöcker, A. M., Gutte, H. M., Bender, R. L., Otto, S. A., Sguotti, C., and Möllmann, C. 2023. Regime shift dynamics, tipping points and the success of fisheries management. Scientific Reports, 13: 1–11. Nature Publishing Group UK. https://doi.org/10.1038/s41598-022-27104-y.

Bowers, D. G., Gaffney, S., White, M., and Bowyer, P. 2002. Turbidity in the southern Irish Sea. Continental Shelf Research, 22: 2115–2126.

Brenko, M. H., and Calabrese, A. 1969. The combined effects of salinity and temperature on larvae of the mussel Mytilus edulis. Marine Biology, 4: 224–226.

Brierley, A. S., and Kingsford, M. J. 2009. Impacts of Climate Change on Marine Organisms and Ecosystems. Current Biology, 19: R602–R614. Elsevier Ltd. http://dx.doi.org/10.1016/j.cub.2009.05.046.

Brown, C. J., Cooper, K. M., Meadows, W. J., Limpenny, D. S., and Rees, H. L. 2002. Small-scale mapping of sea-bed assemblages in the eastern English Channel using sidescan sonar and remote sampling techniques. Estuarine, Coastal and Shelf Science, 54: 263–278.

Brown, C. J., Mitchell, A., Limpenny, D. S., Robertson, M. R., Service, M., and Golding, N. 2005. Mapping seabed habitats in the Firth of Lorn off the west coast of Scotland: Evaluation and comparison of habitat maps produced using the acoustic ground-discrimination system, RoxAnn, and sidescan sonar. ICES Journal of Marine Science, 62: 790–802.

Brown, C. J., Smith, S. J., Lawton, P., and Anderson, J. T. 2011. Benthic habitat mapping: A review of progress towards improved understanding of the spatial ecology of the seafloor using acoustic techniques. Estuarine, Coastal and Shelf Science, 92: 502–520. Elsevier Ltd. http://dx.doi.org/10.1016/j.ecss.2011.02.007.

Brown, J., Carrillo, L., Fernand, L., Horsburgh, K. J., Hill, A. E., Young, E. F., and Medler, K. J. 2003. Observations of the physical structure and seasonal jet-like circulation of the Celtic Sea and St. George's Channel of the Irish Sea. Continental Shelf Research, 23: 533–561.

Browne, T. J. 1904. Report on the Shell-fish Layings on the Irish Coast. 270 pp. http://dx.doi.org/10.1016/j.cirp.2016.06.001%0Ahttp://dx.doi.org/10.1016/j.powtec.2016.12.055%0Ahttps://doi.org/10.1016/j.ijfatigue.2019.02.006%0Ahttps://doi.org/10.1016/j.matlet.2019.04.024%0Ahttps://doi.org/10.1016/j.matlet.2019.127252%0Ahttp://dx.doi.o.

Calderwood, J., O'Connor, N. E., and Roberts, D. 2016. Efficiency of starfish mopping in reducing predation on cultivated benthic mussels (Mytilus edulis Linnaeus). Aquaculture, 452: 88–96. Elsevier B.V. http://dx.doi.org/10.1016/j.aquaculture.2015.10.024.

Capelle, J. J., Wijsman, J. W. M., Schellekens, T., van Stralen, M. R., Herman, P. M. J., and Smaal, A. C. 2014. Spatial organisation and biomass development after relaying of mussel seed. Journal of Sea Research, 85: 395–403. Elsevier B.V. http://dx.doi.org/10.1016/j.seares.2013.07.011.

Capelle, J. J., Hartog, E., van den Bogaart, L., Jansen, H. M., and Wijsman, J. W. M. 2021a. Adaptation of gill-palp ratio by mussels after transplantation to culture plots with different seston conditions. Aquaculture, 541: 736794. Elsevier B.V. https://doi.org/10.1016/j.aquaculture.2021.736794.

Capelle, J. J., Garcia, A. B., Kamermans, P., Engelsma, M. Y., and Jansen, H. M. 2021b. Observations on recent mass mortality events of marine mussels in the Oosterschelde, the Netherlands. Aquaculture International, 29: 1737–1751.

Chipperfield, P. N. J. 1953. Observations on the breeding and settlement of mytilus edulis (L.) in British waters. Journal of the Marine Biological Association of the United Kingdom, 32: 449–476.

Clements, J. C., Hicks, C., Tremblay, R., and Comeau, L. A. 2018. Elevated seawater temperature, not pCO2, negatively affects post-spawning adult mussels (Mytilus edulis) under food limitation. Conservation Physiology, 6.

Clements, J. C., Ramesh, K., Nysveen, J., Dupont, S., and Jutfelt, F. 2021. Animal size and sea water temperature, but not pH, influence a repeatable startle response behaviour in a wide-ranging marine mollusc. Animal Behaviour. Elsevier Ltd. https://doi.org/10.1016/j.anbehav.2020.12.008.

Cochard, M.-L., and Paul, C. 2016. Les gisements mouliers de l ' Est Cotentin - Compte-rendu de la prospection 2016. https://archimer.ifremer.fr/doc/00370/48094/48206.pdf.

Cochrane, G. R., and Lafferty, K. D. 2002. Use of acoustic classification of sidescan sonar data for mapping benthic habitat in the Northern Channel Islands, California. Continental Shelf Research, 22: 683–690.

Coghlan, B., and Gosling, E. 2007. Genetic structure of hybrid mussel populations in the west of Ireland: Two hypotheses revisited. Marine Biology, 150: 841–852.

Commito, J. A., and Rusignuolo, B. R. 2000. Structural complexity in mussel beds: The fractal geometry of surface topography. Journal of Experimental Marine Biology and Ecology, 255: 133–152.

Commito, J. A., and Dankers, N. M. J. A. 2001. Dynamics of Spatial and Temporal Complexity in European and North American Soft-Bottom Mussel Beds: 39–59.

Commito, J. A., Commito, A. E., Platt, R. V., Grupe, B. M., Piniak, W. E. D., Gownaris, N. J., Reeves, K. A., *et al.* 2014. Recruitment facilitation and spatial pattern formation in soft-bottom mussel beds. Ecosphere, 5.

Copernicus Marine Service. 2022. Ocean Physical and Biogeochemical reanalysis: 1–29.

Coscia, I., Robins, P. E., Porter, J. S., Malham, S. K., and Ironside, J. E. 2013. Modelled larval dispersal and measured gene flow: Seascape genetics of the common cockle Cerastoderma edule in the southern Irish Sea. Conservation Genetics, 14: 451–466.

Coste, V. 1861. Voyage D'Exploration sur le Littoral de la france et de L'Italie. Musée Maritime de la Tremblade. https://www.biodiversitylibrary.org/bibliography/39381#/summary.

Crawford, T. W., Commito, J. A., and Borowik, A. M. 2006. Fractal characterization of Mytilus edulis L. spatial structure in intertidal landscapes using GIS methods. Landscape Ecology, 21: 1033–1044.

Crépin, A.-S., Biggs, R., Polasky, S., Troell, M., and de Zeeuw, A. 2012. Regime shifts and management. Ecological Economics, 84: 15–22. Elsevier B.V. http://dx.doi.org/10.1016/j.ecolecon.2012.09.003.

DAFM. 2018. Irish Sea Mussel Seed Fishery. http://www.fishingnet.ie/sea-fisheriesinnaturaareas/currentconsultation/irishseamusselseedfishery/.

Dankers, N., Brinkman, A. G., Meijboom, A., and Dijkman, E. 2001. Recovery of intertidal mussel beds in the Waddensea: Use of habitat maps in the management of the fishery. Hydrobiologia, 465: 21–30.

Dardignac-Corbeil, M. J., and Prou, J. 1995. A propos des problèmes de captage de naissain de moules (Mytilus edulis L .) dans le Pertuis Breton de 1989 à 1991 : Observations préliminaires. Haliotis, 31: 13–31.

Dare, P. J. 1982. Notes on the Swarming Behaviour and Population Density of Asterias Rubens L. (Echinodermata: Asteroidea) Feeding on the Mussel, Mytilus Edulis L. ICES Journal of Marine Science, 40: 112–118.

Davenport, J., and Chen, X. 1987. A comparison of methods for the assessment of condition in the mussel (Mytilus edulis L.). Journal of Molluscan Studies, 53: 293–297.

Demmer, J., Robins, P., Malham, S., Lewis, M., Owen, A., Jones, T., and Neill, S. 2022. The role of wind in controlling the connectivity of blue mussels (Mytilus edulis L.) populations. Movement Ecology, 10: 1–15. BioMed Central. https://doi.org/10.1186/s40462-022-00301-0.

Dereli, M. A., and Tercan, E. 2020. Assessment of Shoreline Changes using Historical Satellite Images and Geospatial Analysis along the Lake Salda in Turkey. Earth Science Informatics, 13: 709–718. Earth Science Informatics.

Derolez, V., Malet, N., Fiandrino, A., Lagarde, F., Richard, M., Ouisse, V., Bec, B., *et al.* 2020. Fifty years of ecological changes: Regime shifts and drivers in a coastal Mediterranean lagoon during oligotrophication. Science of the Total Environment, 732.

deYoung, B., Barange, M., Beaugrand, G., Harris, R., Perry, R. I., Scheffer, M., and Werner, F. 2008. Regime shifts in marine ecosystems: detection, prediction and management. Trends in Ecology and Evolution, 23: 402–409.

Diaz, R. J., Solan, M., and Valente, R. M. 2004. A review of approaches for classifying benthic habitats and evaluating habitat quality. Journal of Environmental Management, 73: 165–181.

Diesing, M., Green, S. L., Stephens, D., Lark, R. M., Stewart, H. A., and Dove, D. 2014. Mapping seabed sediments: Comparison of manual, geostatistical, object-based image analysis and machine learning approaches. Continental Shelf Research, 84: 107–119. Elsevier. http://dx.doi.org/10.1016/j.csr.2014.05.004.

Dingemanse, N. J., and Dochtermann, N. A. 2013. Quantifying individual variation in behaviour: Mixed-effect modelling approaches. Journal of Animal Ecology, 82: 39–54.

Dutertre, M., Beninger, P. G., Barillé, L., Papin, M., and Haure, J. 2010. Rising water temperatures, reproduction and recruitment of an invasive oyster, Crassostrea gigas, on the French Atlantic coast. Marine Environmental Research, 69: 1–9. Elsevier Ltd. http://dx.doi.org/10.1016/j.marenvres.2009.07.002.

Edward, C. A., and Sibinski, D. O. . 1987. Genetic variation of mitochondrial DNA in mussel (Mytilus edulis and M.galloprovinicialis) population from South West England and South Wales, 556: 547–556.

Elliott, J., Holmes, K., Chambers, R., Leon, K., and Wimberger, P. 2008. Differences in morphology and habitat use among the native mussel Mytilus trossulus, the non-native M. galloprovincialis, and their hybrids in Puget Sound, Washington. Marine Biology, 156: 39–53.

Elner, R. W. 1978. The mechanics of predation by the shore crab, Carcinus maenas (L.), on the edible mussel, Mytilus edulis L. Oecologia, 36: 333–344.

ESRI. (n.d.). How IDW works. https://desktop.arcgis.com/en/arcmap/10.3/tools/spatial-analyst-

toolbox/how-idw-works.htm.

ESRI. (n.d.). ArcGIS Field Maps. https://www.esri.com/en-us/arcgis/products/arcgis-field-maps/overview.

European Environment Agency. 2019. Mytilus edulis beds on littoral sediments. https://eunis.eea.europa.eu/habitats/1925.

Fakiris, E., Blondel, P., Papatheodorou, G., Christodoulou, D., Dimas, X., Georgiou, N., Kordella, S., *et al.* 2019. Multi-frequency, multi-sonar mapping of shallow habitats-efficacy and management implications in the National Marine Park of Zakynthos, Greece. Remote Sensing, 11.

Feser, F., Barcikowska, M., Krueger, O., Schenk, F., Weisse, R., and Xia, L. 2015. Storminess over the North Atlantic and northwestern Europe-A review. Quarterly Journal of the Royal Meteorological Society, 141: 350–382.

Fly, E. K., and Hilbish, T. J. 2013. Physiological energetics and biogeographic range limits of three congeneric mussel species. Oecologia, 172: 35–46.

Fly, E. K., Hilbish, T. J., Wethey, D. S., and Rognstad, R. L. 2015. Physiology and Biogeography: The Response of European Mussels (Mytilus spp.) to Climate Change * . American Malacological Bulletin, 33: 136–149.

Folmer, E. O., Drent, J., Troost, K., Büttger, H., Dankers, N., Jansen, J., van Stralen, M., *et al.* 2014. Large-Scale Spatial Dynamics of Intertidal Mussel (Mytilus edulis L.) Bed Coverage in the German and Dutch Wadden Sea. Ecosystems, 17: 550–566.

Frederick, C., Villar, S., and Michalopoulou, Z.-H. 2020. Seabed classification using physics-based modeling and machine learning. The Journal of the Acoustical Society of America, 148: 859–872.

Fuentes-Santos, I., and Labarta, U. 2015. Spatial patterns of larval settlement and early post-settlement survivorship of Mytilus galloprovincialis in a Galician Ría (NW Spain). Effect on recruitment success. Regional Studies in Marine Science, 2: 1–10. Elsevier B.V. http://dx.doi.org/10.1016/j.rsma.2015.08.006.

Garland, E. D., Zimmer, C. A., and Lentz, S. J. 2002. Larval distributions in inner-shelf waters: The roles of wind-driven cross-shelf currents and diel vertical migrations. Limnology and Oceanography, 47: 803–817.

Gilg, M. R., and Hilbish, T. J. 2003a. Patterns of Larval Dispersal and Their Effect on the Maintenance of a Blue Mussel Hybrid Zone in Southwestern England. Society for the Study of Evolution, 57: 1061–1077.

Gilg, M. R., and Hilbish, T. J. 2003b. The Geography of Marine Larval Dispersal : Coupling Genetics with Fine-Scale Physical Oceanography. Ecology, 84: 2989–2998.

Godet, L., Fournier, J., Toupoint, N., and Olivier, F. 2009. Mapping and monitoring intertidal benthic habitats: A review of techniques and a proposal for a new visual methodology for the european coasts. Progress in Physical Geography, 33: 378–402.

Gosling, E., Doherty, S., and Howley, N. 2008. Genetic characterization of hybrid mussel (Mytilus) populations on Irish coasts. Journal of the Marine Biological Association of the United Kingdom, 88:

341–346.

Gosling, E. 2015. Marine Bivalve Molluscs - Second Edition. John Wiley & Sons, Ltd (10.1111).

Gosling, E. 2022. Marine Mussels: Ecology, Physiology, Genetics and Culture. Wiley. 874 pp.

Gosling, E. M., and Wilkins, N. P. 1981. Ecological Genetics of the Mussels Mytilus edulis and M. galloprovincialis on Irish Coasts. Marine Ecology Progress Series, 4: 221–227.

Guinan, J., McKeon, C., O'Keeffe, E., Monteys, X., Sacchetti, F., Coughlan, M., and Nic Aonghusa, C. 2020. NFOMAR data in the EMODnet Geology data portal supports marine spatial planning and offshore energy development in the Irish offshore. Quarterly Journal of Engineering Geology and Hydrogeology INFOMAR, Mapping th. http://qjegh.lyellcollection.org/ by.

Gurney-Smith, H. J., Wade, A. J., and Abbott, C. L. 2017. Species composition and genetic diversity of farmed mussels in British Columbia, Canada. Aquaculture, 466: 33–40. Elsevier B.V. http://dx.doi.org/10.1016/j.aquaculture.2016.08.038.

Haase, A. T., Eggleston, D. B., Luettich, R. A., Weaver, R. J., and Puckett, B. J. 2012. Estuarine , Coastal and Shelf Science Estuarine circulation and predicted oyster larval dispersal among a network of reserves. Estuarine, Coastal and Shelf Science, 101: 33–43. Elsevier Ltd. http://dx.doi.org/10.1016/j.ecss.2012.02.011.

Hastings, R. A., Rutterford, L. A., Freer, J. J., Collins, R. A., Simpson, S. D., and Genner, M. J. 2020. Climate Change Drives Poleward Increases and Equatorward Declines in Marine Species. Current Biology, 30: 1572-1577.e2. Elsevier Ltd. https://doi.org/10.1016/j.cub.2020.02.043.

Hervas, A., Tully, O., Hickey, J., Keeffe, E. O., and Kelly, E. 2008. Assessment, Monitoring and Management of the Dundalk Bay and Waterford Estuary Cockle (*Cerastoderma edule*) Fisheries in 2007. 38 pp.

Hibbert, A., Royston, S. J., Horsburgh, K. J., Leach, H., and Hisscott, A. 2015. An empirical approach to improving tidal predictions using recent real-time tide gauge data. Journal of Operational Oceanography, 8: 40–51.

Hilbish, T. J., Mullinax, A., Dolven, S. I., Meyer, A., Koehn, R. K., and Rawson, P. D. 2000. Origin of the antitropical distribution pattern in marine mussels (Mytilus spp.): Routes and timing of transequatorial migration. Marine Biology, 136: 69–77.

Hilgerloh, G. 1997. Predation by birds on blue mussel Mytilus edulis beds of the tidal flats of Spiekeroog (southern North Sea). Marine Ecology Progress Series, 146: 61–72.

Hlavac, and Marek. 2022. stargazer: Well-Formatted Regression and Summary Statistics Tables. https://cran.r-project.org/package=stargazer.

Hughes, D. J., and Atkinson, R. J. A. 1997. A towed video survey of megafaunal bioturbation in the north-eastern Irish Sea. Journal of the Marine Biological Association of the United Kingdom, 77: 635–653. Prifysgol Bangor University CBO.

Hunt, H. L., and Scheibling, R. E. 1996. Physical and biological factors influencing mussel (Mytilus trossulus, M. edulis) settlement on a wave-exposed rocky shore. Marine Ecology Progress Series,

142: 135–145.

Huston, M. A., and Deangelis, D. L. 1987. Size bimodality in monospecific populations: a critical review of potential mechanisms. American Naturalist, 129: 678–707.

Ireland, G. of the R. of. 2006. Sea-Fisheries and Maritime Jurisdiction Act 2006.

James, M. K., Polton, J. A., Brereton, A. R., Howell, K. L., Nimmo-smith, W. A. M., and Knights, A. M. 2019. Reverse engineering field-derived vertical distribution profiles to infer larval swimming behaviors: 1–6.

Janowski, L., Wroblewski, R., Rucinska, M., Kubowicz-Grajewska, A., and Tysiac, P. 2022. Automatic classification and mapping of the seabed using airborne LiDAR bathymetry. Engineering Geology, 301: 106615. Elsevier B.V. https://doi.org/10.1016/j.enggeo.2022.106615.

Johansson, I., Saurel, C., Taylor, D., and Kjerulf, J. 2024. Longevity of subtidal mussel beds (Mytilus edulis) in eutrophic coastal areas. Journal of Sea Research: 102506. Journal of Sea Research. https://doi.org/10.1016/j.seares.2024.102506.

Kartavtsev, Y. P., Masalkova, N. A., and Katolikova, M. V. 2018. Genetic and Morphometric Variability in Settlements of Two Mussel Species (Mytilus ex. gr. Edulis), Mytilus trossulus a. Journal of Shellfish Research, 37: 103–119.

Kijewski, T., Śmietanka, B., Zbawicka, M., Gosling, E., Hummel, H., and Wenne, R. 2011. Distribution of Mytilus taxa in European coastal areas as inferred from molecular markers. Journal of Sea Research, 65: 224–234.

Kijewski, T., Zbawicka, M., Strand, J., Kautsky, H., Kotta, J., Rätsep, M., and Wenne, R. 2019. Random forest assessment of correlation between environmental factors and genetic differentiation of populations: Case of marine mussels Mytilus. Oceanologia, 61: 131–142. Elsevier B.V. http://dx.doi.org/10.1016/j.oceano.2018.08.002.

King, N. G., Wilmes, S. B., Smyth, D., Tinker, J., Robins, P. E., Thorpe, J., Jones, L., *et al.* 2021. Climate change accelerates range expansion of the invasive non-native species, the Pacific oyster, Crassostrea gigas. ICES Journal of Marine Science, 78: 70–81.

King, P. A., McGrath, D., and Gosling, E. M. 1989. Reproduction and settlement of mytilus edulis on an exposed rocky shore in galway bay, west coast of ireland. Journal of the Marine Biological Association of the United Kingdom, 69: 355–365.

Knights, A. M., Crowe, T. P., and Burnell, G. 2006. Mechanisms of larval transport: Vertical distribution of bivalve larvae varies with tidal conditions. Marine Ecology Progress Series, 326: 167–174.

Knights, A. M. 2012. Spatial variation in body size and reproductive condition of subtidal mussels: Considerations for sustainable management. Fisheries Research, 113: 45–54. Elsevier B.V. http://dx.doi.org/10.1016/j.fishres.2011.09.002.

Koehn, M. R. K., Hilbish, T. J., Mullinax, a., Meyer, a., Rawson, P. D., Dolven, S. I., and Koehn, R. K. 2000. Origin of the antitropical distribution pattern in marine mussels (Mytilus spp .): routes and timing of transequatorial migration. Marine Biology, 136: 69–77.

Lapworth, A. 2011. Wind against tide. Weather, 66: 100–102.

Larsson, J., Lind, E. E., Corell, H., Grahn, M., Smolarz, K., and Lönn, M. 2017. Regional genetic differentiation in the blue mussel from the Baltic Sea area. Estuarine, Coastal and Shelf Science, 195: 98–109.

Le Gendre, R., Morin, J., Maheux, F., Fournier, F., Simon, B., Cochard, M.-L., Pierre-Duplessix, O., *et al.* 2014a. DILEMES DIspersion LarvairE de Mytilus Edulis en baie de Seine. 1–75 pp. https://archimer.ifremer.fr/doc/00188/29916/28376.pdf.

Le Gendre, R., Morin, J., Maheux, F., Fournier, F., Simon, B., Cochard, M.-L., Pierre-Duplessix, O., *et al.* 2014b. DILEMES DIspersion LarvairE de Mytilus Edulis en baie de Seine. 1–75 pp. https://archimer.ifremer.fr/doc/00188/29916/28376.pdf.

Liu, Q. X., Weerman, E. J., Herman, P. M. J., Olff, H., and van de Koppel, J. 2012. Alternative mechanisms alter the emergent properties of self-organization in mussel beds. Proceedings of the Royal Society B: Biological Sciences, 279: 2744–2753.

Liu, Q. X., Doelman, A., Rottschafer, V., De Jager, M., Herman, P. M. J., Rietkerk, M., and Van De Koppel, J. 2013. Phase separation explains a new class of selforganized spatial patterns in ecological systems. Proceedings of the National Academy of Sciences of the United States of America, 110: 11905–11910.

Liu, Q. X., Herman, P. M. J., Mooij, W. M., Huisman, J., Scheffer, M., Olff, H., and Van De Koppel, J. 2014. Pattern formation at multiple spatial scales drives the resilience of mussel bed ecosystems. Nature Communications, 5: 1–7. Nature Publishing Group. http://dx.doi.org/10.1038/ncomms6234.

Lüdecke, D. 2018. “ggeffects: Tidy Data Frames of Marginal Effects from Regression Models.” Journal of Open Source Software. https://doi.org/10.21105/joss.00772.

Lupo, C., Bougeard, S., Le Bihan, V., Blin, J. L., Allain, G., Azéma, P., Benoit, F., *et al.* 2021. Mortality of marine mussels Mytilus edulis and M. galloprovincialis: systematic literature review of risk factors and recommendations for future research. Reviews in Aquaculture, 13: 504–536.

Lynch, S. A., Morgan, E., Carlsson, J., Mackenzie, C., Wooton, E. C., Rowley, A. F., Malham, S., *et al.* 2014. The health status of mussels, Mytilus spp., in Ireland and Wales with the molecular identification of a previously undescribed haplosporidian. Journal of Invertebrate Pathology, 118: 59–65. Elsevier Inc. http://dx.doi.org/10.1016/j.jip.2014.02.012.

Lynch, S. A., Leary, A. C. B. O., and Culloty, E. M. S. C. 2020. Northward establishment of the mediterranean mussel Mytilus galloprovincialis limited by changing climate. Biological Invasions, 6. Springer International Publishing. https://doi.org/10.1007/s10530-020-02294-6.

Maguire, J., Knights, T., Burnell, G., Crowe, T., O’Beirn, F., McGrath, D., Ferns, M., *et al.* 2007. Management recommendations for the sustainable exploitation of mussel seed in the Irish Sea.

Marine Institute, and BIM. 2020. Shellfish Stocks and Fisheries Review.

Mc Quaid, C. D., and Phillips, T. E. 2000. Limited wind-driven dispersal of intertidal mussel larvae: in situ evidence from the plankton and the spread of the invasive species Mytilus galloprovincialis in South Africa. Marine Ecology Progrees Series, 201: 211–220. https://www.int-

res.com/abstracts/meps/v201/p211-220/.

Minnett, P. J. 2014. Sea surface temperature. Encyclopedia of Earth Sciences Series: 754–759.

Molinet, C., Díaz, M., Marín, S. L., Astorga, M. P., Ojeda, M., Cares, L., and Asencio, E. 2017. Relation of mussel spatfall on natural and artificial substrates: Analysis of ecological implications ensuring long-term success and sustainability for mussel farming. Aquaculture, 467: 211–218. Elsevier B.V. http://dx.doi.org/10.1016/j.aquaculture.2016.09.019.

Morello, S. L., and Yund, P. O. 2016. Response of competent blue mussel (Mytilus edulis) larvae to positive and negative settlement cues. Journal of Experimental Marine Biology and Ecology, 480: 8–16. Elsevier B.V. http://dx.doi.org/10.1016/j.jembe.2016.03.019.

Morgan, S. G., and Fisher, J. L. 2010. Larval behavior regulates nearshore retention and offshore migration in an upwelling shadow and along the open coast. Marine Ecology Progress Series, 404: 109–126.

Newell, C. R., Hidu, H., McAlice, B. J., Podniesinski, G., Short, F., and Kindblom, L. 1991. Recruitment and Commercial Seed Procurement of the Blue Mussel Mytilus edulis in Maine. Journal of the World Aquaculture Society, 22: 134–152.

Nicolle, A., Dumas, F., Foveau, A., Foucher, E., and Thiébaut, E. 2013. Modelling larval dispersal of the king scallop (Pecten maximus) in the English Channel: Examples from the bay of Saint-Brieuc and the bay of Seine. Ocean Dynamics, 63: 661–678.

Pechenik, J. A., Eyster, L. S., Widdows, J., and Bayne, B. L. 1990. The influence of food concentration and temperature on growth and morphological differentiation of blue mussel Mytilus edulis L. larvae. Journal of Experimental Marine Biology and Ecology, 136: 47–64.

Pecl, G. T., Araújo, M. B., Bell, J. D., Blanchard, J., Bonebrake, T. C., Chen, I. C., Clark, T. D., *et al.* 2017. Biodiversity redistribution under climate change: Impacts on ecosystems and human well-being. Science, 355.

Pépin, J. F., Benabdelmouna, A., Degremont, L., Guesdon, S., Le Moine, O., Morga, B., Bierne, N., *et al.* 2017. Mortalités de moules bleues dans les secteurs mytilicoles charentais et vendéens: description et facteurs liés-MORBLEU Rapport scientifique de l'étude MORBLEU, convention DPMA-Ifremer 2016. https://archimer.ifremer.fr/doc/00391/50288/50978.pdf.

Pérez-Camacho, A., Labarta, U., and Beiras, R. 1995. Growth of mussels (Mytilus edulis galloprovincialis) on cultivation rafts: influence of seed source,. Aquaculture, 138: 349–362. http://www.sciencedirect.com/science/article/pii/0044848695011390.

Pérez, A. F., Boy, C. C., Curelovich, J., Pérez-Barros, P., and Calcagno, J. A. 2013. Relationship between energy allocation and gametogenesis in Aulacomya atra (Bivalvia: Mytilidae) in a sub-Antarctic environment. Revista de biología marina y oceanografía, 48: 459–469.

Petraitis, P. S. 1998. Timing of mussel mortality and predator activity in sheltered bays of the Gulf of Maine, USA. Journal of Experimental Marine Biology and Ecology, 231: 47–62.

Pineda, J., Porri, F., Starczak, V., and Blythe, J. 2010. Causes of decoupling between larval supply and settlement and consequences for understanding recruitment and population connectivity. Journal

of Experimental Marine Biology and Ecology, 392: 9–21. Elsevier B.V. http://dx.doi.org/10.1016/j.jembe.2010.04.008.

Pleissner, D., Eriksen, N. T., Lundgreen, K., and Riisgård, H. U. 2012. Biomass Composition of Blue Mussels, Mytilus edulis , is Affected by Living Site and Species of Ingested Microalgae . ISRN Zoology, 2012: 1–12.

Plets R., Dix J., B. R. 2013. Marine Geophysics Data Acquisition, Processing and Interpretation. Guidance notes. English Heritage: 1–92.

Powell, E. N., Ashton-Alcox, K. A., Kraeuter, J. N., Ford, S. E., and Bushek, D. 2008. Long-term trends in oyster population dynamics in Delaware Bay: Regime shifts and response to disease. Journal of Shellfish Research, 27: 729–755.

Pulfrich, A. 1996. Attachment and settlement of post-larval mussels (Mytilus edulis L.) in the Schleswig-Holstein Wadden Sea. Journal of Sea Research, 36: 239–250. http://www.sciencedirect.com/science/article/B6VHH-498RR4D-2B/2/bea0ac48656d13c51f4c350d06000c87.

R Core Team. 2022. R: A language and environment for statistical computing. R Foundation for Statistical Computing, Vienna, Austria. https://www.r-project.org/.

Robins, P. E., Neill, S. P., Giménez, L., Stuart, R., Jenkins, S. R., and Malham, S. K. 2013. Physical and biological controls on larval dispersal and connectivity in a highly energetic shelf sea. Limnology and Oceanography, 58: 505–524.

Rodhouse, P. G., Roden, C. M., Burnell, G. M., Hensey, M. P., McMahon, T., Ottway, B., and Ryan, T. H. 1984. Food Resource, Gametogenesis And Growth Of Mytilus Edulis On The Shore And In Suspended Culture: Killary Harbour, Ireland. Journal of the Marine Biological Association of the United Kingdom, 64: 513–529.

Sarà, G., Manganaro, A., Cortese, G., Pusceddu, A., and Mazzola, A. 1998. The relationship between food availability and growth in Mytilus galloprovincialis in the open sea (southern Mediterranean). Aquaculture, 167: 1–15.

Sea, M. A., Hillman, J. R., and Thrush, S. F. 2022. Enhancing multiple scales of seafloor biodiversity with mussel restoration. Scientific Reports, 12: 1–14. Nature Publishing Group UK. https://doi.org/10.1038/s41598-022-09132-w.

Seed, R. 1969. The Ecology of Mytilus edulis L . (Lamellibranchiata) on Exposed Rocky Shores I. Breeding and Settlement. Oecologia, 3: 277–316.

Sloan, N. A., and Aldridge, T. H. 1981. Observations on an aggregation of the starfish asterias rubens l. In morecambe bay, lancashire, england. Journal of Natural History, 15: 407–417.

Smaal, A., Herman, P., Capelle, J., Wijsman, J., and van Stralen, M. 2017. Population dynamics of subtidal blue mussels Mytilus edulis and the impact of cultivation. Aquaculture Environment Interactions, 9: 155–168.

Smaal, A. C. 1991. The ecology and cultivation of mussels: new advances. Aquaculture, 94: 245–261.

Smaal, A. C. 2002. European mussel cultivation along the Atlantic coast: Production status, problems and perspectives. Hydrobiologia, 484: 89–98.

Smaal, A. C., Ferreira, J. G., Grant, J., Petersen, J. K., and Strand, Ø. (Eds). 2018. Goods and Services of Marine Bivalves. Springer Open. 485–506 pp. https://link.springer.com/book/10.1007%2F978-3-319-96776-9.

Smaal, A. C., Craeymeersch, J. A., and van Stralen, M. R. 2021. The impact of mussel seed fishery on the dynamics of wild subtidal mussel beds in the western Wadden Sea, The Netherlands. Journal of Sea Research, 167: 101978. Elsevier B.V. https://doi.org/10.1016/j.seares.2020.101978.

Smith, M. T., and Addison, J. T. 2003. Methods for stock assessment of crustacean fisheries. Fisheries Research, 65: 231–256.

Solan, M., Germano, J. D., Rhoads, D. C., Smith, C., Michaud, E., Parry, D., Wenzhöfer, F., *et al.* 2003. Towards a greater understanding of pattern, scale and process in marine benthic systems: A picture is worth a thousand worms. Journal of Experimental Marine Biology and Ecology, 285–286: 313–338.

Sotheran, I. S., Foster-Smith, R. L., and Davies, J. 1997. Mapping of marine benthic habitats using image processing techniques within a raster-based geographic information system. Estuarine, Coastal and Shelf Science, 44: 25–31. Academic Press Limited. http://dx.doi.org/10.1016/S0272-7714(97)80004-2.

South, P. M. 2016. An experimental assessment of measures of mussel settlement: Effects of temporal, procedural and spatial variations. Journal of Experimental Marine Biology and Ecology, 482: 64–74. Elsevier B.V. http://dx.doi.org/10.1016/j.jembe.2016.05.002.

Sprung, M. 1984a. Physiological Energetics of Mussel Larvae (Mytilus edulis) II. Food Uptake. Marine Ecology Progress Series, 17: 295–306.

Sprung, M. 1984b. Physiological energetics of mussel larvae (Mytilus edulis). III. Respiration. Marine Ecology, 18: 171–178.

Sprung, M. 1984c. Physiological energetics of mussel larvae (Mytilus edulis) I.Shell growth and biomass. Marine Ecology, 17: 283–293.

Steenbergen, J., Baars, J. M. D. D., Stralen, M. R. Van, and Craeymeersch, J. A. 2005. Winter survival of mussel beds in the intertidal part of the Dutch Wadden Sea. Monitoring and Assessment in the Wadden Sea. Proceedings from the 11. Scientific Wad- den Sea Symposium, NERI Techn: 107–112.

Stewart, I. J., and Hamel, O. S. 2014. Bootstrapping of sample sizes for length- or age-composition data used in stock assessments. Canadian Journal of Fisheries and Aquatic Sciences, 71: 581–588.

Strong, J. A., and Service, M. 2011. Using optimum allocation analysis to improve seed mussel stock assessments. Journal of Shellfish Research, 30: 1–6.

Svane, I., and Setyobudiandi, I. 1996. Diversity of associated fauna in beds of the ble mussel Mytilus edulis L. : effects of location, patch size, and position within a patch. Ophelia.

Telesca, L., Michalek, K., Sanders, T., Peck, L. S., Thyrring, J., and Harper, E. M. 2018. Blue mussel shell

shape plasticity and natural environments: A quantitative approach. Scientific Reports, 8: 1–15. Springer US. http://dx.doi.org/10.1038/s41598-018-20122-9.

Travers, M.-A., PEPIN, J.-F., SOLETCHNIK, P., GUESDON, S., and LE MOINE, O. 2016. Mortalités de moules bleues dans les Pertuis Charentais: description et facteurs liés – MORBLEU: 126p. http://archimer.ifremer.fr/doc/00324/43539/.

Troost, K., van der Meer, J., and van Stralen, M. 2022. The longevity of subtidal mussel beds in the Dutch Wadden Sea. Journal of Sea Research, 181: 102174. Elsevier B.V. https://doi.org/10.1016/j.seares.2022.102174.

Tully, O., and Clarke, S. 2012. The Status and Management of Oyster (Ostrea edulis) in Ireland. Irish Fisheries Investigations: 40.

Unna, P. J. . 1942. Waves and Tidal Streams. Nature, 149: 220.

van der Schatte Olivier, A., Jones, L., Vay, L. Le, Christie, M., Wilson, J., and Malham, S. K. 2018. A global review of the ecosystem services provided by bivalve aquaculture. Reviews in Aquaculture: 1–23.

Van Lancker, V., Du Four, I., Papili, S., Verfaillie, E., Schelfout, K., Rabout, M., and Degraer, S. 2007. Habitat signature catalogue, Belgian Part of the North Sea.

van Overmeeren, R., Craeymeersch, J., van Dalfsen, J., Fey, F., van Heteren, S., and Meesters, E. 2009. Acoustic habitat and shellfish mapping and monitoring in shallow coastal water - Sidescan sonar experiences in The Netherlands. Estuarine, Coastal and Shelf Science, 85: 437–448. Elsevier Ltd. http://dx.doi.org/10.1016/j.ecss.2009.07.016.

Venables, W. N., and Ripley, B. D. 2002. Modern Applied Statistics with S. Fourth Edition. Springer, New York. http://www.stats.ox.ac.uk/pub/MASS4/.

Verdier-Bonnet, C., Carlotti, F., Rey, C., and Bhaud, M. 1997. A model of larval dispersion coupling wind-driven currents and vertical larval behaviour: application to recruitment of annelid Owenia fusiformis in Banuyls Bay, France. Marine Ecology Progrees Series, 160:217–23.

wa Kangeri, A. K., Jansen, J. M., Joppe, D. J., and Dankers, N. M. J. A. 2016. In situ investigation of the effects of current velocity on sedimentary mussel bed stability. Journal of Experimental Marine Biology and Ecology, 485: 65–72. Elsevier B.V. http://dx.doi.org/10.1016/j.jembe.2016.08.011.

Wickham, H. 2016. ggplot2: Elegant Graphics for Data Analysis. Springer-Verlag New York.

Widdows, J. 1991. Physiological responses of mussel larvae. Aquaculture, 94: 147–163. Settlement and Recruitment.

Wilcox, M., and Jeffs, A. 2017. Is attachment substrate a prerequisite for mussels to establish on soft-sediment substrate? Journal of Experimental Marine Biology and Ecology, 495: 83–88.

Wilcox, M., and Jeffs, A. 2019. Impacts of sea star predation on mussel bed restoration. Restoration Ecology, 27: 189–197.

Wilson, B. R., Brown, C. J., Sameoto, J. A., Lacharité, M., and Gazzola, V. 2021. Mapping seafloor habitats in the Bay of Fundy to assess megafaunal assemblages associated with Modiolus modiolus beds. Estuarine, Coastal and Shelf Science: 107294. Elsevier Ltd.

https://doi.org/10.1016/j.ecss.2021.107294.

Zilhão, J., Angelucci, D. E., Araújo Igreja, M., Arnold, L. J., Badal, E., Callapez, P., Cardoso, J. L., *et al.* 2020. Last Interglacial Iberian Neandertals as fisher-hunter-gatherers. Science, 367.

Zippay, M. L., and Helmuth, B. 2012. Effects of temperature change on mussel, Mytilus. Integrative Zoology, 7: 312–327.

Appendix

Chapter 2: New approaches to mapping and quantifying the Biomass of Subtidal Seed Mussel Beds

IDW interpolation biomass (metric tonnes) estimation for Rosslare pre-fishing (a), Rusk Channel pre-fishing (b)

a)

Density Classes	Areas in hectares	N samples	Mean Wt per 0.1 m^{-2} in Kg	Tonnes/Area
40	1.16	8	0.00	0.00
250	10.38	11	0.16	164.83
500	18.26	10	0.34	624.53
750	10.47	4	0.63	660.58
1000	6.38	2	0.90	573.83
1250	3.09	3	1.18	363.66
1500	1.80	1	1.46	262.73
1750	0.81	0	0.00	0.00
2000	0.34	1	1.76	60.19
2250	0.13	1	2.05	26.31
2500	0.01	1	2.28	1.33
Total area	***52.82***		***Total tonnage***	***2737.99***

b)

Density Classes	Areas in hectares	N samples	Mean Wt per 0.1 m^{-2} in Kg	Tonnes/Area
0	0.58	4	0.00	0.00
250	2.53	5	0.13	33.33
500	8.26	2	0.33	272.50
750	6.88	6	0.64	442.90
1000	7.27	1	0.92	668.92
1250	6.79	4	1.13	763.97
1500	5.46	3	1.41	768.19
1750	2.79	3	1.59	442.18
2000	0.70	2	1.80	126.09
2500	0.31	1	2.28	70.39
Total area	***41.57***		***Total tonnage***	***3588.49***

IDW interpolation biomass (metric tonnes) estimation for Rosslare post-fishing (a), Rusk Channel post-fishing (b)

a)

Density Classes in g	Areas in hectares	N samples	Mean Wt per 0.1 m^{-2} in Kg	Tonnes/Area
0	6.73	7	0.00	0.00
3 to 10	6.17	2	0.01	3.40
10 to 25	13.30	6	0.02	20.17
25 to 50	13.24	5	0.04	48.71
50 to 75	6.89	5	0.06	43.81
75 to 100	3.20	1	0.08	24.98
100 to 150	1.60	3	0.12	19.26
150 to 305	1.18	1	0.30	35.39
Total area	***52.30***		***Total tonnage***	***195.71***

b)

Density Classes in g	Areas in hectares	N samples	Mean Wt per 0.1 m^{-2} in Kg	Tonnes/Area
0	3.69	6	0.00	0.00
13 to 25	3.77	3	0.02	6.16
25 to 50	5.69	7	0.03	18.05
50 to 75	7.32	1	0.07	47.61
75 to 100	6.72	6	0.08	56.03
100 to 150	6.51	4	0.13	86.31
150 to 200	2.46	1	0.15	37.22
200 to 250	1.92	1	0.24	45.97
250 to 300	1.09	1	0.25	27.42
300 to 400	1.74	1	0.38	66.06
400 to 550	0.54	2	0.49	26.72
Total area	***41.48***		***Total tonnage***	***417.56***

Chapter 3: The Relation between sea water temperature and recruitment variations of subtidal seed mussels on the Southeast coast of Ireland

Process in R Studio

```
####Structure data per classes

## Daily Cumul Temp

bin_temp <- function(daily_cumul_temp) {

  ifelse(daily_cumul_temp <=970 , "Low",

         ifelse(daily_cumul_temp <=1040, "Medium",

                ifelse(daily_cumul_temp <=1105, "High")))

}

wexford$DCT_class <- bin_temp(wexford$daily_cumul_temp)

cahore$DCT_class <- bin_temp(cahore$daily_cumul_temp)


## Sampling time

bin_numbers <- function(sampling_weeks) {

  ifelse(sampling_weeks <= 22, "Early",

         ifelse(sampling_weeks <=30, "midway",

                ifelse(sampling_weeks <=38, "Late")))

}
```

```
#ggplot(wexford, aes(x = size_mm, colour = DCT_class)) +
  geom_histogram() + facet_wrap(~year) +
  theme_bw() +
  labs(x = "Seed Mussel Size in mm", y = "Size Frequency")


ggplot(cahore, aes(x = size_mm, colour = DCT_class)) +
  geom_histogram() + facet_wrap(~year) +
  theme_bw() +
  labs(x = "Seed Mussel Size in mm", y = "Size Frequency")### Histograms Temperature classes
```

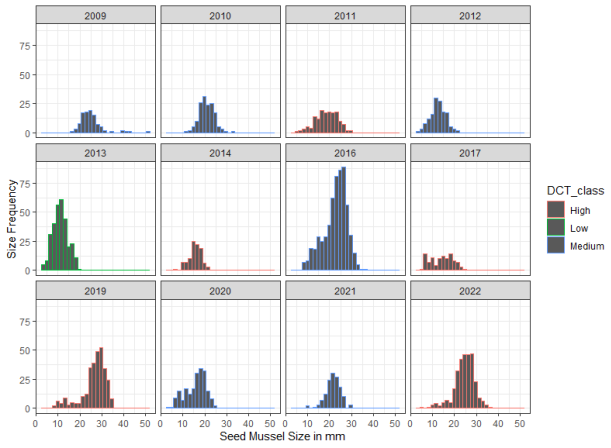

Seed mussel length distribution and DCT variations from 2009 to 2022 for Wexford/ Rosslare (p.71)

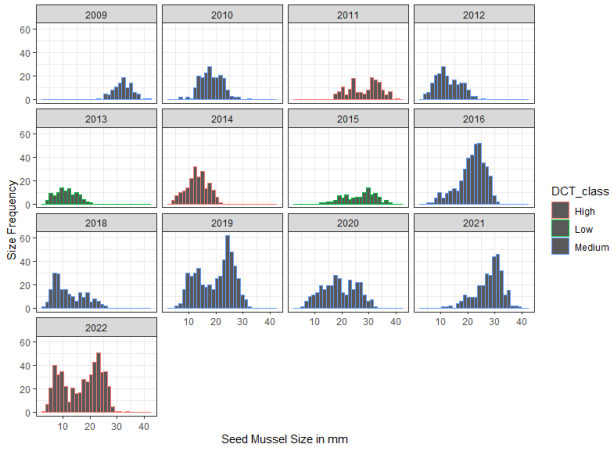

Seed mussel length distribution and DCT variations from 2009 to 2022 for Cahore/ Rusk Channel (p.74)

```
#### Histograms Sampling timing

 ggplot(wexford, aes(x = size_mm, colour = sample_timing)) +

 geom_histogram() + facet_wrap(~year) +

 theme_bw() +

 labs(x = "Seed Mussel Size in mm", y = "Size Frequency")

ggplot(cahore, aes(x = size_mm, colour = sample_timing)) +

 geom_histogram() + facet_wrap(~year) +

 theme_bw() +

 labs(x = "Seed Mussel Size in mm", y = "Size Frequency")
```

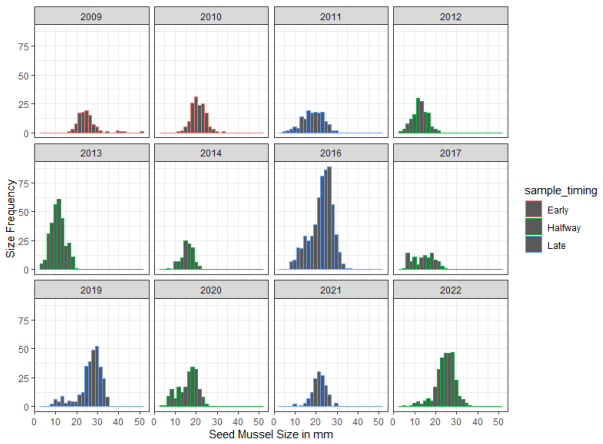

Seed mussel length distribution and sampling time from 2009 to 2022 for Wexford/ Rosslare (p.72)

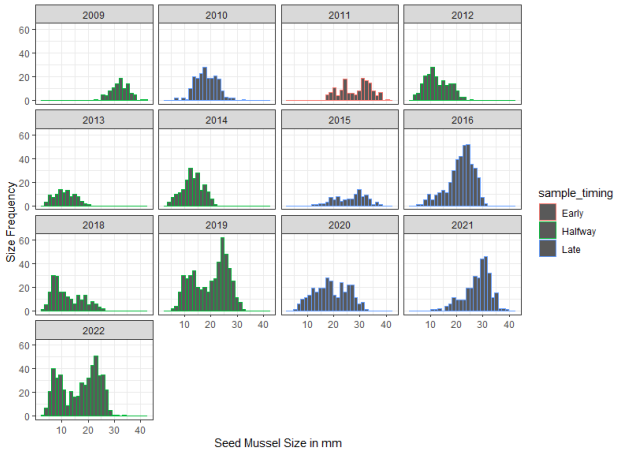

Seed mussel length distribution and sampling time from 2009 to 2022 for Cahore/ Rusk Channel (p.75)

```
###plot_wexford <- ggplot(wexford, aes(x = year2, y = size_mm, colour = DCT_class, fill = sample_timing)) +
  geom_boxplot()+
  labs(x = "Year", y = "Seed Mussel sizes in mm",
       title = "Seed Mussel Size Distribution, Sampling Time and Sea Temperature variation for Wexford")


plot_wexford + scale_color_grey() + theme_dark()


plot_cahore <- ggplot(cahore, aes(x = year2, y = size_mm, colour = DCT_class, fill = sample_timing)) +
  geom_boxplot()+
  labs(x = "Year", y = "Seed Mussel sizes in mm",
       title = "Seed Mussel Size Distribution, Sampling Time and Sea Temperature variation for Cahore")


plot_cahore + scale_color_grey() + theme_dark()# Cumulative graphs
```

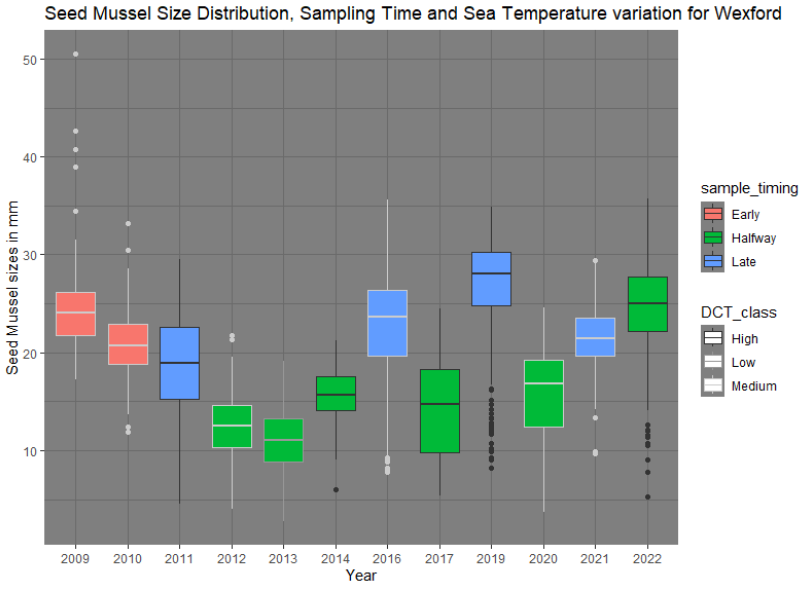

Seed mussel size distribution, with Daily Cumulative Temperature classes and sampling time period for the Wexford/Rosslare sector from 2009 to 2022 (p.73)

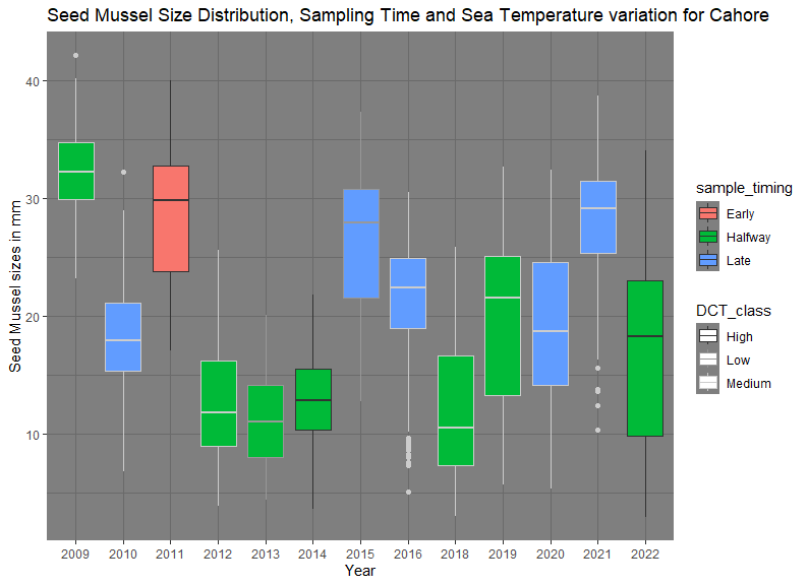

Seed mussel size distribution, indicating Daily Cumulative Temperature classes and sampling time period for the Cahore/ Rusk Channel sector from 2009 to 2022. (p.76)

Results

Results from par 1: 2009 and 2010 for Wexford, likely year previous settlement, 2011 for Cahore,

Low DCT for Wexford and Cahore may equal lower size for 2013,

Decreasing size pattern for Wexford from 2009 to 2013, no pattern in Cahore

```
## Part 2: significance of temp variations on size

#Run lmm with log size

#Wexford

sizewx.log <- log(wexford$size_mm)

mod_wex_temp <- lmer(sizewx.log ~ year_deci +

                daily_cumul_temp + (1|factor(vct_yearwx)), data = wexford)

summary(mod_wex_temp)

plot(mod_wex_temp)

qqnorm(resid(mod_wex_temp))

qqline(resid(mod_wex_temp), col=2)

plotNormalHistogram(sizewx.log)

##Cahore

sizech.log <- log(lenght_mm2)

mod_ch_temp <- lmer(sizech.log ~ year_deci +

                daily_cumul_temp + (1|factor(vct_yearch)), data = cahore)

summary(mod_ch_temp)

qqnorm(resid(mod_ch_temp))

qqline(resid(mod_ch_temp), col=2)
```

Summary results Model 1

1- Wexford Model 1 with log size

```
Linear mixed model fit by REML ['lmerMod']
Formula: sizewx.log ~ year_deci + daily_cumul_temp + (1 | factor(vct_yearwx))
   Data: wexford

REML criterion at convergence: 916

Scaled residuals:
    Min      1Q  Median      3Q     Max
-5.2986 -0.3809  0.2044  0.6163  2.5531

Random effects:
 Groups             Name        Variance Std.Dev.
 factor(vct_yearwx) (Intercept) 0.09335  0.3055
 Residual                       0.08089  0.2844
Number of obs: 2584, groups:  factor(vct_yearwx), 12

Fixed effects:
                  Estimate Std. Error t value
(Intercept)      -14.486697  42.630818  -0.340
year_deci          0.007401   0.021483   0.345
daily_cumul_temp   0.002360   0.002122   1.112

Correlation of Fixed Effects:
            (Intr) yer_dc
year_deci   -0.999
dly_cml_tmp  0.284 -0.330
```

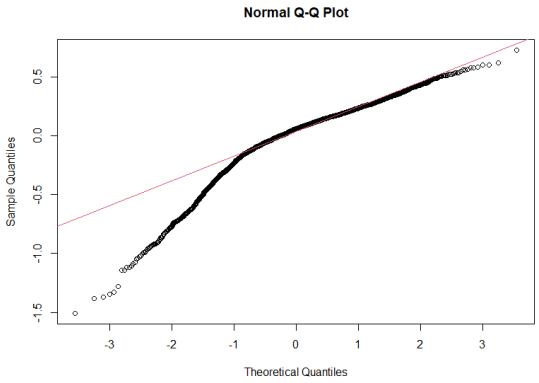

Q-Q plot for residual of Wexford Model 1

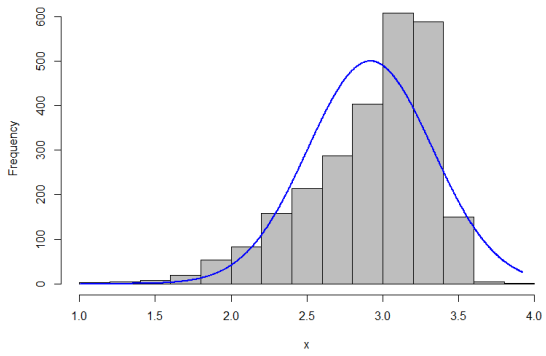

Normal histogram for Wexford log size

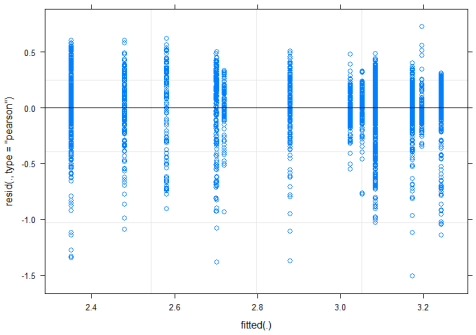

Residuals versus fitted plot for Wexford Model 1

2- Cahore Model 1 with log size

```
Linear mixed model fit by REML ['lmerMod']
Formula: sizech.log ~ year_deci + daily_cumul_temp + (1 | factor(vct_yearcahor
e))
   Data: cahore

REML criterion at convergence: 2805.1

Scaled residuals:
    Min      1Q  Median      3Q     Max
-4.4456 -0.5596  0.1846  0.7093  2.3956

Random effects:
 Groups                 Name        Variance Std.Dev.
 factor(vct_yearcahore) (Intercept) 0.1681   0.4101
 Residual                           0.1351   0.3675
Number of obs: 3251, groups:  factor(vct_yearcahore), 13

Fixed effects:
                 Estimate Std. Error t value
(Intercept)      3.611e-01  5.696e+01   0.006
year_deci        3.197e-04  2.865e-02   0.011
daily_cumul_temp 1.879e-03  2.768e-03   0.679

Correlation of Fixed Effects:
            (Intr) yer_dc
year_deci   -0.999
dly_cml_tmp  0.263 -0.308
```

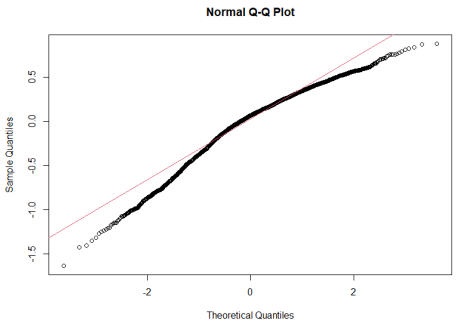

Q-Q plot for residual of Cahore Model 1

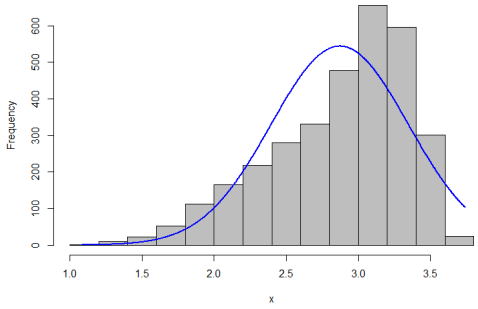

Normal histogram for Cahore log size

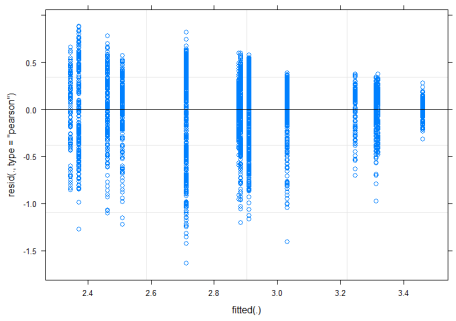

Residuals versus fitted plot for Cahore Model 1

Results from models: residuals not fitting, data may require transformation

```
## transformation of "size_mm" with BoxCox Lambda

#Wexford

l1<-lm(size_mm ~ year_deci +

       daily_cumul_temp, data = wexford)

bc <- boxcox(l1)

lb<-(lambda <- bc$x[which.max(bc$y)])

lb

wexford$trans_size <-wexford$size_mm^lb

Mg_L1 <- lmer(trans_size ~ year_deci +

            daily_cumul_temp + (1|factor(vct_yearwx)), data = wexford)

summary(Mg_L1)

plot(Mg_L1)

qqnorm(resid(Mg_L1))

qqline(resid(Mg_L1),col=2)

plotNormalHistogram(wexford$trans_size)

shapiro.test(wexford$trans_size) ##### W = 0.98421, p-value = 2.336e-16

#Cahore

l2<-lm(size_mm ~ year_deci +

       daily_cumul_temp, data = cahore)

bc2 <- boxcox(l2)

lb2<-(lambda <- bc2$x[which.max(bc2$y)])

lb2

cahore$trans_size <- cahore$size_mm^lb2

g_L2 <- lmer(trans_size ~ year_deci +

            daily_cumul_temp + (1|factor(vct_yearcahore)), data = cahore)

summary(g_L2)

plot(g_L2)

qqnorm(resid(g_L2))
```

Summary results Model 2

1- Wexford Model 2 with Box-Cox transformation

```
Linear mixed model fit by REML ['lmerMod']
Formula: trans_size ~ year_deci + daily_cumul_temp + (1 | factor(vct_yearwx))
   Data: wexford

REML criterion at convergence: 14331.6

Scaled residuals:
    Min      1Q  Median      3Q     Max
-4.1710 -0.5250  0.1126  0.6703  5.3053

Random effects:
 Groups             Name        Variance Std.Dev.
 factor(vct_yearwx) (Intercept) 18.94    4.352
 Residual                       14.63    3.824
Number of obs: 2584, groups:  factor(vct_yearwx), 12

Fixed effects:
                  Estimate Std. Error t value
(Intercept)      -309.95046  606.98949  -0.511
year_deci           0.14693    0.30587   0.480
daily_cumul_temp    0.02912    0.03022   0.963

Correlation of Fixed Effects:
            (Intr) yer_dc
year_deci   -0.999
dly_cml_tmp  0.284 -0.330
```

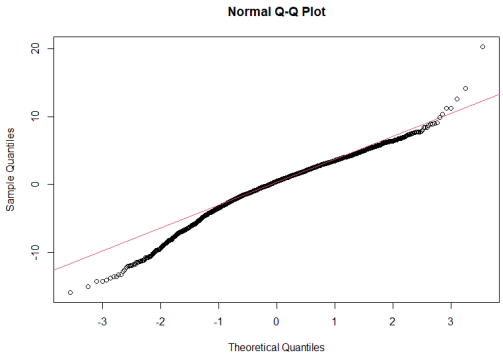

Q-Q plot for residual of Wexford Model 2

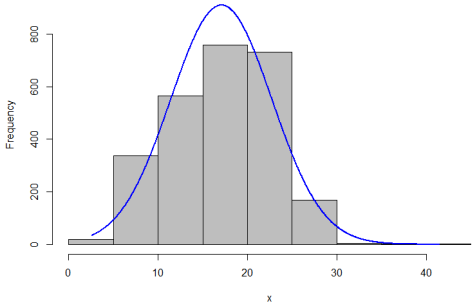

Normal histogram for Wexford Box-Cox sizes

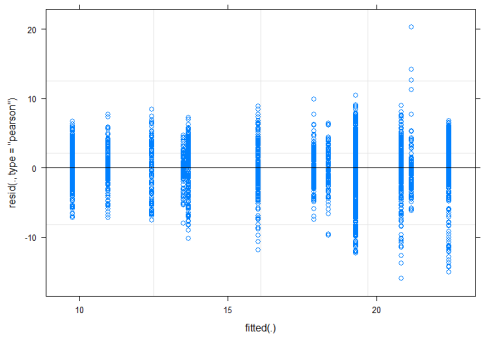

Residuals versus fitted plot for Wexford Model 2

2- Cahore Model 2 with Box-Cox transformation

```
Linear mixed model fit by REML ['lmerMod']
Formula: trans_size ~ year_deci + daily_cumul_temp + (1 | factor(vct_yearcahor
e))
   Data: cahore

REML criterion at convergence: 15157.9

Scaled residuals:
    Min      1Q  Median      3Q     Max
-3.0658 -0.7031  0.1068  0.7702  2.8417

Random effects:
 Groups                 Name        Variance Std.Dev.
 factor(vct_yearcahore) (Intercept) 9.973    3.158
 Residual                           6.052    2.460
Number of obs: 3251, groups:  factor(vct_yearcahore), 13

Fixed effects:
                  Estimate Std. Error t value
(Intercept)      -18.481522 438.264061  -0.042
year_deci          0.008234   0.220408   0.037
daily_cumul_temp   0.012297   0.021301   0.577

Correlation of Fixed Effects:
            (Intr) yer_dc
year_deci   -0.999
dly_cml_tmp  0.263 -0.307
```

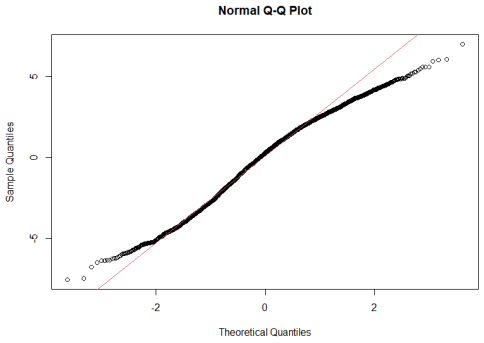

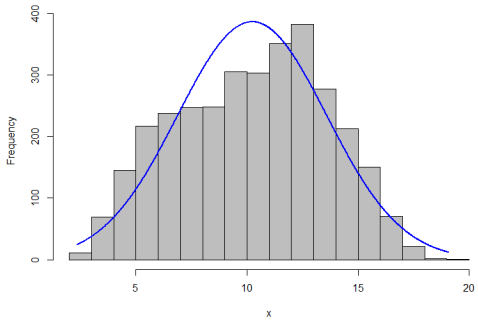

Q-Q plot for residual of Cahore Model 2 Normal histogram for Cahore Box-Cox sizes

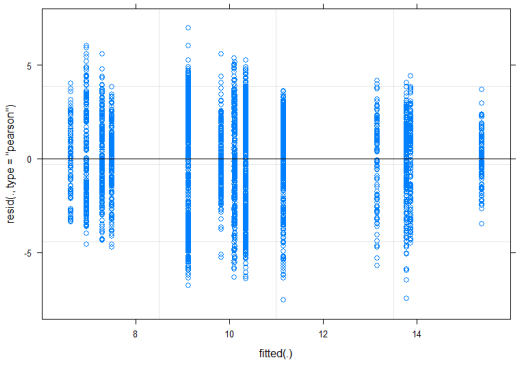

Residuals versus fitted plot for Cahore Model 2

###Results: Better fitting of the residuals for both locations, REML higher than with Log-size, insert interaction term for possible improvements, possible issue with cumul_temp values, use average values instead

```
####model with interaction term using larvae time average temp

#Wexford

mod_interact_wex2 <- lmer(sizewx.log ~ deci_year + sb_temp + deci_year:sb_temp +

                    (1 | factor(vct_yearwx)), data = wexford)

summary(mod_interact_wex2)

plot(mod_interact_wex2)

qqnorm(resid(mod_interact_wex2))

qqline(resid(mod_interact_wex2), col=2)


#Cahore

mod_interact_ch2 <- lmer(sizech.log ~ deci_year + sb_temp + deci_year:sb_temp +

                   (1 | factor(vct_yearch)), data = cahore)

summary(mod_interact_ch2)

plot(mod_interact_ch2)

qqnorm(resid(mod_interact_ch2))

qqline(resid(mod_interact_ch2), col=2)
```

Summary results Model 3

1- Wexford Model 3 with log size and average sea temperature value

```
Linear mixed model fit by REML ['lmerMod']
Formula: sizewx.log ~ deci_year + sb_temp + deci_year:sb_temp + (1 | factor(vc
t_yearwx))
   Data: wexford

REML criterion at convergence: 877.4

Scaled residuals:
    Min      1Q  Median      3Q     Max
-5.3278 -0.3698  0.2074  0.6196  2.5634

Random effects:
 Groups             Name        Variance Std.Dev.
 factor(vct_yearwx) (Intercept) 0.22141  0.4705
 Residual                       0.08007  0.2830
Number of obs: 2584, groups:  factor(vct_yearwx), 12

Fixed effects:
                  Estimate Std. Error t value
(Intercept)         76.368     22.627   3.375
deci_year         -146.479     42.581  -3.440
sb_temp             -6.612      2.011  -3.288
deci_year:sb_temp   13.152      3.781   3.478

Correlation of Fixed Effects:
            (Intr) dec_yr sb_tmp
deci_year   -0.990
sb_temp     -1.000  0.990
dc_yr:sb_tm  0.990 -1.000 -0.990
```

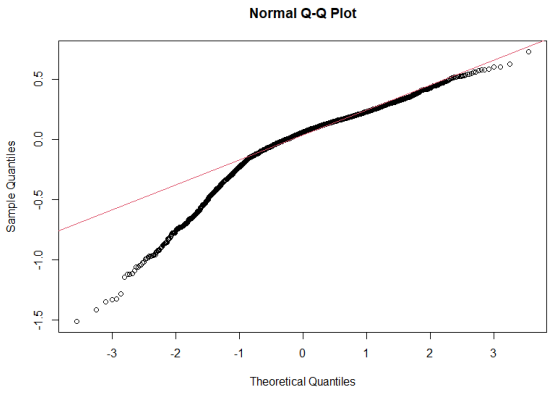

Q-Q plot for residual of Wexford Model 3

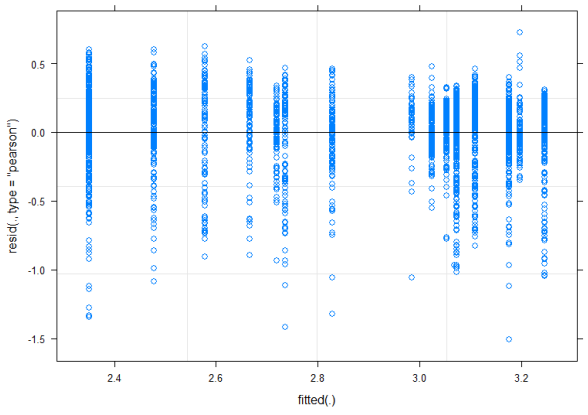

Residuals versus fitted plot for Wexford Model 3

2- Cahore Model 3 with log size and average sea temperature value

```
Linear mixed model fit by REML ['lmerMod']
Formula: sizech.log ~ deci_year + sb_temp + deci_year:sb_temp + (1 | factor(vc
t_yearch))
   Data: cahore

REML criterion at convergence: 2616.8

Scaled residuals:
    Min      1Q  Median      3Q     Max
-4.4682 -0.5558  0.1991  0.7034  2.4668

Random effects:
 Groups             Name        Variance Std.Dev.
 factor(vct_yearch) (Intercept) 0.6274   0.7921
 Residual                       0.1276   0.3573
Number of obs: 3251, groups:  factor(vct_yearch), 13

Fixed effects:
                  Estimate Std. Error t value
(Intercept)         82.576     16.872   4.894
deci_year         -147.612     27.131  -5.441
sb_temp             -7.055      1.446  -4.880
deci_year:sb_temp   13.125      2.309   5.683

Correlation of Fixed Effects:
            (Intr) dec_yr sb_tmp
deci_year   -0.953
sb_temp     -1.000  0.947
dc_yr:sb_tm  0.953 -1.000 -0.947
```

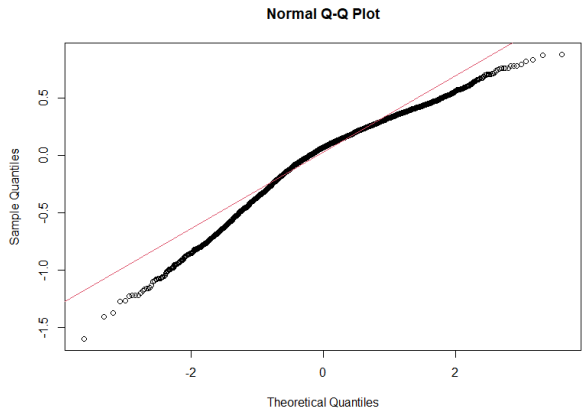

Q-Q plot for residual of Cahore Model 3

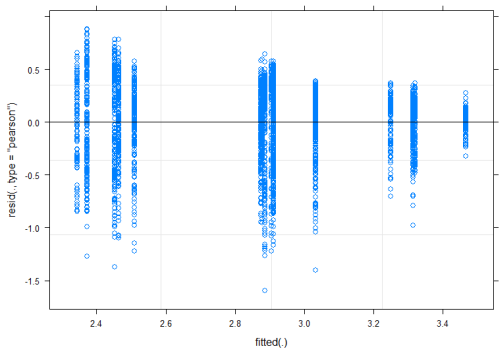

Residuals versus fitted plot for Cahore Model 3

#Results: improvement of the REML convergence value, residuals not fitting, replicate model with boxcox transformation. Histogram of log size distribution on p.107 (Wexford) and p.108(Cahore)

```
#### model intercation term with boxcox size transformation

#Wexford

lbwx<-lm(size_mm ~ year_deci +

        sb_temp, data = wexford)

bc_wexford <- boxcox(lbwx)

lbwxf<-(lambda <- bc_wexford$x[which.max(bc_wexford$y)])

lbwxf

wexford$lba_size <- wexford$size_mm^lbwxf

mod_interact_wex_lba <- lmer(lba_size ~ deci_year + sb_temp + deci_year:sb_temp +

                        (1 | factor(vct_yearwx)), data = wexford)

summary(mod_interact_wex_lba)

plot(mod_interact_wex_lba)

qqnorm(resid(mod_interact_wex_lba))

qqline(resid(mod_interact_wex_lba), col=2)

#Cahore

lbch<-lm(size_mm ~ year_deci +

        sb_temp, data = cahore)

bc_cahore <- boxcox(lbch)

lbchr<-(lambda <- bc_cahore$x[which.max(bc_cahore$y)])

lbchr

cahore$lba_size <- cahore$size_mm^lbchr

mod_interact_ch_lba <- lmer(lba_size ~ deci_year + sb_temp + deci_year:sb_temp +

                    (1 | factor(vct_yearch)), data = cahore)

summary(mod_interact_ch_lba)

plot(mod_interact_ch_lba)

qqnorm(resid(mod_interact_ch_lba))

qqline(resid(mod_interact_ch_lba), col=2)
```

Summary results Model 4:

1- Wexford Model 4 with Box-Cox transformation and average sea temperature value

```
Linear mixed model fit by REML ['lmerMod']
Formula: lba_size ~ deci_year + sb_temp + deci_year:sb_temp + (1 | factor(vct_
yearwx))
   Data: wexford

REML criterion at convergence: 14271.9

Scaled residuals:
    Min      1Q  Median      3Q     Max
-4.2096 -0.5031  0.1184  0.6607  5.3480

Random effects:
 Groups             Name        Variance Std.Dev.
 factor(vct_yearwx) (Intercept) 59.80    7.733
 Residual                       14.37    3.791
Number of obs: 2584, groups:  factor(vct_yearwx), 12

Fixed effects:
                 Estimate Std. Error t value
(Intercept)       1191.69     319.07   3.735
deci_year        -2328.08     597.59  -3.896
sb_temp           -106.22      28.36  -3.745
deci_year:sb_temp  209.97      53.07   3.956

Correlation of Fixed Effects:
            (Intr) dec_yr sb_tmp
deci_year   -0.987
sb_temp     -1.000  0.987
dc_yr:sb_tm  0.987 -1.000 -0.987
```

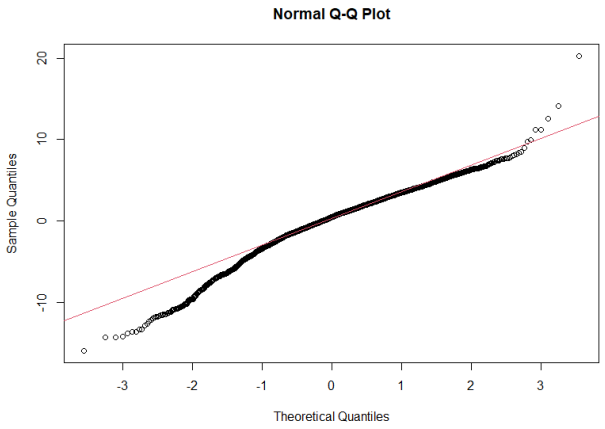

Q-Q plot for residual of Wexford Model 4

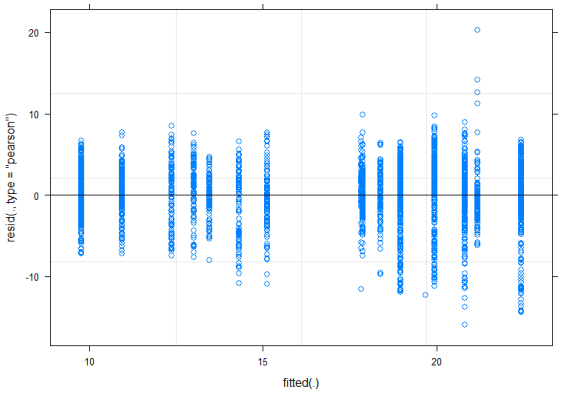

Residuals versus fitted plot for Wexford Model 4

2- Cahore Model 4 with Box-Cox transformation and average sea temperature value

```
Linear mixed model fit by REML ['lmerMod']
Formula: lba_size ~ deci_year + sb_temp + deci_year:sb_temp + (1 | factor(vct_
yearch))
   Data: cahore

REML criterion at convergence: 14964.6

Scaled residuals:
    Min      1Q  Median      3Q     Max
-3.1575 -0.6985  0.1399  0.7640  2.5244

Random effects:
 Groups             Name        Variance Std.Dev.
 factor(vct_yearch) (Intercept) 64.636   8.040
 Residual                        5.706   2.389
Number of obs: 3251, groups:  factor(vct_yearch), 13

Fixed effects:
                  Estimate Std. Error t value
(Intercept)         840.03     138.88   6.049
deci_year         -1482.54     217.03  -6.831
sb_temp             -72.31      11.93  -6.062
deci_year:sb_temp   129.66      18.45   7.029

Correlation of Fixed Effects:
            (Intr) dec_yr sb_tmp
deci_year   -0.928
sb_temp     -0.999  0.919
dc_yr:sb_tm  0.928 -1.000 -0.919
```

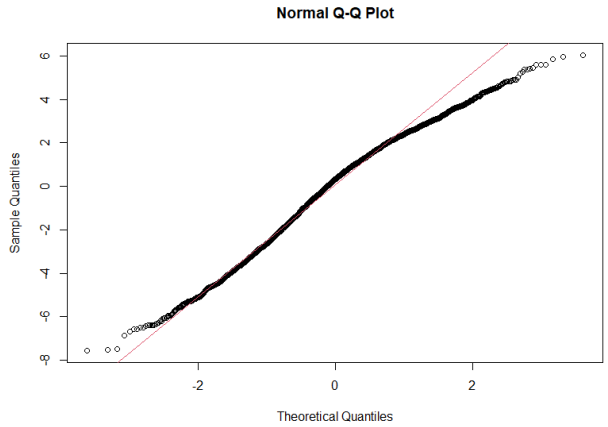

Q-Q plot for residual of Cahore model 4

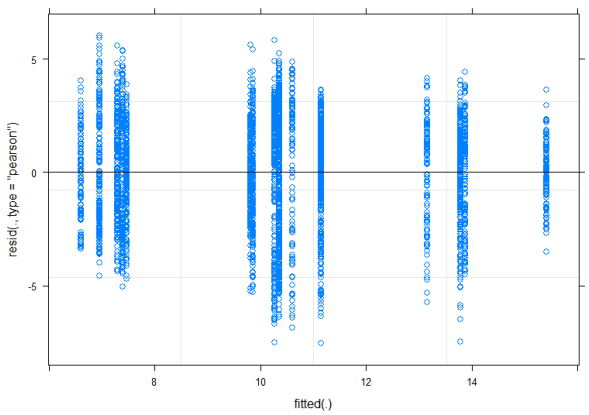

Residuals versus fitted plot for Cahore model 4

#Results: REML lower than previous box Cox transformation lmm, residual fit better, add prediction model to current results. Histogram of Box-Cox size distribution on p. 110 (Wexford) and p.111 (Cahore)

```
Prediction model

#Wexford

pred.mod_interact_wex3 <- ggpredict(mod_interact_wex_lba, terms = c("sb_temp"))

plot(pred.mod_interact_wex3)

(ggplot(pred.mod_interact_wex3) +

geom_line(aes(x = x, y = predicted)) +         # slope

   geom_ribbon(aes(x = x, ymin = predicted - std.error, ymax = predicted + std.error),

               fill = "lightgrey", alpha = 0.5) +  # error band

   geom_point(data = wexford,

              aes(x = sb_temp, y = lsize_mm, colour = factor(year))) +

   labs(x = "average sea bottom temperature", y = "mussel size log") +

   theme_light())


#Cahore

pred.mod_interact_ch3 <- ggpredict(mod_interact_ch_lba, terms = c("sb_temp"))

plot(pred.mod_interact_ch3)

(ggplot(pred.mod_interact_ch3) +

geom_line(aes(x = x, y = predicted)) +         # slope

   geom_ribbon(aes(x = x, ymin = predicted - std.error, ymax = predicted + std.error),

               fill = "lightgrey", alpha = 0.5) +  # error band

   geom_point(data = cahore,

              aes(x = sb_temp, y = lsize_mm, colour = factor(year))) +

   labs(x = "average sea bottom temperature", y = "mussel size log") +

   theme_light())
```

Wexford prediction model plot (size, temperature and year), also on p.78

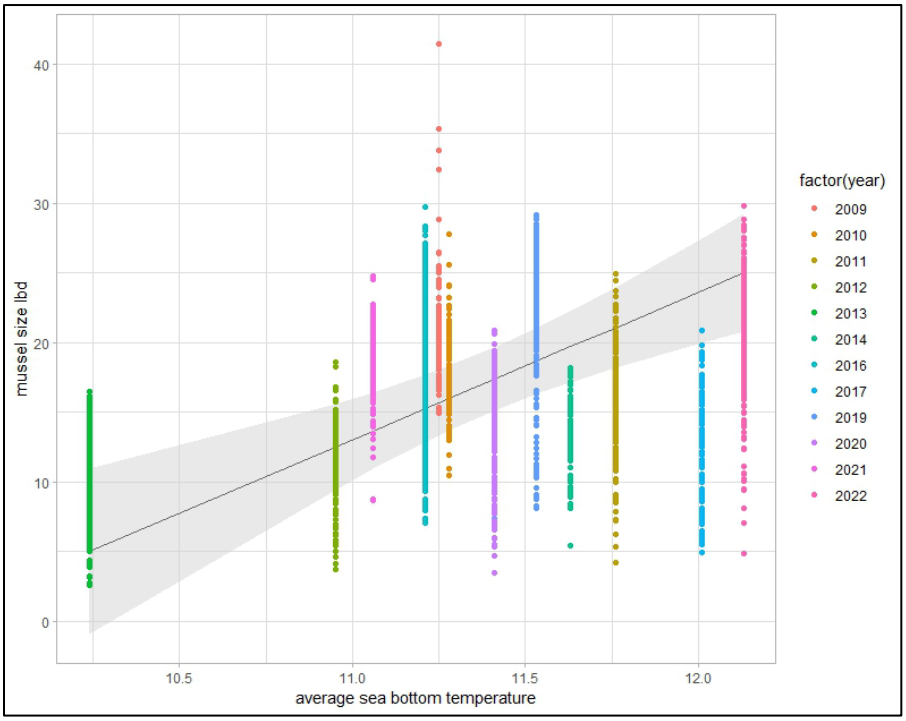

Cahore prediction model plot(size, temperature and year),also on p.79

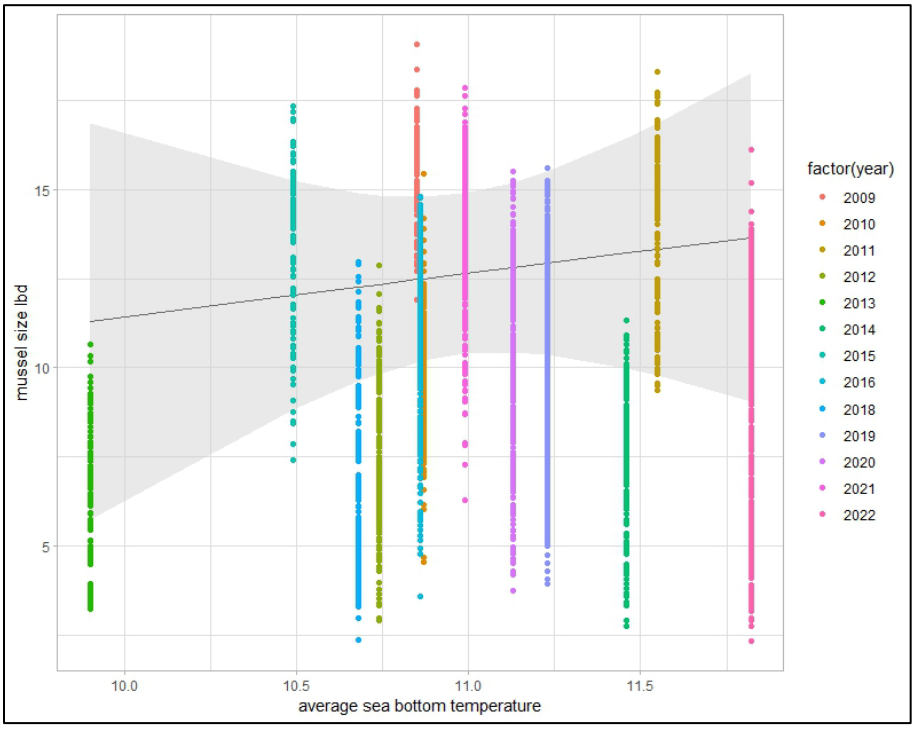

```
# Create a summary table using stargazer

table_output_wx <- stargazer(mod_interact_wex_lba, type = "html")

table_output_ch <- stargazer(mod_interact_ch_lba, type = "html")


# Capture the html code from the stargazer output

html_code_wx <- capture.output(cat(table_output_wx))

html_code_ch <- capture.output(cat(table_output_ch))


# export tables

writeLines(html_code_wx, "Wexford_lmm_table.html")

writeLines(html_code_ch, "cahore_lmm_table.html")
```

	Dependent variable:
	lba_size
deci_year	-2,328.080***
	(597.586)
sb_temp	-106.217***
	(28.361)
deci_year:sb_temp	209.966***
	(53.071)
Constant	1,191.693***
	(319.066)
Observations	2,584
Log Likelihood	-7,135.947
Akaike Inf. Crit.	14,283.890
Bayesian Inf. Crit.	14,319.040
Note:	*p<0.1; **p<0.05; ***p<0.01

Model results for Wexford/ Rosslare

	Dependent variable:
	lba_size
deci_year	-1,482.542***
	(217.035)
sb_temp	-72.312***
	(11.929)
deci_year:sb_temp	129.656***
	(18.445)
Constant	840.031***
	(138.882)
Observations	3,251
Log Likelihood	-7,482.293
Akaike Inf. Crit.	14,976.590
Bayesian Inf. Crit.	15,013.110
Note:	*p<0.1; **p<0.05; ***p<0.01

Models results for Cahore/ Rusk Channel

Evaluation of the assumptions based on diagnostic results

```
# Fit final model

modwex_final <- lmer(lba_size ~ deci_year + sb_temp + deci_year:sb_temp + (1 | factor(vct_yearwexford)), data = wexford_data)



modch_final <- lmer(lba_size ~ deci_year + sb_temp + deci_year:sb_temp + (1 | factor(vct_yearcahore)), data = cahore_data)

# Residuals vs Fitted Plot

plot(fitted(modwex_final), resid(modwex_final), main = "Residuals vs Fitted Wexford", xlab = "Fitted values", ylab = "Residuals")

abline(h = 0, col = "red")



plot(fitted(modch_final), resid(modch_final), main = "Residuals vs Fitted Cahore", xlab = "Fitted values", ylab = "Residuals")

abline(h = 0, col = "red")
```

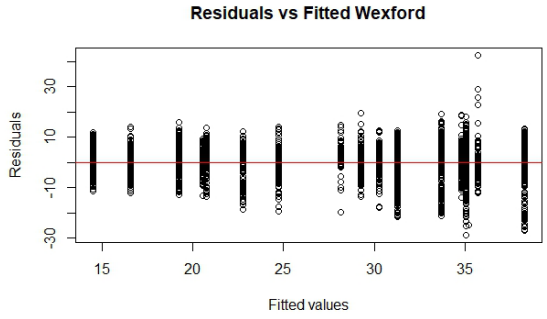

Residuals vs Fitted plot for Wexford model 4

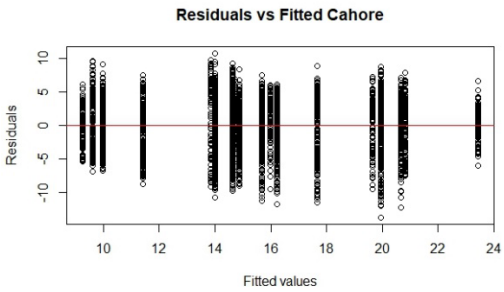

Residuals vs Fitted plot for Cahore model 4

```
# Residuals vs Independent Variables

plot(wexford_data$deci_year, resid(modwex_final), main = "Residuals vs deci_year Wexford", xlab =
"deci_year", ylab = "Residuals")

abline(h = 0, col = "red")


plot(wexford_data$sb_temp, resid(modwex_final), main = "Residuals vs sb_temp Wexford", xlab =
"sb_temp", ylab = "Residuals")

abline(h = 0, col = "red")


plot(cahore_data$deci_year, resid(modch_final), main = "Residuals vs deci_year Cahore", xlab = "deci_year",
ylab = "Residuals")

abline(h = 0, col = "red")


plot(cahore_data$sb_temp, resid(modch_final), main = "Residuals vs sb_temp Cahore", xlab = "sb_temp",
ylab = "Residuals")

abline(h = 0, col = "red")
```

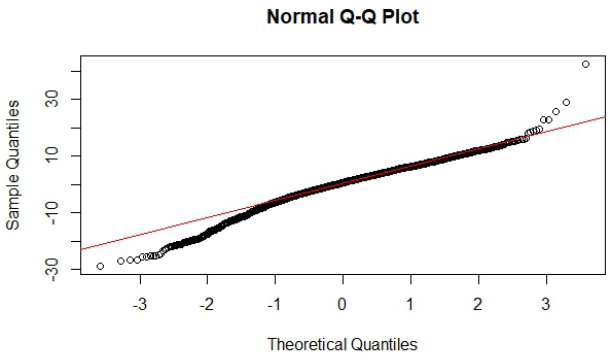

Q-Q plot for Wexford model 4

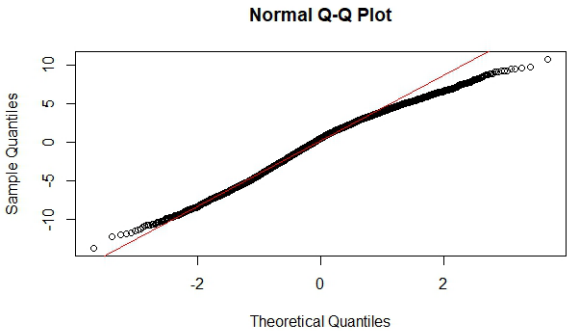

Q-Q plot for Cahore model 4

```
# Residuals vs Independent Variables

plot (wexford_data$deci_year, resid(modwex_final), main = "Residuals vs deci_year Wexford", xlab = "deci_year", ylab = "Residuals")

abline(h = 0, col = "red")

plot(wexford_data$sb_temp, resid(modwex_final), main = "Residuals vs sb_temp Wexford", xlab = "sb_temp", ylab = "Residuals")

abline(h = 0, col = "red")

plot(cahore_data$deci_year, resid(modch_final), main = "Residuals vs deci_year Cahore", xlab = "deci_year", ylab = "Residuals")

abline(h = 0, col = "red")

plot(cahore_data$sb_temp, resid(modch_final), main = "Residuals vs sb_temp Cahore", xlab = "sb_temp", ylab = "Residuals")

abline(h = 0, col = "red")
```

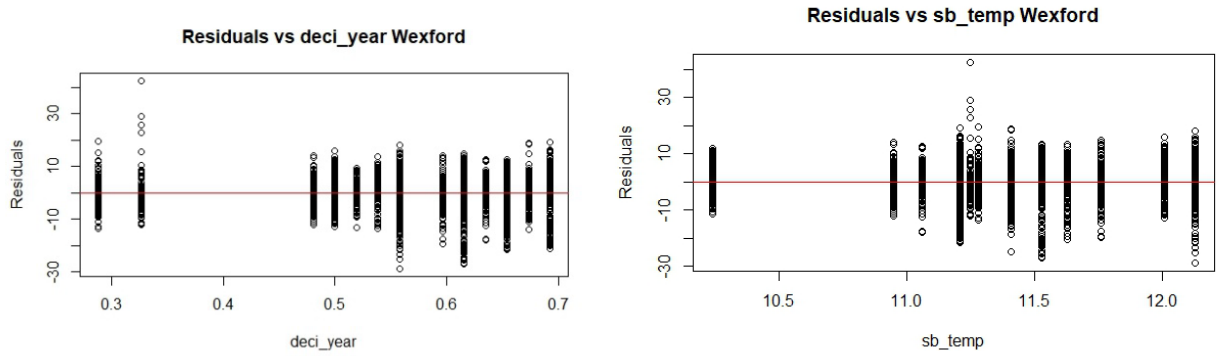

Plots for Residuals versus Independent Variables for Wexford model 4 (year and temperature)

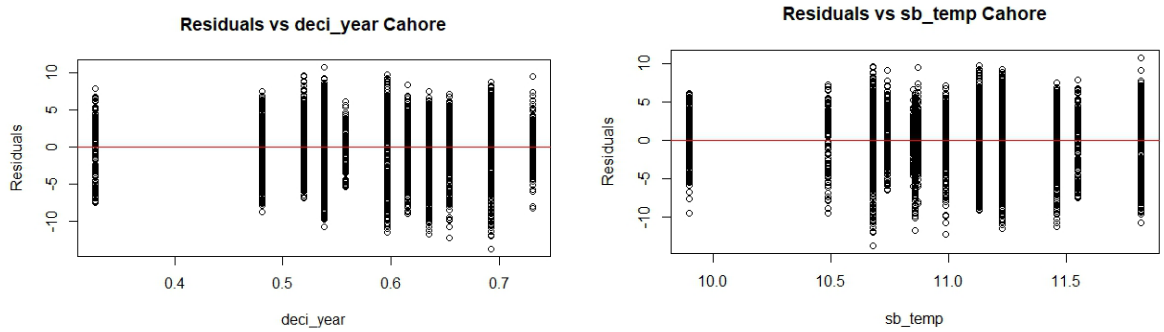

Plots for Residuals versus Independent Variables for Cahore model 4 (year and temperature)

```
# Q-Q Plot of Random Effects
qqnorm(ranef(modwex_final)$`factor(vct_yearwexford)`[, "(Intercept)"])
qqline(ranef(modwex_final)$`factor(vct_yearwexford)`[, "(Intercept)"], col = "red")


qqnorm(ranef(modch_final)$`factor(vct_yearcahore)`[, "(Intercept)"])
qqline(ranef(modch_final)$`factor(vct_yearcahore)`[, "(Intercept)"], col = "red")
```

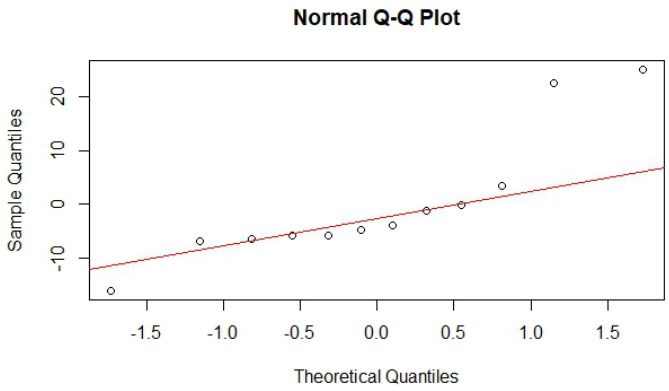

Q-Q Plot of Random Effects for Wexford Model 4

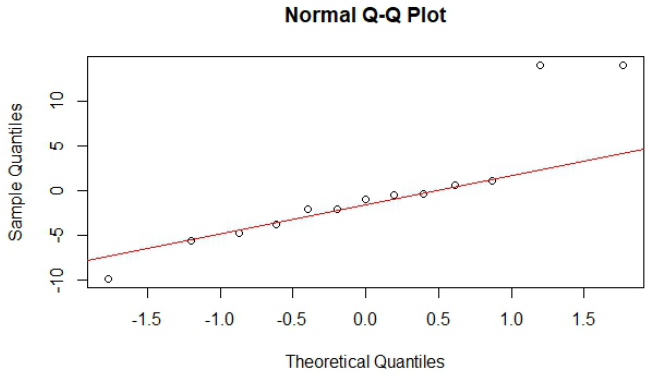

Q-Q Plot of Random Effects for Cahore Model 4

```
# Shapiro-Wilk test for normality of residuals


Shapiro.test(resid(modwex_final))

        Shapiro-Wilk normality test

    data:  resid(modwex_final)

    W = 0.97202, p-value < 2.2e-16


Shapiro.test(resid(modch_final))

        Shapiro-Wilk normality test

   data:  resid(modch_final)

  W = 0.9853, p-value < 2.2e-16
```

```
# Durbin-Watson test for autocorrelation of residuals

dwtest(resid(modwex_final) ~ fitted(modwex_final))

       Durbin-Watson test

 data:  resid(modwex_final) ~ fitted(modwex_final)

 DW = 0.17824, p-value < 2.2e-16

 alternative hypothesis: true autocorrelation is greater than 0


dwtest(resid(modch_final) ~ fitted(modch_final))

    Durbin-Watson test

 data:  resid(modch_final) ~ fitted(modch_final)

 DW = 0.084437, p-value < 2.2e-16

 alternative hypothesis: true autocorrelation is greater than 0
```